Distribution Agreement

In presenting this thesis or dissertation as a partial fulfillment of the requirements for an advanced degree from Emory University, I hereby grant to Emory University and its agents the non-exclusive license to archive, make accessible, and display my thesis or dissertation in whole or in part in all forms of media, now or hereafter known, including display on the world wide web. I understand that I may select some access restrictions as part of the online submission of this thesis or dissertation. I retain all ownership rights to the copyright of the thesis or dissertation. I also retain the right to use in future works (such as articles or books) all or part of this thesis or dissertation.

Signature:

_____ _____

Jun Liu Date

Ferritin as a Transgenic MRI Reporter in Mouse Embryonic Stem Cells

By

Jun Liu
Doctor of Philosophy

Graduate Division of Biological and Biomedical Sciences
Neuroscience

_____

Anthony Chan
Advisor

_____

Marie Csete
Committee Member

_____

Hui Mao
Committee Member

_____

Yoland Smith
Committee Member

_____

Lary Walker
Committee Member

Accepted:

_____

Lisa A. Tedesco, Ph.D.
Dean of the Graduate School

_____

Date

Ferritin as a Transgenic MRI Reporter in Mouse Embryonic Stem Cells

By

Jun Liu

B.A., Beijing Foreign Studies University, 2001
M.S., Georgia Institute of Technology, 2004

Advisor: Anthony W. S. Chan, Ph.D.

An abstract of

A dissertation submitted to the Faculty of the Graduate School of Emory University in partial fulfillment of the requirements for the degree of Doctor of Philosophy

in

Graduate Division of Biological and Biomedical Sciences
Neuroscience Program

2009

Abstract

Ferritin as a Transgenic MRI Reporter in Mouse Embryonic Stem Cells

By Jun Liu

Embryonic stem cells hold great promise for regenerative medicine. To facilitate their translation into clinical practice, new methods to monitor stem cell transplant *in vivo* using transgenic MRI reporter are explored in the current study.

Among potential choices for MRI reporter genes, we focused on two critical players in iron homeostasis: ferritin heavy chain (FTH) and transferrin receptor (Tfrc), and began our study with parallel comparisons of the function and safety of FTH, Tfrc and their co-expression in clonal transgenic 293HEK and C6 glioma cell lines. It was discovered that un-regulated co-expression of FTH and Tfrc was associated with insignificant functional improvement but severe toxicity, so this combination was eliminated as a strategy. When expressed individually, FTH and Tfrc each were shown to be safe and effective MRI reporters. Closer examination of the underlying mechanisms of their reporter function suggested FTH was potentially the safer option between the two, being able to achieve the same level of MRI contrast with less intracellular iron accumulation, while retaining the capacity for effective regulation of iron uptake. FTH was subsequently chosen for introduction into mouse embryonic stem cells (mESCs).

In mESCs, moderate levels of FTH expression did not impair cell growth, nor were these levels disruptive to ESC pluripotency. When transplanted and monitored *in vivo*, FTH transgenes induced significant MRI contrast comparable to those achieved in

other cell types. These findings suggest that FTH can function as a safe and effective molecular reporter in mESCs without external contrast agent. This has opened up new possibilities for stem cell imaging include longitudinal monitoring of cell transplants and, at the molecular level, potential to monitor differentiation status of stem cells and to detect expression of therapeutic genes in stem cell based gene therapies. Further efforts are needed to provide an accurate guideline of applicability and to improve on detection sensitivity of the transgenic reporter, before the full benefit of a MRI reporter-ESC combination can be realized.

Ferritin as a Transgenic MRI Reporter in Mouse Embryonic Stem Cells

By

Jun Liu

B.A., Beijing Foreign Studies University, 2001
M.S., Georgia Institute of Technology, 2004

Advisor: Anthony W. S. Chan, Ph.D.

A dissertation submitted to the Faculty of the Graduate School of Emory University in partial fulfillment of the requirements for the degree of Doctor of Philosophy

in

Graduate Division of Biological and Biomedical Sciences
Neuroscience Program

2009

TABLE OF CONTENTS

FIGURES AND TABLES

CHAPTER I: GENERAL INTRODUCTION

CHAPTER II: Seeking the Right Reporter

Chapter I

General Introduction

1.1 Embryonic Stem Cells

Life starts as a single cell, it is thus a certainty that at an early developmental stage some cells have the potential to divide and ultimately differentiate into all the cell types of the adult organism (zygote being the quintessential example). The possibility of maintaining such cells *in vitro* is of immense interest to research and medicine, and efforts over the past decades have culminated in successful isolation of pluripotent stem cells from many species, notably of mouse in 1981(Evans and Kaufman, 1981; Martin, 1981), of non-human primates in 1995 (Thomson et al., 1995) and of humans in 1998 (Thomson et al., 1998). These successes were built upon the insights that self renewing cells with extensive differentiation potential can be isolated from the inner cell mass (ICM) of blastocyst stage embryos and maintained in an undifferentiated state in culture, hence the name "embryonic stem cells" (ESCs).

Among the many features characteristic of ESCs, two are considered the hallmarks: unlimited self-renewal (generate additional unspecialized embryonic stem cells through division) and pluripotency (give rise to all cell types of the adult organism through differentiation) (Smith, 2001). In contrast, adult stem cells (ASCs), undifferentiated cells isolated from more differentiated tissues, have more limited differentiation potential (multipotent) and cannot proliferate indefinitely in culture. Here is where names can become a bit misleading: ostensibly the nomenclature refers to the source of stem cell derivation (ASCs from adult tissue vs. ESCs from blastocyst stage embryo); however in reality, ASCs can be isolated from any stage of development. And with technological advances, ES-like cells have been derived from other (adult) cell sources using techniques such as somatic cell nuclear transfer (SCNT) (Byrne et al.,

2007), or parthenogenesis (Revazova et al., 2008). ES-like cells can be derived from non-blastocyst embryonic developmental stages (Brons et al., 2007), from fetal tissue destined for gonads (Shamblott et al., 1998) as well as adult gonads (Conrad et al., 2008), and now from epigenetic modification of adult cells resulting in induced pluripotent stem cells (iPSCs) (Takahashi et al., 2007; Yu et al., 2007). For the purpose of this thesis, the important functional definition of ESCs is that they are pluripotent stem cells with unlimited renewing potential.

Ever since the successful isolation of human embryonic stem cells (hESCs) in 1998 (Thomson et al., 1998), the ESC has remained one of the hottest topics in biomedicine, and for good reasons. While the use of ASCs is less controversial, their applications are also constrained by ASCs' replicative senescence and more limited differentiation potential. In contrast, ESCs, which combine long term self-renewal and pluripotency, could provide a source of unlimited supply of any cell type of interest. The potential applications of ESCs are many; they are invaluable as platforms for studying the very earliest stages of embryonic development, for studying cancer origins and progression, and are already widely used as models for drug development/ toxicity screening. For our interest in regenerative medicine, the current and future impact of ESCs on cell replacement therapy cannot be overstated. ESCs have two clear advantages here, one is supply: Cell replacement therapies have shown promise in the treatment of conditions ranging from Parkinson's (Freed et al., 2001) to Type I diabetes (Efrat, 2002), and access to graft tissue has been one of the major bottlenecks to extend these successes (Bjorklund and Lindvall, 2000; McKay, 2000). The combination of self-renewal and pluripotency of ESCs could one day make the supply concerns obsolete. (It should also

be pointed out that for diseases with complex etiology like Parkinson's, at current stage stem cells therapy are no panacea but only a promising alternative, and has so far produced mixed results).The other advantage is gene therapy (Wobus and Boheler, 2005): ESCs can be maintained indefinitely *in vitro* and are conducive to genetic engineering, which makes them natural complements to gene therapies. To start with, transgenic ESCs lines can be established to provide an undepletable source of cell based delivery of therapeutic genes. (It is important to note, however, that homologous recombination is much more difficult in human ESCs than in mouse ESCs.) Unlike therapeutic strategies based on direct transduction of host cells with viral vectors, transplanting genetically modified stem cells could provide a renewable source of therapeutic gene product that can be selected and fine-tuned *in vitro* before *in vivo* delivery, a clear advantage under some circumstances. With further technological advances, they offer hope for even the most seemingly intractable cases of neurodegenerative disease from genetic defects. For example, it may be possible to witness one day treatment options involving iPSCs custom created for Huntington's disease patients, genetically engineered *in vitro* to remove the inherited defects, differentiated into neural progenitor cells (NPCs) and autologously grafted back to the patients without the fear of rejection. Such a strategy has already been successfully applied in treating sickle cell anemia in a rodent model (Hanna et al., 2007).

Despite the great promises, ESCs have a rather thin resume when it comes to actual clinical applications; it wasn't until the beginning of this year that the first human clinical trial of embryonic stem cell based therapy was authorized. On Jan 23rd 2009 FDA approved Geron to test embryonic stem cell derived pre-oligodendrocytes on patients

with acute, severe thoracic spinal cord injuries. Considering that human ESCs were only identified a decade ago, and the difficulties in handling human ESCs and political obstacles to their widespread use, this development of a therapy was not as delayed as it may first appear. Besides regulatory hurdles, the relative slow introduction of ESCs based therapies also reflects healthy scientific caution: ESCs not only hold great promise but can also carry significant risks. Transplants of undifferentiated ESCs are known to aggressively proliferate and form teratoma *in vivo*, even grafts post-differentiation are not risk free as exemplified by studies in which dopaminergic cell grafts derived from hESCs alleviated behavioral symptoms in rat model of Parkinson's disease and were at the same time tumorigenic (Roy et al., 2006). Before pluripotent stem cells can be fully integrated into clinical practice, further technological advances in their maintenance, differentiation, graft selection, scaled production, organ/tissue engineering, *in vivo* monitoring etc. are necessary.

Our efforts focused on molecular imaging, that is, non-invasive *in vivo* investigation of cellular and molecular events involved in normal and pathological processes (Hoehn et al., 2008). More specifically, we focused on molecular imaging of stem cells with MRI reporter genes. In experimental models, stem cell grafts are already routinely monitored at the cellular level (often with the help of MRI contrast agents in the form of magnetic nanoparticles (Bulte et al., 2002) to follow their localization, migration and survival; and cellular imaging gained new urgency because of the potential for undifferentiated ESCs in a cell product to form tumors. Monitoring can also be extended to events at the molecular level that bear great relevance to ESCs based cell therapies, like the differentiation status of ESC-derived grafts or the activation status of therapeutic

genes that stem cell grafts are carrying. Effective monitoring of all these events can potentially be realized with the help of genetic engineering-- with the introduction of reporter genes into ESCs whose gene products can be visualized through a wide range of mechanisms across multiple imaging modalities. By non-invasively providing *in vivo* monitoring of stem cell grafts, of their localization, migration, survival, differentiation status, gene expression, and potential tumor formations (which can also be controlled with genetic engineering using suicide genes); molecular imaging has been and will continue to be an indispensable tool in the development of effective stem cell therapies.

1.2 Brief review of imaging modalities

Three imaging modalities are commonly used for the purpose of *in vivo* monitoring: optical imaging, nuclear imaging and magnetic resonance imaging, all of which have adopted reporter gene systems to varying degrees.

Optical Imaging: The basis for optical imaging is the sensitive detection of photons of a specific light spectrum. Two major techniques of optical imaging are fluorescence imaging and bioluminescence imaging (Weissleder and Ntziachristos, 2003). The most familiar example of the fluorescence imaging camp is green fluorescence protein (GFP) and its variant, enhanced green fluorescence protein (EGFP). In a typical *in vivo* scenario, tissue of interest expressing an EGFP transgene will emit green (509 nm) light in response to excitation, which can be visualized as long as the target is located sufficiently close to the body surface. An alternative fluorescence imaging approach uses the near infrared spectrum, which requires exogenous administration of fluorochromes for the benefit of improved tissue penetration and reduced

autofluorescence. Both these approaches are limited by tissue penetration of photons, with effective penetration depth measured only in the millimeter range. Bioluminescence imaging follows the same general principles as fluorescence imaging. The difference lies in the reporter gene (luciferase) used and its corresponding substrate (luciferin). Unlike fluorescence imaging, bioluminescence imaging does not require excitation light, thus is less confounded by background light or autofluorescence. Bioluminescence has greater sensitivity and improved tissue penetration (1-2 cm) (Massoud and Gambhir, 2003) than fluorescence imaging.

As an imaging modality, optical imaging is easy and inexpensive to perform with good sensitivity. It has relied heavily on reporter gene systems and found applications in both cell trafficking (Kaneko et al., 2001) and monitoring gene expression (Spergel et al., 2001). Its greatest limitation is the scattering and attenuation of photons as they transmit through tissues, which effectively limits *in vivo* applications of optimal imaging to very small animals. From the perspective of reporter genes for stem cells, optimal imaging is a decent choice for small animal imaging but not a practical choice for *in vivo* monitoring on large animals. Still, thanks to its many conveniences fluorescence reporters like GFP can serve as good auxiliary reporters for double confirmation of other reporter genes of interest, a strategy that has been successfully used in the past and adopted in the current study.

Nuclear Imaging: Both Positron emission tomography (PET) and Single photon emission computed tomography (SPECT) imaging, the two prominent modalities nuclear imaging, rely on administration of radioactive tracer that allows detection of gamma ray emissions from targets of interest, from which three dimensional images are constructed

(Rosenthal et al., 1995; Cherry and Gambhir, 2001). Early nuclear imaging efforts mostly relied upon the direct measurements of metabolic activities, like PET imaging of glucose utilization ([18F] fluorodeoxyglucose FDG), but the versatility of PET imaging has since been greatly expanded owing to the development of reporter gene systems, which allow visualization of selective interactions between radiolabeled probes and their many potential targets of enzymes, receptors or transporters (Gambhir, 2002). One prominent example of a PET reporter gene is herpes simplex virus type 1 thymidine kinase (HSV1-TK) (Gambhir et al., 1999; Gambhir et al., 2000). HSV1-TK is capable of phosphorylating a number of thymidine analogs that are unresponsive to mammalian thymidine kinase, and its expression can be visualized by trapping phosphorylated radiolabeled substrates inside the cell.

As an imaging modality, PET imaging has multiple advantages when it comes to sensitivity, versatility, quantification and tissue penetration (no limit). Its reporter gene system has already found applications in embryonic stem cells, with the additional benefit that HSV1-TK could function as a suicide gene when a pharmacological dosage of ganciclovir is administrated (Schuldiner et al., 2003; Cao et al., 2007), a strategy used in experimental therapies of human tumors. Image resolution, in the 1-2 mm range, is a limitations that can be overcome when PET is linked to MRI or CT systems (Jacobs and Cherry, 2001). The most significant limitation of PET imaging is the prohibitive cost associated with its establishment, maintenance and functioning (short half-life of many radioactive tracers often requires onsite synthesis), which in turn limits the availability of PET systems in stem cell research.

Magnetic Resonance Imaging: When placed in a strong magnetic field, the unpaired nuclear spins align with the field forming a net magnetization vector parallel to the magnetic field. In response to radiofrequency pulses that match the Larmor frequency of hydrogen atoms (hydrogen atoms are preferably targeted due to the abundance of water in the body); the spins absorb energy and the magnetization vector changes orientation. Afterwards the spins will release energy and revert to the original state, a process called relaxation which varies depending on the physicochemical environment. The relaxation process is detected by the scanner and translated into MRI signal; thanks to the fact that differences in tissue composition have significant impact on relaxation parameters. By careful design of the imaging paradigm, those differences can be captured and recreated as MRI contrasts(Massoud and Gambhir, 2003).

As an imaging modality, MRI is ideal for many applications involving stem cell grafts. Like PET, it has no limit of tissue penetration. It boasts great spatial resolution and tissue contrast, and has the potential to combine anatomical, functional (fMRI) and molecular imaging (Hoehn et al., 2008). Since MRI does not require radioactive probes and thus is free from major safety (dosage of radiation) and logistic (onsite cyclotron/chemical lab) concerns of PET imaging, it can be performed repeatedly in most patients. Both the system and its maintenance are significantly less expensive than PET (despite the fact medical bills involving MRI services often compel people to conclude otherwise), and it is widely available thanks to its clinical relevance.

Given the current stage of developments in molecular imaging, we decided to pursue an MRI based reporter gene system for *in vivo* molecular imaging of ESCs. The choice of MRI over other systems reflects the following considerations: (1) Originality,

the fact that MRI is the only modality that has not seen application of reporter genes in ESCs poses both a challenge and an opportunity. (2) Clinical/research relevance, many promising ideas on stem cells are poised to progress to the stages where trials on non-human primates or human are necessary, thus optical imaging was ruled out because of its severe limitations with tissue penetration while MRI is preferred for its strong clinical and research presence. (3) Between MRI and PET, MRI has many advantages in terms of resolution, contrast, safety, cost and availability, all of which were factored positively into our planning. We expect that if a viable reporter gene system equivalent to HSV1-TK for PET can be established for MRI, it will doubtless find applications in stem cell research. The choice of MRI is also a practical one: While both MRI and PET systems are available on campus, the cost of MRI research scanners can be brought down to $150/hr level, a fraction of that of PET, which leaves room for mistakes and continuous efforts, both indispensable for the current exploratory study. The following table (Table I-1) summarizes the strengths and weakness of different imaging modalities, modified from (Massoud and Gambhir, 2003).

1.3 Choice of MRI reporter genes

Study of molecular reporters for MRI is still in an early stage with less than a dozen reports available, and few consensus or established protocols to rely upon. Consequently, the choice of "appropriate" reporter genes for MRI constitutes the first challenge we faced in this study. As will be reviewed in Chapter II, no less than 6 candidates have been proposed for this function (Koretsky et al., 1996; Weissleder et al., 1997; Louie et al., 2000; Weissleder et al., 2000; Alfke et al., 2003; Cohen et al., 2005;

Genove et al., 2005; Gilad et al., 2007b; Zurkiya et al., 2008). Two candidates, transferrin receptor and ferritin, are the dominant players in endogenous iron regulation and are the two candidates with independent confirmations of utility (though the case of transferrin receptor was controversial). We focused our attention on three possible transgene scenarios: transferrin receptor only, ferritin only and combined usage of the two, and explored the best options among them using transgenic 293HEK and C6 glioma cells, both *in vitro* and *in vivo*. All of our efforts with non-ESC characterization in seeking the best candidate MRI reporter gene will be covered in Chapter II. The somewhat surprising conclusion, that ferritin alone is the best candidate for MRI reporter, laid the foundation for our effort with transgenic mESCs.

Chapter III covers studies of ferritin heavy chain introduced into mESCs as a reporter gene. The ESC model posed new challenges including the compatibility between transgene expression and ESC viability/pluripotency, and finding a proper balance between safety and effectiveness. Our efforts in addressing these concerns and the success with *in vivo* MRI monitoring of mESCs after transplantation constitute the bulk of Chapter III.

Accordingly, the experimental efforts presented in this manuscript focused on two aims

Chapter II

Aim One: Identify the best reporter gene that combines efficacy and safety

- Establish clonal cell lines that represents transferrin receptor only, ferritin only, and co-expression of the two in 293HEK and C6 glioma cell models.
- Characterize the impact of transgene expression on iron homeostasis.

- Characterize the safety of transgene expression based on cell proliferation.
- Characterize the function of reporter genes based on *in vitro* and *in vivo* MRI.

Chapter III

Aim Two: Test the compatibility and functionality of reporter gene in mESCs

- Establish clonal mESC lines that express the reporter gene of choice.
- Characterize the impact of transgene expression on iron homeostasis.
- Characterize the safety of transgene expression based on cell proliferation.
- Characterize the pluripotency of transgenic mESCs.
- Confirm the function of reporter gene in *in vivo* monitoring of mESCs grafts.

The last chapter, Chapter IV, summarizes our findings, the lessons learned and insights gained over the past three years of research, and offers a perspective on the future efforts needed to transform this promising ESC tracking modality into practical applications on MRI monitoring of stem cell grafts.

Table I-1. Comparisons of imaging modalities

Imaging modalities	Optical imaging	PET	MRI
Measurements	photon	Gamma ray	microwave
Tissue Penetration	<2 cm	unlimited	unlimited
Resolution	2-3 mm	1-2 mm	25-100 um
Probe	Fluorochrome or luciferin, but not required in many cases of fluorescence protein	Requires radioactive probe	Magnetic nanoparticles often used, but not required in all cases
Sensitivity	high	high	low
Invasive	no	yes	no
Cost	low	high	moderate
Availability	wide	limited	wide
Reports on ES cell application	yes	yes	not yet

Chapter II

Seeking the Right Reporter

2.1 Introduction

The first step towards an MRI reporter-ESC combination is to decide which reporter gene to introduce into ESCs. Molecular MRI reporting is a nascent field with less than a dozen reports to date, but a diversity of candidates to choose from: β-galactosidase (Louie et al., 2000), tyrosinase (Weissleder et al., 1997; Alfke et al., 2003), transferrin receptor (Tfrc) (Koretsky et al., 1996; Weissleder et al., 2000), ferritin (FT) (Cohen et al., 2005; Genove et al., 2005; Cohen et al., 2007), MagA (Zurkiya et al., 2008) and Lysine rich protein (Gilad et al., 2007b). With application in cell replacement therapy in mind, some candidates have been eliminated due to their clear limitations: β-galactosidase was ruled out because it required administration of substrates that had difficulty with tissue penetration *in vivo*; tyrosinase was ruled out because melanin production was associated with significant toxicity from ROS; the report on Lysine rich protein relied on a very high strength (11.7T) MRI unit to demonstrate a rather weak contrast, making it an unlikely candidate with our current access to hardware.

We thus focused on Tfrc and ferritin, two ubiquitous proteins that are tightly linked in the process of intracellular iron homeostasis. After hydrogen, iron is considered the most important atoms to MRI; and it is arguably the most important trace element when it comes to imaging of cell transplants. To understand how Tfrc and ferritin might function as MRI reporters, it would be useful to start with a brief review on how iron is distributed and stored in the body.

Iron distribution and storage in the body

Iron is essential to life and the human body is very sensitive to both iron deficiency and iron excess. Iron plays key roles in oxygen transport, muscle functions, and various enzymatic activities including the synthesis of DNA and neurotransmitters (Crichton and Ward, 1998). It is also capable of contributing to toxicity as excessive iron contributes to chemical reactions yielding the very reactive hydroxyl radicals that inflict tissue damage through their attack on lipids, proteins and nuclei acids (Berlett and Stadtman, 1997; Henle and Linn, 1997; Steinberg, 1997; Stadtman and Berlett, 1998).

A typical human body has 3-4 grams of iron, of which close to 65% is incorporated into hemoglobin (Andrews, 1999). The second largest compartment (20% of total) is stored iron, mostly in the form of ferritin-bound iron. Tissues with high iron contents include liver, spleen macrophages, muscle and the brain (Jocobs and Worwood, 1978). Circulating iron in the plasma, bound to transferrin (Tf), represents only 0.1% of total body iron despite its great functional significance. Since the human body does not have effective methods to remove iron, at the systemic level iron balance is mostly achieved through control of iron absorption, normally at a level of 1-2 mg per day (Brissot et al., 2002).

Transferrin, transferrin receptor and ferritin

At the cellular level, the iron balance is achieved through complex interactions among a number of players, including, but not limited to 1) Tf: the iron transport protein, each transferrin is capable of strong and reversible binding to two ferric (FeIII) iron atoms. Since ferric iron is not soluble, it is circulated through the body in Tf-bound form. The transporter protein provides solubility, reduces toxicity, and helps with selective

uptake (Aisen, 1998). 2) Tfrc: the ligand-receptor complex between Tf-Tfrc is the major gateway cells use to regulate iron uptake. Once holo-transferrin (h-Tf, also known as diferric transferrin---transferrin carrying two atoms of ferric iron) is bound to Tfrc , the Tf-Tfrc complex is internalized into the cell, fused to endosome, and releases ferric iron in the more acidic environment (PH 5.5-6.5) before being recycled back to the membrane (Dautry-Varsat et al., 1983; Hopkins and Trowbridge, 1983). 3) Labile iron pool (LIP): once ferric iron is released from Tf, it is transported into the cytoplasm to become part of the LIP--- a pool of chelatable and redox-active iron which serves as the interface between iron in active function and iron in storage form. (Breuer et al., 1995; Konijn et al., 1999) 4) FT: iron storage protein, consists of 24 subunits of ferritin heavy and light chains. Through its ferroxidase center (iron binding site), FT protein can incorporate excessive iron from LIP into its core as ferrihydrite crystal (non-reactive mineral form). Each FT protein is capable of storing up to 4500 iron atoms (Harrison and Arosio, 1996; Treffry et al., 1997). The relationships between Tf, Tfrc and FT can be summarized as: Tf delivers ferric iron to cells through the process of Tf-Tfrc binding, internalization, and iron release. Released iron goes into LIP; part of which will be diverted for storage in FT-bound form. (Figure II-1)

Iron Regulation

An elaborate system of iron regulation has evolved to maintain iron homeostasis in the event of excess or deficiency in iron supply (Aisen et al., 1999). Mechanisms are in place to quickly modulate the expression of both Tfrc and FT at a posttranscriptional level, mostly through the interaction between iron responsive elements (IREs) --- stem loop structures on the non-coding regions of Tfrc and FT mRNA, and iron regulatory

protein (IRP) --- proteins that are capable of binding to IRE to influence translation. (Hentze et al., 1988; Hanson and Leibold, 1999; Theil, 2000) As an example of an ingenious, evolved solution in regulation, IRP has opposing effects on Tfrc and FT expression. IRE sequence is located at the 5' region of FT mRNA and IRP binding inhibits translation (hinders recruitment of 43S translation pre-initiation complex) (Aziz and Munro, 1987; Caughman et al., 1988); in contrast, IRE is located at the 3' region of Tfrc mRNA and IRP binding stabilizes mRNA (prevent RNases endonucleolytic attack) to facilitated translation (Casey et al., 1988; Casey et al., 1989).

IRPs also bind to iron and iron-bound IRPs lose their ability to bind IRE. In the event of excessive intracellular iron, an increase in LIP and more iron binding to IRP means less IRP regulation on FT and Tfrc mRNA. With increased production of FT and reduction in Tfrc, the cell initiates the appropriate response to iron excess---more storage (FT) and reduced intake (Tfrc). The reverse is true for iron deficiency, a decrease in LIP and less iron-bound IRP means more IRP regulation over FT and Tfrc. With reduction in FT and increase in Tfrc, the cells will store less and uptake more in response to iron deficiency. In both cases, iron homeostasis is delicately maintained (Ponka et al., 1998). (Figure II-2)

Response to transgene

One obvious approach to create MRI contrast is to increase cellular iron content. In order for that to happen *in vivo*, the baseline for iron equilibrium needs to be shifted toward increased iron storage. Given what is known about the functions of Tfrc, FT and IRP in iron homeostasis, in theory this may be realized by introducing either Tfrc or FT

transgenes to influence cellular iron homeostasis. Of course IRE sequences would have to be removed from the transgenes so their translation will be free from endogenous regulatory control. In the case of FT, expression of IRE-free FT will increase levels of storage protein and divert more intracellular iron from LIP into FT-bound storage form. This will temporarily create a reduction in LIP (total cellular iron remains constant, with a higher proportion in storage form), which in turn through IRP will lead to an up-regulation of Tfrc expression. With more iron uptake to replenish the LIP, a greater amount will also be diverted to iron storage. Eventually when a semblance of balance is reached, the cell is expected to have accumulated more iron during the process, and the iron will have been distributed in more ferritin proteins (total cellular iron now increased, with higher proportion in storage).

The expected outcome from Tfrc transgene overexpression is conceptually similar: Expression of IRE-free Tfrc will directly increase iron uptake into LIP, the cell will respond by up-regulating FT expression through IRP to provide more storage protein. During the process of rebalancing, excessive iron from LIP will be continuously diverted to FT and the end result would also be similar to FT transgenesis: Increase in total cellular iron stored in FT bound form (Figure II-3).

Still there are subtle but important differences between the two approaches. From the perspective of iron content, Tfrc transgenesis will have more direct impact on iron uptake and will possibly lead to greater accumulation; the downside of increasing LIP may also put the cell at greater risk for ROS damage. In contrast, FT transgenesis is expected to induce less dramatic iron content increases as it relies upon indirect compensatory boosts in response to decreases in LIP; this may offer some protection

against toxicity (Arosio and Levi, 2002; Pham et al., 2004) (though insufficient iron supply could also slow cell growth). On top of these, total intracellular iron content may not be the sole determinant in MRI contrast. Both *in vitro* and likely *in vivo,* iron loading factor of ferritin protein may also influence MR relaxivity (Vymazal et al., 1996; Vymazal et al., 1998). Thus the relative strength of Tfrc versus FT transgenes are hard to predict purely from theoretical models and have to be determined experimentally.

Three approaches

Appreciating the potential of manipulating iron homeostasis for MRI contrast through genetic engineering, a few groups of researchers have performed the pioneering studies on metalloprotein-based MRI reporters. Three designs have been adopted: Tfrc only, FT only, and combining Tfrc with FT.

Tfrc only design: The earliest report on metalloprotein MRI reporter dates back to 1996, when Koretsky et al. reported that Tfrc-overexpressing transformed fibroblasts exhibited a 3-fold increase in iron content, and the transgenic transplants showed significant contrast comparing to WT controls *in vivo* on T2 weighted MR images (Koretsky et al., 1996). Subsequent studies using Tfrc overexpressing 9L rat gliosarcoma cell lines (Moore et al., 1998; Weissleder et al., 2000) confirmed the increase in iron uptake from Tfrc expression, but did not observe significant MRI contrast from Tfrc expression alone. Instead Weissleder et al. proposed using Tf linked MION to target Tfrc-expressing cells and succeeded in distinguishing transgenic cells both *in vitro* and *in vivo*. (It should be noted that in the case of Tf-MION targeted Tfrc-transgenic cells, the magnetic nanoparticle functioned as the MRI reporter and the Tf-Tfrc combination only

provided a receptor-ligand pathway for MION delivery, which was not contingent upon their role in iron homeostasis.) To this day, while the utility of Tfrc as a reporter gene is well recognized, it remains an open question whether Tfrc transgene alone can effectively mobilize an endogenous iron supply to function as an MRI reporter without external administration of contrast agents.

FT only design: Inspired by earlier success (or should we say controversy) of Tfrc, more recent studies on metalloprotein reporters have focused on Tfrc's partner in iron regulation--FT. The logic, as outlined previously, is FT expression will induce compensatory increases in iron content safely sequestered in the additional storage proteins (along with redistribution of stored iron). This approach has been proven successful, with three studies following different paradigms: C6 glioma transplant (Cohen et al., 2005), direct viral injection (Genove et al., 2005), transgenic animal (Cohen et al., 2007); all reported positive *in vivo* results from FT transgenesis. Beyond the many differences in methodology, it is the similarities among these studies that are most revealing: (1) all of them relied on high field strength MRI units (4.7T-11.7T); (2) all of them used T2 weighted MRI sequences, with additional T2* sequence used in the direct viral injection into CNS (3) all transgene introduction focused on the heavy chain subunits of ferritin (FTH). These designs point to a few critical properties of ferritin worth emphasizing from the beginning: Ferritin is a relatively weak MRI contrast agent and its efficacy increases with field strength (Vymazal et al., 1992), its ferroxidase activity is exclusively linked to its heavy chain (though the presence of light chain improves effectiveness in iron uptake) (Levi et al., 1988; Lawson et al., 1989; Levi et al., 1992), and T2/ T2* weighted sequences are more sensitive for detection of ferritin-based

contrast than T1 sequences (Wood et al., 2004; Cohen et al., 2005; Rogers et al., 2006). In sum, there is considerable evidence that FT could function as an MRI reporter on high field strength MRI units.

Tfrc+FT combination design: This idea was first proposed by Deans and colleagues (Deans et al., 2006), and their work remains the only published study following a combinatory design to date. It has its intuitive appeals: One would expect greater MRI contrast from expressing Tfrc and FT together as both are known to increase cellular iron content. Deans proposed greater safety from the combination, arguing that instead of relying on the endogenous iron regulatory system to compensate (by up-regulating Tfrc or FT in response to transgenesis of their counterpart), co-expression would balance intake and storage from the beginning. However the strategy was difficult to judge as, in the original study, no Tfrc-only or FT-only control was available for comparison with Tfrc+FT combined cell line to validate the claims of co-expression superiority. The original study also failed to detect MRI contrast *in vivo* from transgenic transplants without iron supplement (which may have more to do with their design of *in vivo* study than issues with transgene function). Consequently, Tfrc-FT combination remains an interesting but not adequately tested idea for MRI reporter.

Current plan

Having pinned the candidates for stem cell MRI reporter down to Tfrc and FT, it becomes very difficult to further decide among the three remaining possibilities, namely: Tfrc, FT and Tfrc/FT. There were no pair-wise comparisons of them from earlier studies to justify strong preferences. As a matter of fact, different research paradigms adopted

previously only added to the uncertainties. Findings on Tfrc are controversial (Koretsky et al., 1996; Weissleder et al., 2000). FT benefits from independent confirmations from different groups (Cohen et al., 2005; Genove et al., 2005), though we found it hard to reconcile the negative findings from Tfrc with positive ones from FT; after all they tap the same regulatory pathway and produce a similar outcome--more iron stored in ferritin. As for Tfrc-FT combination, the idea remains attractive but largely untested (Deans et al., 2006).

The best course of action, it seems, is to conduct parallel comparisons among all four conditions of interest (WT, Tfrc, FT and Tfrc/FT) to produce a clearer picture on their relative strengths and weaknesses, before an informed decision could be made. Our study employed lentiviral vectors to transduce different combinations of transgenes to establish clonal cell lines that correspond to the four conditions of interest; and characterized the resultant transgenic cell lines on cell viability, cellular iron content, and *in vitro* and *in vivo* MRI; before making a recommendation on the best reporter gene candidate for stem cells based on empirical support.

2.2 Materials and Methods

Lentiviral construct design

cDNA for human ferritin heavy chain (gene bank accession number: BC015156) and human transferrin receptor (accession number: BC001188) were obtained from Openbiosystems. Both were cloned into FUGW lentiviral backbones to create lentiviral vectors that constitutively express the transgenes of interest. In addition, FTH cDNA was

also cloned into a Tet-on lentiviral vector that expresses FTH in response to tetracycline (Tet)/doxycycline (Dox) induction.

FUGW is a self inactivating lentiviral vector with a number of desirable features (Lois et al., 2002): an internal human ubiquitin-C promoter (U) that provides reliable transgene expression across cell types, woodchuck hepatitis virus posttranscriptional regulatory element (W) that increases transcription level and human immunodeficiency virus-1 (HIV-1) flap element (F) that increases the titer of the virus. In our study, an internal ribosome entry site (IRES) was placed before GFP (G) to modify FUGW into a bicistronic reporter vector---FU-IRES-GW.

FTH cDNA was PCR modified to remove Iron Responsive Element (IRE) and create Hemagglutinin (HA)-tag at the N-terminus (primer sequences 5'-3' FTH sense first: ATG TTC CAG ATT ACG CTA TGA CGA CCG CGT CCA CC, FTH sense second: AGC TAG CAT GTA CCC ATA CGA TGT TCC AGA TTA CGC, FTH antisense both times: CTT AGC TTT CAT TAT CAC TGT CTC CCA GGG) before it was sub-cloned into the multiple cloning site of FU-IRES-GW. The resultant vector is named pLVU-HA FTH-IRES-EGFP (Figure II-4). The coding sequence of Tfrc cDNA was released from pOTB7 vector (supplied by Openbiosystems) by restriction enzyme digestion and during the process its IRE sequence located in the 3' non-coding region was removed. The IRE-free fragment was sub-cloned into the multiple cloning site of FU-IRES-GW with the resultant vector named pLVU-Tfrc-IRES-EGFP. (Figure II-4)

LV-mCMV-G-Ubi-rTetR is a self inactivating lentiviral vector with Tet-on inducible system incorporated into its design. The transgene of interest is expressed under the miCMV promoter and its expression controlled under the tetracycline-dependent

binding of reverse tetracycline Transactivator (rtTA) to Tetracycline Response Element (TRE). HA tagged FTH sequence was inserted to replace EGFP (G) sequence downstream of TRE-miCMV so that its expression would be under tetracycline induction; and IRES-ZeoR sequence was inserted downstream of ubiquitin promoter to confer constitutively expressed Zeocin Resistance sequence as a selection marker. The resultant vector was named pLV-mCMV-HA FTH- Ubi-rtTA-IRES-ZeocinR. (Figure II-5)

To summarize, three lentiviral vectors have been constructed for the project:

(1) pLVU-HA-FTH-IRES-EGFP: constitutively expresses FTH along with EGFP. FTH is HA-tagged with IRE sequence removed; expression of EGFP enables visual confirmation and facilitates selection.

(2) pLVU-Tfrc-IRES-EGFP: constitutively expresses Tfrc (IRE removed, not tagged) along with EGFP to enable visual confirmation and to facilitate selection.

(3) pLV-mCMV-HA-FTH- Ubi-rtTA-IRES-ZeocinR: inducibly expresses FTH under tetracycline/doxycycline. No EGFP sequence has been incorporated into the inducible vector; instead, selection was made possible with ZeocinR sequence.

Establishing clonal cell lines through transduction

Lentiviruses carrying trangenes of interest were generated by co-transfecting each of the three plasmids (pLVU-HA FTH-IRES-EGFP, pLVU-Tfrc-IRES-EGFP, pLV-mCMV-HA FTH- Ubi-rTetR-IRES-Zeocin) with packaging plasmid pΔ8.9 and envelope vector pVSV-G into 293FT human embryonic kidney packaging cells (Invitrogen). On the day of transfection, 293FT cells were in exponential growth phase reaching 60%

confluence in 35 mm dish and cultured in D/F medium (Dulbecco's modified Eagle's medium with 10% fetal bovine serum supplemented with 2 mM L-glutamine and 100U/ml penicillin/ 100ug/ml streptomycin). Following calcium phosphate transfection protocol (Invitrogen), an optimal combination of 1.35 ug lentiviral plasmid DNA, 1 ug pΔ8.9 and 0.68 ug pVSV-G per were introduced into the culture medium. 48 hrs later, virus-containing medium was harvested and filtered.

Targeted cells (including C6 glioma, 293HEK and U87glioma, all subject to the same transduction protocol) have been cultured in D/F medium in parallel. Transduction was initiated by replacing culture medium with freshly harvested viral medium supplemented with polybrene (concentration 8 ug/ml) and cultured overnight. The next day, virus-containing medium was removed and replaced with standard D/F medium. Transduced cells were then passaged as single cells at low concentration into 10 cm plates for selection (200 cells per 10 cm plate).

Clonal selection procedures were dependent upon lentiviral vectors employed. FTH constitutive expression and Tfrc constitutive expression colonies were manually selected based on EGFP expression. Tet-on inducible clones were first selected with zeocin treatment (400 ug/ml for 293 cells, 600 ug/ml for cancer cell lines C6 and U87) over 6-10 days, with surviving colonies individually expanded into clonal cell lines. From each group, clonal transgenic lines that maintained stable and highest level of transgene expression were selected for subsequent studies.

Immunocytochemistry

Cell samples were fixed in 4% paraformaldehyde for 15 minutes followed by thorough washes in phosphate buffered saline (PBS); they were then incubated overnight at 4^{o}C with primary antibodies monoclonal Tfrc antibody (1:1000 Zymed), which recognize both murine and human Tfrc; and monoclonal HA antibody (1:1000 Chemicon), which specifically recognize HA tagged human FTH but not endogenous FTH; followed by thorough wash and incubation with secondary antibodies conjugated with appropriate fluorochromes for 45 minutes at room temperature. The specificity of all the antibodies used in the study has been previously confirmed by in-lab testing.

Western blot

Samples (both cell pellets and tumor tissues) were lysed in pre-chilled radio immunoprecipitation assay (RIPA) buffer with protease inhibitor cocktail and homogenized by sonication. Protein concentration was determined by Bradford assay (Bio-Rad) and equal amounts (30 μg) of proteins from each sample were loaded into 15% SDS polyacrylamide gel and separated by electrophoresis. Proteins were transferred onto a PVDF membrane (Millipore) using Bio-Rad's transblot, the membranes were blocked for 3 hrs in 5% milk in Tris Buffered Saline Tween buffer (TBST), and incubated overnight at 4°C with monoclonal HA antibody (1:1000 Chemicon) and monoclonal Tfrc antibody (1:1000 Zymed), followed by 45 minutes incubation with horseradish peroxidase (1:10000 Jackson Immunoresearch) at room temperature. Proteins were visualized with Amersham ECL kit (Amersham).

Cell growth

To determine the growth rate of clonal lines of interest, 5 x 10^5 cells from each clonal line were seeded as single cells into 60-mm culture plates and cultured in D/F medium. Using a hemacytometer, cell number was determined in triplicate at 48 hrs post cell attachment. Doubling time was calculated with the following formula: Doubling time = Total culture time/log2 (Total cell count/Initial seeding number)

Iron content

Iron contents have been determined using two methods: For cell pellet samples, o-phenanthroline iron determination method was used. Cell lines of interest (C6 and 293) were cultured in 10 cm culture plates over 4 days selectively supplemented with doxycycline (4 ug/ml) and iron supplements according to experimental designs. After thorough wash to remove trace of supplements, 6 x 10^6 cells were counted and pelleted in water before sonication to release cellular contents. 0.15% v/v mercaptoacetic acid was added to each sample and incubated overnight. For iron determination, buffer solution sodium citrate was added to the sample to maintain acidic pH along with 0.2% hydroxylamine hydrochloride to reduce iron to the ferrous state. At the last step o-Phenanthroline was added to a final concentration of 0.0075% w/v. Ferrous iron reacts with o-Phenanthroline to form orange-red Fe-phenanthroline complex that can be quantified with spectrophotometric reading of light absorbance at 510 nm. A standard for comparison was established with $FeSO_4$. The absorbance reading was performed with an ELISA Reader.

For tumor samples, Inductively Coupled Plasma Optical Emission Spectrometry (ICP-OES) was used: Tissue samples were first processed into dry powders before they

were atomized in the nebulizer and introduced into direct contact with a plasma flame. Every element will emit light at a characteristic wavelength with intensity dependent upon concentration, enabling accurate measurement of trace metals. Chemical analysis lab at University of Georgia performed all the ICP-OES experiments for the current study.

In vitro MRI

Cell pellets (full confluence in 10 cm culture plate for each sample) were collected after three PBS washes, 0.05% trypsin-EDTA treatment, and pelleted in 96 well PCR tubes at 1000 rpm. MRI of cell pellets was performed on a 4.7-Tesla horizontal bore (33 cm) MRI scanner (Oxford Magnet Technology, Oxford, UK), interfaced to a Unity INOVA console (Varian, Palo Alto, CA, USA). Using T2 weighted Fast Spin Echo sequence with TR of 5000 ms (or 2000ms) and multiple effective TE between 20 to 100 ms, two averages, matrix 256 x 256, Field of View (FOV) 40 mm x 70 mm, slice thickness 0.5mm and a gap of 0.15 mm. Multi-echo images of slices cutting through the center of cell pellets across samples were used for calculating T2 and R2 maps with MRI analysis calculator plugin (Dr. Karl Schmidt of Harvard University) of ImageJ (National Institutes of Health).

T2 weighted sequences were used in the current study to probe transgene induced MRI contrast because expression of both Tfrc and FTH are believed to shorten the T2 time of transgenic cells/tissues, which will lead to faster spin-spin relaxation. Depending on the choice of TE (echo time) this may reveal either poor or good contrast between transgenic and wild type tissues. The use of multiple TE sequence enabled reconstruction

of the decay curve and calculation of T2 time (and its reciprocal-R2 relaxivity) for more quantitative comparisons.

In vivo MRI

For *in vivo* imaging, mice were scanned using the same 4.7-Tesla MRI unit. Animals were placed in a custom-built volume coil (5 cm ID, 8 cm long) and anesthetized using 2% isoflurane delivered via a mask throughout the MRI experiments. A set of survey images was obtained using T2 weighted fast spin echo imaging sequence with TR of 5000 ms and TE of 20 ms. This was followed by high resolution images covering the full extent of tumors with T2 weighted fast spin echo sequence with TR of 5000 ms multiple effective TE of 20, 40, 60, 80 ms, matrix 256 x 256. Typically, an FOV of 40 mm x 70 mm, slice thickness 0.5 mm and a gap of 0.15 mm were used. Multi-echo images of slices cutting through the center of tumors across samples were used for calculating T2 and R2 maps using MRI analysis calculator plugin of ImageJ.

Statistical analysis

Data were presented as mean ± SD. Two-tailed t test was used in data analysis with $p<.05$ considered statistically significant (represented as * in figures, ** signifies significance at $p<.01$ level). The assumption of normal distribution was met to allow the use of Student's T test. All experiments have at least three replicates.

2.3 Results

Established cell lines

We used lentiviral vectors to establish clonal transgenic C6 glioma cell lines. Lentiviral vectors helped achieve high levels of stable transgene expression (Cherry et al., 2000; Lois et al., 2002), and selection of clonal lines ensured homogeneity of the cell populations and consistency of results. Standard transduction protocols were followed to infect wild type (WT) C6 cells with vectors that constitutively/inducibly express human FTH as well as vector that constitutively expresses human Tfrc. Clonal cell lines were selected based on co-expressed selection markers.

Specifically, clonal C6 cell lines overexpressing FTH were obtained through lentiviral transduction of WT C6 cells using bicistronic vector pLVU-HA-FTH-IRES-EGFP that co-expresses HA tagged FTH and EGFP. Colonies grown from transduced single cells were manually selected based on homogenous EGFP expression, from which the one with the highest level of transgene expression was chosen for the subsequent studies and named C6-FTH. (Figure II-6) Clonal C6 cell lines overexpressing Tfrc were similarly established with bicistronic vector pLVU-Tfrc-IRES-EGFP transduction and selected based on EGFP expression. The clonal line with highest level of transgene expression was named C6-Tfrc and expanded for subsequent studies. (Figure II-7) Cell lines that inducibly express FTH were established with Tet-On inducible vector pLV-mCMV-HA FTH- Ubi-rtTA-IRES-ZeocinR and selected with zeocin, among them the line with the highest expression in response to doxycycline induction was chosen and named C6-Tet-FTH. C6-Tet-FTH was then transduced with pLVU-Tfrc-IRES-EGFP (vector used in creating C6-Tfrc) to select cell lines that combine overexpression of Tfrc with inducible expression of FTH, the resultant line was named C6-Combined. (Figure II-8)

C6 glioma was not the only cell model explored in MRI reporter gene characterization; other cell lines including 293HEK (human embryonic kidney), U87 (human glioma) and Mda-231 (human breast cancer line) also received varying degrees of experimental attention. *In vitro* characterizations on both C6 glioma and 293HEK lines are reported in this chapter. (Transgenic 293HEK clonal lines followed the same selection protocol and naming convention as used for C6; for example: 293-Tfrc = 293HEK cell line constitutively expresses Tfrc, 293-Tet-FTH = 293HEK cell line inducibly expresses FTH etc.) As it turned out, comparisons between cell models have brought further insights into reporter gene functions. We chose C6 glioma as our cell model for *in vivo* studies as it represents the best combination of some desirable features: It was capable of sustaining high level of transgene expression (advantage over Mda-231), effective for *in vivo* tumor formation (advantage over 293HEK) and had previous confirmation of its compatibility with MRI reporter gene (Cohen et al., 2005) thus removing potential confounds based on cell model choice (advantage over U87).

Iron content

As outlined in the introduction, the iron homeostasis model predicts that unregulated (due to removal of IRE) expression of either transgenic FTH or Tfrc will lead to compensatory net increase in intracellular iron content. Thus measuring changes in intracellular iron content of transgenic cell lines could serve as an indicator of transgene function. Iron content has been measured under two culture conditions: Standard cell culture condition (D/F medium, in 10 cm plate, medium change every 3 days) with serum being the only source of iron, or cell culture with iron supplement in the form of ferric

citrate or holo-transferrin. Changes in iron content in response to external iron supplement were of interest because: 1) iron supply in standard culture medium was often insufficient to allow sensitive detection of changes in iron content; and 2) Tfrc expression, which is directly linked to iron uptake, should respond well to changes in environmental iron supplies.

O-phenanthroline iron determination method was used to measure iron content of cells cultured *in vitro*. O-phenanthroline forms colored complexes with Fe that can be easily visualized and quantified (by comparing its absorbance with pre-generated standards). Our protocol was modified from standard O-phenanthroline methods to incorporate steps that facilitate release of intracellular iron (sonication to disrupt cell membrane and incubation with mercaptoacetic acid). Based on a recent reference on supplemental regime for Tfrc/FTH transgenesis (Deans et al., 2006), iron supplement was first chosen as Ferric citrate (FC 200uM) + 1 mg/ml holo-transferrin (h-Tf) over 3 days in D/F medium.

When iron content comparisons was first made between WT 293 and 293-Tfrc cells with and without iron supplement, it was revealed that Tfrc expression significantly increased cellular iron content. Under standard culture conditions, Fe content was estimated at 30.4 femtogram ($1X10^{-15}$ g) per cell (fg/cell) for 293-Tfrc and 20.8 fg/cell for WT 293 cells, a significant increase of 46.4% (p=0.001). With iron supplement (in the form of FC + h-Tf), Fe content of WT 293 increased to 79.4 fg/cell and that of 293-Tfrc reached 131.3 fg/cell, a difference of 65.3% (P=0.01), suggesting FC + h-Tf supplement was capable of not only increasing cellular iron in general, but also amplified the enhancement of Tfrc expression on Fe content (Figure II-9A).

Capable but not optimal: When the same supplement was applied to C6 cell lines, no difference in Fe content was observed between WT and Tfrc transgenic cell lines (both seemed to reach a high plateau). Further investigation revealed two contributing factors 1) Inherent difference between cell lines, as C6 glioma cells more readily took up environmental iron than 293HEK cells 2) More importantly, the original FC + h-Tf formula was problematic: FC turned out to be a poor supplement choice to study Tfrc function as it indiscriminately increases cellular iron content, while h-Tf alone turned out to be a much more selective supplement choice to probe metalloprotein functions. When the two supplements were separately administrated, the Fe difference between WT 293 (26.6 fg/cell) and 293-Tfrc (57.7 fg/cell) increased to 117% (P=0.003) under h-Tf only treatment. However, under FC supplement, it shrunk to 33.6% from 46.4% before supplement, with Fe content of WT 293 at 77.4 fg/cell and 293-Tfrc at 103.4f g/cell (Figure II-9A; Note that FC was still effective in boosting iron content, but in a much less selective fashion). The difference was even more dramatic in C6 cells (Figure II-9B): without supplement, Fe content was 58.2% higher (p=0.01, C6 WT=15.6 fg/cell, C6-Tfrc=24.7 fg/cell) in C6-Tfrc than WT C6 under standard culture conditions. H-Tf supplement selectively targeted C6-Tfrc cells and increased the difference to 181.8% ($p<0.001$ C6 WT=21.4fg/cell, C6-Tfrc=60.4fg/cell). Such distinctions, however, were completely obliterated using 200 uM FC as a supplement over 3 days (C6 WT=105.3 fg/cell, C6-Tfrc=101.9 fg/cell, -3% difference).

Given greater sensitivity of C6 cells to environmental iron and better selectivity of h-Tf as an iron supplement, further Fe content characterization on C6 cell lines was conducted either under standard culture or with h-Tf (1 mg/ml, 4 days) supplementation.

Fe content comparisons among 4 conditions of interest: WT, FTH expression only, Tfrc expression only, and Tfrc/Combined expression (Figure II-10) revealed that 1) consistent with previous findings, constitutive expression of Tfrc in C6 cells induces significant increase in Fe content under standard culture (86% increase, $p=0.003$; C6 WT=15.2 fg/cell, C6-Tfrc=28.2 fg/cell); which can be further amplified by h-Tf supplement (195% increase, $p<0.001$; C6 WT=20.1 fg/cell, C6-Tfrc=59.5 fg/cell); 2) constitutive expression of FTH in C6 cells induces more moderate but still significant increase in Fe content (49% increase, $p=0.02$; C6 WT=15.2 fg/cell, C6-FTH=22.6f g/cell); which was also amplified by h-Tf supplement (80% increase, $p=0.02$; C6 WT=20.1 fg/cell, C6-Tfrc=36.2f g/cell); 3) Combined Tfrc/FTH expression, after Dox treatment (4 ug/ml 4 days) induced FTH expression on top of Tfrc overexpression, with similar Fe content compared to Tfrc overexpression only without supplements, C6-Tfrc=28.2 fg/cell vs. C6-Combined=28.6 fg/cell); with supplement, combined Tfrc/FTH expression had a positive influence on Fe content over Tfrc only, but did not reach statistical significance (C6-Tfrc=59.5 fg/cell vs. C6-Combined=66.8 fg/cell, $p=0.138$).

To summarize, with proper selection of assay and iron supplements, the impact of metalloprotein transgenes on cellular iron content can be effectively probed. Our observations were consistent with predictions from the iron homeostasis model and expression of both Tfrc and FTH led to increases in cellular iron. Consistent with their proposed functions, Tfrc transgenesis responded more readily to environmental iron and resulted in greater increase in iron content across conditions; in contrast, FTH transgenesis, which is believed to influence iron uptake through indirect compensatory mechanisms, was indeed less responsive to environmental iron and led to more moderate

iron increase. We should point out that comparing to other FTH transgenic cell lines like 293-FTH, C6-Tet-FTH and 293-Tet-FTH which usually show increases between 10-20% without supplement; C6-FTH already manifested the greatest iron increase (49%) *in vitro*. This may partially explain the non-significant iron increase from FTH induction under co-expression (C6-Combined) condition.

Growth rate

Some cautionary notes on cell proliferation: As an exploratory study on transgene function, we used the highest expression clonal cell lines for various characterizations, including growth rate (measured as doubling times). These high expression clonal lines are ideal for most purposes, but could be misleading in interpreting cell viability. If a high expression transgenic line has growth rates similar to WT controls, that is strong evidence (though not complete proof) of the safety of the transgene; however, if the high expression line has a much reduced growth rate, that may be attributable to any of the following: 1) the transgene is toxic, or 2) the transgene itself is not toxic in the conventional sense, but like most transgenes when expressed at very high levels it influences proliferation (and perversely, it is the non-toxicity of the transgene that enables creation of very high expression clonal line in the first place), or 3) the change is independent of transgene function, random insertion of lentiviral transduction has changed the genetic background of the host cells and altered its baseline growth rate (position effect). Not to mention that growth rates are specific to *in vitro* culture conditions, and could be significantly different *in vivo*. In short, a slower proliferating clonal line does not necessarily imply transgene-induced toxicity.

When combined with other manipulations, like response to iron challenge and induced transgene expression, the growth rate outcome can become more informative. In the current experiment, doubling time of four C6 cell lines (C6-WT, C6-FTH, C6-Tfrc and C6-Combined) were quantified under either standard culture condition (D/F medium) or with iron challenge (Chemically Defined Iron Supplement-CDIS from Sigma as h-Tf replacement, with final Fe content at 0.54 ug/ml. Sigma recommend 0.13-0.54 ug/ml for cell culture, we chose a concentration that represents high iron but is still physiologically relevant). Doxycycline treatment at 4 ug/ml over 72 hrs was used to induce FTH expression.

The baseline doubling time of WT C6 control line was estimated at 16.2 hrs which matched previous estimates following similar protocols (Naus et al., 1992). WT C6 with doxycycline induction had essentially the same doubling time (16.5 hrs) suggesting doxycycline itself at 4 ug/ml has little impact on C6 cell proliferation. The doubling time for C6-Tfrc is estimated at 19.6 hrs while that of C6-FTH was calculated at a significantly slower rate of 41.7 hrs. C6-Combined (Tfrc overexpression + induced FTH expression) had a doubling time of 23.3 hrs. When iron challenge was introduced as CDIS (Fe=0.54ug/ml) in D/F medium and growth rate estimated following the same protocol, some interesting observations were made: WT C6 cells slightly slowed their proliferation rate in response to increased iron concentration in the medium, with doubling time increased from 16.2 hrs to 18.9 hrs (17%); C6-Tfrc showed greater reduction in proliferation rate, from a doubling time of 19.6 hrs to 24.3 hrs (24.2%); iron challenge had a reverse effect on C6-FTH, instead of slowing its proliferation, its doubling time actually accelerated from 41.7 hrs to 36.5 hrs (-12.5%). The most dramatic

change in growth rate came from C6-Combined: in response to iron challenge, its doubling time increased from 23.3 hrs to 42.2 hrs (81.5% Figure II-11). Not shown in the figure are doubling times of C6-combined without doxycycline induction, which is functionally equivalent to Tfrc overexpression and it indeed had growth rate closely matched to that of C6-Tfrc: 19.3 hrs (C6-Combined no induction) and 19.6 hrs (C6-Tfrc) respectively without supplement, 25.1 hrs and 24.3 hrs respectively with iron challenge.

Most of these observations on iron challenge were consistent with what was previously known about FTH and Tfrc function. Tfrc expression increases vulnerability to iron challenge presumably due to toxicity associated with high LIP (Meneghini, 1997; Kotamraju et al., 2002; Kruszewski, 2003); while FTH expression at high levels reduces LIP that manifests an iron-deficiency phenotype: reduced growth rate that is partially reversed by iron supplementation (Arosio and Levi, 2002). The real surprise came from C6-Combined line, where expression of FTH on top of Tfrc reduces viability both under standard culture conditions and with iron challenge (despite a theoretical safety advantage of co-expression (Deans et al., 2006).

Another peculiarity was the extent of reduction in growth rate of the FTH overexpressing line C6-FTH (158.3% increase in doubling time compared to WT control). While the behavior of this clone was most consistent with an iron deficiency phenotype (Arosio and Levi, 2002) and not necessarily a sign of toxicity, we would also like to point out this does not automatically translate into a growth slowing effect of FTH transgenesis. Indeed, the difference in growth rate between high FTH expression 293 HEK cells and WT controls was much more moderate (293-FTH, 21.6 hrs vs. WT control 18.2 hrs). More reliable comparisons can be made in FTH-inducible lines (against the same genetic

background), and in both C6-Tet-FTH and 293-Tet-FTH lines, expression of FTH had no negative impact on cell proliferation (Figure II-12). These results suggested that moderate level increases in FTH expression would have no perceivable impact on growth rate. (This finding was also consistent with Cohen et al.'s (Cohen et al., 2005) observation of FTH transgenesis in C6 cells).

To summarize, evidence *in vitro* suggests that both FTH and Tfrc are reasonably safe transgenes on their own. At high expression levels, our observations on FTH were consistent with an iron deficiency phenotype while that of Tfrc transgenic cells hinted at slightly increased vulnerability to iron toxicity. The much reduced viability from co-expression of Tfrc and FTH is perplexing. We suspect this might be related to disruption of iron regulation as in the combined scenario both Tfrc and FTH are unresponsive to regulatory control, but a conclusion on co-expression viability requires further experimentation *in vivo*.

In vitro **MRI**

Having confirmed transgene expression in clonal lines and corresponding changes in iron content, the logical next step is to explore the functions of metalloproteins as MRI reporters. The initial MRI characterizations were performed *in vitro* looking for MRI contrast between transgenic cell pellets and their WT controls. Ferritin-bound iron is an example of compartmentalization of a superparamagentic substance that lead to rapid loss of phase coherence of spins, which decreases transverse relaxation time T2 (T2, measured in milliseconds, is the amount of time needed for transverse magnetization to

decay by 63%). Thus on T2 weighted MR images, samples with shorter T2 time (faster signal decay) would appear darker (hypointense) than controls.

In the earliest stage, pilot *in vitro* MRI studies were performed on different FTH transgenic 293HEK cell lines (293-FTH, and 3 different clones of 293-Tet-FTH). Fast spin echo (FSE) sequence with Repetition Time (TR) of 2 seconds and a single Echo Time (TE) of 72 ms was used to provide a T2 weighted snap shot across conditions. We observed that under standard culture conditions, FTH expression in 293HEK cells was only marginally effective in creating MRI contrast, with signal hypointensity in transgenic lines ranging between 4-15%. Since it was impossible to calculate T2 time from a single TE time, we were unable to make quantitative comparisons to previous reports at this stage.

The imaging protocols have since been updated to incorporate multiple TE times to enable calculation of T2 time. One example with such characterization was performed on WT and Tfrc transgenic 293HEK cells cultured under three different iron supplement conditions for either 3 or 7 days: 1) No iron supplement, 2) 1 mg/ml h-Tf , and 3) 200 uM FC (these are the same treatments used in iron content determination of 293HEK cells). As would be expected from its role in iron uptake, Tfrc expression indeed shortened *in vitro* MRI T2 time (corresponding to increase in R2 relaxation rate, R2=1/T2) in 293-Tfrc cell pellets under certain conditions, namely with longer culture periods (7 days) when no supplement was provided (WT 293 R2=9.6 S^{-1} 293-Tfrc R2=11.4 S^{-1} $p<0.01$), or with FC supplement (WT 293 R2=10.1 S^{-1} 293-Tfrc R2=13.6 S^{-1} $p=0.02$ on day 3, WT 293 R2=12.9 S^{-1} 293-Tfrc R2=16.2 S^{-1} $p<0.01$ on day 7) (Figure II-13). It is interesting to note that while h-Tf was more selectively taken up by cells based on O-phenanthroline

iron absorbance assay, it did not create sufficient MRI contrast in the cell pellet under the current imaging protocol; while 200 uM FC, the less selective but stronger (in the sense of greater increase in total iron content) iron supplement, significantly amplified MRI contrast based on Tfrc expression.

The last phase of the *in vitro* MRI study focused on transgenic C6 cell lines without administration of any iron supplement. The shift to C6 cells, as explained earlier, was due to its tumorigenicity and greater sensitivity to environmental iron, making it an ideal model for further study *in vivo*. The termination of the iron supplement practice was due to our realization (from this and parallel projects with different metalloproteins) that supplement-based artificial amplifications of MRI contrast *in vitro* had little predictive value of transplant behavior *in vivo* and we were interested in whether sufficient MRI contrast can be generated without external supplement (as would be the case *in vivo*). MRI of C6 cell pellets with T2 weighted FSE sequences confirmed that overexpression of both FTH (C6-FTH) and Tfrc (C6-Tfrc) could generate significant changes in R2 transverse relaxation rate on a 4.7 T MRI unit without iron supplementation (Figure II-14). The R2 value of WT C6 cell pellets was estimated at 6.4 s^{-1}, significantly lower than that of C6-FTH (8.0 s^{-1}, p=0.01) and C6-Tfrc (7.1 s^{-1} p=0.05). Inducible expression of FTH alone (Dox 4ug/ml, 3 days) had a positive but not statistically significant influence on relaxation rate (C6-Tet-FTH R2= 6.7 s^{-1} p=0.18); similarly, inducible expression of FTH on top of Tfrc overexpression had a positive but not statistically significant impact on R2 (R2 of C6-Combined=7.6 s^{-1} compared to 7.1 s^{-1} of C6-Tfrc, p=0.19). Note that increase in FTH expression and corresponding iron content changes were much more pronounced in C6-FTH than other FTH transgenic lines, which may explain the varied

effectiveness between C6-FTH and its inducible counterparts (C6-Tet-FTH) in generating MRI contrast.

Positive outcomes from *in vitro* MRI characterization provided additional support for function of both metalloprotein transgenes and warranted further experimentation *in vivo*. However, we should emphasize positive results from *in vitro* MRI are neither necessary nor sufficient to qualify transgenes as MRI reporters (in the sense that they can function effectively *in vivo* for monitoring purposes). Over-reliance on *in vitro* MRI confirmation could (and indeed has) led to both Type I (false positive) and Type II (false negative) errors; this issue will be covered in detail in the discussion.

In vivo MRI

The final verdict on whether metalloprotein transgenes qualify as MRI reporters could only come from *in vivo* MRI characterizations. Characterizations on gene expression, iron content and *in vivo* MRI have shown promise for both Tfrc and FTH as reporter genes, so in the final *in vivo* study all four conditions: (1) wild type, (2) Tfrc overexpression, (3) FTH overexpression, and (4) Combined expression (Tfrc overexpression + Inducible FTH expression) were incorporated. The experiment followed a between subject design with 3 CD-1 nude mice assigned to each condition. C6 cells were inoculated subcutaneously adjacent to mammary pads (3 million cells were inoculated at each site). Tumor growth was monitored daily and MRI scans were first performed when tumor size reached 6-10 mm in diameter with T2 weighted FSE sequence (with TR/TE 5s/20, 40, 60, 80 ms), with repeat scans performed 7 days later on the same set of tumors following the same imaging protocols. Under the C6-Combined

condition, the transplants remained Dox free before the first scan. Induction of FTH expression (using 0.5 mg doxycycline/ml in 30% sucrose) was initiated immediately upon completion of the first scan and continued for 7 days until repeat scans were performed.

In vivo proliferation rate of C6 glioma cells had significant impact on the experimental design. Normally for such *in vivo* MRI experiments a within-subject design would be preferred to reduce individual variations and allow pair-wise comparisons of transplants within the same image. However, in the current study there were significant variations in proliferation rate of different clonal lines. As we have observed in pilot studies, such variations quickly translated into dramatic difference in tumor size within a short period of 2-3 weeks. Within the same animal, significant difference in tumor size makes proper imaging and data interpretation extremely difficult: Small tumors from slowly proliferating cells were difficult to localize and more susceptible to imaging artifacts. And before the slow proliferating transplants could reach proper size for imaging, the fast proliferating ones started to show signs of necrosis (noted often once the tumor grew beyond 15 mm in diameter), which could significantly alter tissue relaxivity. Due to these concerns, we adopted the current between-subject design with each mouse receiving only one type of transplant and imaging performed only when tumor diameter reached a pre-determined 6-10 mm range.

Based on our observations of the *in vivo* transplant growth, the following relationship held true for proliferation rate of transplants of different origins: C6 WT> C6-FTH > C6 Tfrc> C6 combined. The *in vivo* doubling time (based on tumor volume) estimated for WT transplants was 46.2 hrs, followed by 60.5 hrs of C6-FTH and 71.2 hrs

of C6-Tfrc. Without induction C6-Combined was functionally equivalent to C6-Tfrc and had a similar doubling time of 74.0 hrs. With 0.5mg/ml Dox induction its proliferation slowed to a doubling time of 101.8 hrs; at higher Dox dosage of 2mg/ml, the induction was clearly toxic to C6-Combined transplant and lysed the tumor (Figure II-15).

There are two points of interest here: First, the relative growth rate between C6-FTH and C6-Tfrc was reversed *in vivo.* (*In vitro* the relationship was C6 WT> C6-Tfrc > C6 FTH> C6 combined). As hypothesized earlier, the reduction of *in vitro* growth of C6-FTH was not necessarily a sign of toxicity, but more likely attributable to an iron deficiency phenotype and could be reversed with better access to iron supply. While long term Tfrc expression might introduce greater risks by making the cells more vulnerable to iron mediated ROS damage. The current *in vivo* observations are in line with these positions, though firmer conclusions can only be made when additional LIP and ROS assays were performed to elucidate the underlying mechanisms (not incorporated in the current experimental design).

Second, the unexpected toxicity from combined FTH/Tfrc expression, first observed *in vitro*, was further confirmed in our *in vivo* characterizations. We are confident that the toxicity was the consequence of co-expression because 1) in our pilot studies, 2 mg/ml Dox treatment lysed C6-Combined tumor without reducing growth of C6-Tfrc transplants within the same animal, 2) the toxicity was observed in different C6-combined lines that had distinct genetic backgrounds, and 3) neither FTH or Tfrc when expressed alone were toxic to host cells. Taken together, the toxicity observed in co-expression was not attributable to Dox, variation in genetic background, individual animals, or the effects of single transgenes. The most likely explanation we espouse at

this stage is that the toxicity was related to the disruption of iron homeostasis when both FTH and Tfrc have been rendered unregulatable and expressed at arbitrary ratios dictated by the expression vectors instead of intracellular conditions.

Similar to the *in vitro* study, the MRI contrasts of transplants across conditions were reported here as T2 maps and their corresponding R2 relaxation rates calculated from multiple TE times. The average T2 for WT C6 tumors was estimated at 75.2 ms ($R2=13.3\ s^{-1}$). Against this reference, both FTH and Tfrc overexpression were found to significantly reduce T2 time (increase R2) in C6-FTH (T2=55.9ms, $R2=17.9\ s^{-1}$ p=0.003) and C6-Tfrc (T2=59.1ms, $R2=16.9\ s^{-1}$ p=0.02) transplants, respectively. There was no statistically significant difference between the R2 relaxation rate of C6-FTH and C6-Tfrc (p=0.42). This finding was more consistent with *in vitro* cell pellet MRI without iron supplement (where both FTH and Tfrc induced moderate MRI contrast) than *in vitro* MRI with iron supplement (where Tfrc had clear advantages over FTH due to greater iron uptake capacities). This further cautions against inferring *in vivo* transgene function based on results from heavy *in vitro* supplement alone, which may lead to false positive results. (Figure II-16)

We should point out that under these three conditions, only imaging data from the first MRI session were used towards quantification of MRI contrast: the very fast *in vivo* proliferation has resulted in overgrowth and necrosis in WT C6, C6-FTH and C6-Tfrc transplants during the second scan session and those images were used only for quantification of tumor size.

Under high Dox induction (2 mg/ml), C6-Combined transplants suffered from clear toxicity, transplants were lysed and their MRI relaxivity cannot be assessed. At

lower dose induction (0.5 mg/ml), they continued to proliferate albeit at a significantly reduced rate. For aggressively growing C6 transplants this actually has the unintended benefit of allowing repeat scans without the concerns of necrosis or tumor overgrowth, and enabled comparisons between Tet-On and Tet-off conditions within the same animals with repeat scans. Without Dox induction, C6-Combined was functionally equivalent to a Tfrc overexpression line and behaved similarly *in vivo*, with a T2 of 61.8 ms (R2=16.2 s^{-1}); which approximates the R2 (16.9 s^{-1}) of C6-Tfrc and significantly higher than that of WT controls (R2=13.3 s^{-1}). Upon Dox induction for 1 week, we observed slight but not statistically significant increase in R2 relaxation rate from additional induced FTH expression (R2=17.1 s^{-1} p=0.60). We concluded that FTH/Tfrc co-expression was not more effective in producing MRI contrast than individual genes under the current experimental design. We cannot rule out the possibility that higher expression level and/or longer induction period could lead to more significant changes, however, given the toxicity from co-expression and its limited MRI contrast benefit, co-expression cannot be recommended as a practical approach for signal enhancement purposes (Figure II-17).

To summarize, findings with *in vivo* MRI suggested that both constitutive expression of Tfrc and FTH transgenes significantly altered R2 relaxation rate and each transgene could serve as an MRI reporter in a tumor transplant model in CD-1 nude mice. Co-expression of Tfrc and FTH, in the form of week-long induced expression of FTH against the background of Tfrc overexpression, significantly slowed down cell proliferation and generated a similar level of MRI contrast as obtained from Tfrc expression alone, with no convincing evidence of cumulative increase of R2.

Post mortem analysis

Immediately upon completion of MRI sessions, animals were euthanized and tumors recovered for post mortem analysis. The tumor analysis was of particular interest 1) to confirm and quantify the level of transgene expression *in vivo*, and 2) to quantify the iron content of transplanted tumors.

Western blots were performed on tumor samples with antibody against HA tag (specific for HA tagged human FTH, does not interact with endogenous rodent ferritin) and antibody against transferrin receptor (recognizes both human and rodent transferrin receptor). It confirmed HA-FTH expression in both C6-Combined and C6-FTH tumors, and absence of transgenic FTH in WT control and C6-Tfrc transplants (Figure II-18A). The confirmation of induced FTH expression in C6-Combined eliminated the possible confound of negative FTH expression, and further strengthened the link between co-expression and observed toxicity. It should be noted that in the strongest constitutive expression line C6-FTH, the level of FTH transgene expression was significantly higher than that achieved with 0.5 mg/ml Dox induction *in vivo* (152.2% difference estimated by densitometry); this leaves open the possibility of higher expression level and/or longer induction period of FTH transgene to actually produce cumulative increase of R2 in C6-Combined. However, as previously mentioned this option lacks practicality due to toxicity concerns. Taking the FTH protein quantification into account, it seems likely in retrospect that the variations in FTH expression level was at least partially responsible for some *in vitro* differences observed between C6-FTH (higher iron content, slower proliferation rate, stronger MRI contrast) and its inducible counterpart C6-Tet-FTH.

Significantly elevated Tfrc expressions have been confirmed in both tissues of C6-Tfrc and C6-Combined origin, which were estimated at 271.6% and 213.4% respectively of baseline Tfrc level in WT, suggesting the transgenesis was effective. (Note that C6-Tfrc and C6-Combined were of different genetic background, the lower Tfrc level in C6-Combined simply reflects difference between clonal lines and is not the result of induced FTH expression) (Figure II-18A). Tfrc expression level in C6-FTH was equivalent to that of WT C6 tumors, which was somewhat unexpected. The iron homeostasis model predicted endogenous Tfrc upregulation in response to FTH transgene expression, and our *in vitro* characterization of Tfrc levels indeed pointed to significant Tfrc upregulation in C6-FTH based both on protein densitometry and pair-wise comparison of ICC (Figure II-18B). Thus, the un-elevated level of Tfrc 3 weeks post transplant was most likely the consequence of termination of Tfrc upregulation *in vivo*. (One important difference between Tfrc and FTH transgenesis is that the Tfrc level under FTH transgenesis will still be under effective regulatory control through the LIP-IRP-IRE system.) In a scenario most consistent with our observation, FTH expression will initially induce reduction of LIP and compensatory upregulation in Tfrc (as observed in cell culture); over time, the increased iron uptake increases iron stores and replenishes LIP, which should in turn reduce the compensatory increase in Tfrc expression towards its original states (as seen in tumor explants). If this was indeed the case, we would expect an increase in total iron content in C6-FTH tumor samples despite matching Tfrc levels with controls, because earlier upregulation in Tfrc and subsequent iron increase would be a prerequisite to bring LIP and Tfrc back to pre-transduction levels, and iron

accumulation during this earlier period should be detectable with sensitive iron content assays.

ICP-OES was performed on tumor samples to measure iron content quantified as Fe parts per million (ppm) normalized to tissue dry weight. In Tfrc overexpression lines, significant increases in iron content over WT controls were observed. The estimate was 122.4 ppm for WT controls, 222.5 ppm for C6-Tfrc samples (81.7% increase $p<0.01$) and 192.3 ppm for C6-Combined samples (57.1% increase $p=0.01$). The higher iron content in C6-Tfrc samples was consistent with greater Tfrc expression levels. To a lesser extent, FTH overexpression in C6-FTH also increased iron content (174.7 ppm, 42.7% increase, due to large variation in individual samples, the difference did not reach statistical significance $p=0.16$) (Figure II-19).

These findings have several implications: 1) iron content data corroborated with *in vivo* MRI and provided further support for both FTH and Tfrc function as MRI reporters. 2) C6-FTH samples showed moderate increase in iron content despite WT-like Tfrc levels, consistent with the hypothetical scenario that earlier episodes of Tfrc upregulation had restored iron balance in the C6-FTH transplants, which led to its subsequent down-regulation towards baseline levels. And 3) C6-FTH transplants achieved comparable MRI contrast with C6-Tfrc/C6-Combined transplants despite much less pronounced iron increase, suggesting that, in the case of ferritin transgenesis, total iron content may not be the sole determinant of MRI contrast. This is consistent with earlier observations about ferritin with higher relaxivity per iron content, when the iron loading factor of ferritin protein is low (Vymazal et al., 1996; Vymazal et al., 1998).

2.4 Discussion

Studying FTH and Tfrc transgenes in C6 and other cell lines has not only shed light on the functions of metalloprotein reporters, but also brought important insights into the strength and limitations of various experimental procedures. Accordingly, our discussion in this chapter will be divided into two major sections. The first part of the discussion will be dedicated to methodological/technical considerations; and reflections on how our practices on establishing cell lines, using iron supplements in *in vitro* characterizations and the design of MRI experiment might influence experimental outcomes, to help clarify possible confusion and improve on subsequent experiments on ESCs. The second part of the discussion will focus on the theoretical relevance of our findings to the field of molecular MRI reporting and, on a more practical level, which candidate gene should be chosen for introduction into ESCs.

Methodological/Technical Considerations

Construct design, clonal line selection and cell viability

Two considerations have been given priority in our construct design: achieving high level of transgene expression and maintaining stable gene expression across cell divisions. Insufficiency or variation in expression level could confound interpretations of effectiveness of transgenes and undermine the main aim of the current experiment: to identify the appropriate reporter gene for introduction into ES cells.

FUGW, a lentiviral backbone with a proven record of achieving high-level, stable transgene expression, was chosen for the current study (Lois et al., 2002; Yang et al., 2008). In addition, Iron Response Element (IRE), located at 5' end of FTH cDNA and 3'

of Tfrc cDNA, was removed by PCR during the construction process to ensure transgene expression not influenced by endogenous regulation through IRP. Based on experimental findings, this construct design has proven effective.

The same principles were followed when selecting clonal cell lines, transgene expression levels were given priority and the candidate lines chosen for further experimentation were usually the ones with highest expression. This practice had its pros and cons: Given the many uncertainties with transgene function and lack of established protocols, it is a clear advantage to eliminate possible confounds related to expression level in the earliest phase of the experiment. The disadvantage was this selection criterion might also introduce peculiarities into cell viability data that are confusing. Consider that lentiviral vectors randomly insert the transgene into the host genome, and may induce changes in cell viability independent of the function of the transgene. This, coupled with the selection criterion of "clone with highest expression", could possibly lead to confusing observations like the instance where FTH expression in a certain clonal line (C6-FTH) exerts the most significant growth slowing effect, while having no perceivable impact on cell proliferation in most other clonal FTH lines (both overexpression and inducible).

From the perspective of appropriate experimental design, the "high expression" approach was effective for the purpose of confirming reporter gene function. At the current stage variations in proliferation rate was less of a concern than reporter function, thus we consider lentiviral-based transgenesis a fitting choice. However, the situation would be very different when the study moved into the territory of cell replacement therapy. In the case of transgenic ESCs, cell lines with impaired viability would defeat

the purpose of combining reporter gene with cell replacement therapy in the first place. Given this concern, we plan to modify the selection criterion for transgenic ESCs (to be covered in chapter III), instead of aiming outright for the highest expression line, only cell lines that retained normal proliferation rate and morphology will be selected for further characterization.

Iron supplement and in vitro characterization

Iron supplements have been used on several occasions during the study, and the purposes were mainly threefold: (1) Probe for Tfrc function, (2) Iron challenge, and (3) MRI contrast amplifier. This practice had considerable impact on the experimental outcome and warrants some discussion here.

Probe for Tfrc function: Both Tfrc and FTH transgenesis are expected to increase iron uptake (directly in the case of Tfrc transgenesis and through compensatory upregulation in the case of FTH transgenesis). The logic goes as follows: An iron content assay coupled with iron supplement could serve as a convenient probe for transgene function.

This approach has proven effective, though from experience we have also identified a few potential pitfalls that may lead to erroneous conclusions. The first is the choice of type and dose of iron supplements and their interaction with different cell models. FAC and FC, while commonly used as supplements in culture, turned out to be a risky choice for studying C6 glioma lines. When administrated in high doses, they are capable of entering the cell through mechanisms not mediated by the Tf-Tfrc complex (Sturrock et al., 1990; Inman and Wessling-Resnick, 1993; Baker et al., 1998) and if the

cell model in question (C6 as a clear example) is susceptible to alternative routes of iron uptake, the outcome would be of little predictive value of Tfrc expression. Had we not experimented with h-Tf supplement in parallel, we would have come to the wrong conclusion that Tfrc transgenesis was not functional in C6 cells. It should also be pointed out that there are commercial solutions available that offer more sensitive and reliable measures of Tfrc function, typically in the form of engineered holo-transferrin tagged with radioactive or fluorescent labels (Arosio and Levi, 2002; Kotamraju et al., 2002; Deans et al., 2006). For researchers who have access, these could serve as effective probes of metalloprotein function without the aforementioned complications. Another potential confound was the mode of FTH function. Unlike direct Tfrc transgenesis which affects iron uptake strongly and immediately, FTH induced Tfrc increase is more modest and takes longer, exemplified by the moderate Fe increase with FTH overexpression as in C6-FTH, and no significant Fe change with FTH inducible expression. Given these considerations, one needs to be cautious about relying solely on a total iron content assay to confirm FTH function (to avoid the false negatives).

Iron challenge: Iron can also be supplemented in culture to elicit changes in cell proliferation and ROS damage. In our experiment, the observation that Tfrc transgenesis exacerbates the growth slowing effect of iron challenge, while certain FTH transgenic cell line (high expression) increased its proliferation under the same treatment, is consistent with the proposed functions of Tfrc and FTH in influencing LIP (with subsequent vulnerability to or possible protection against ROS damage) (Meneghini, 1997; Arosio and Levi, 2002; Kotamraju et al., 2002; Kruszewski, 2003). While our observations were consistent with the predictions from the prospect of iron homeostasis,

we wish to stress that our experimental efforts were only rudimentary in this aspect. Firmer links between LIP, ROS and metalloprotein transgenesis would require selective measurements of LIP (as opposed to total iron) and additional measurements of ROS. Considering the links between metalloprotein function and LIP are well established, and that the current study focuses instead on their potential role as MRI reporters, the additional measurements of LIP and ROS were not incorporated into the current experimental design. Both are interesting topics that warrants further studies.

MRI contrast amplifier: Under standard culture conditions with limited iron supply, the magnitude of absolute iron change from transgene expression is often quite small and poses challenges for MRI detection. Providing iron supplement could drastically amplify the change in iron content and enhance *in vitro* MRI contrast.

The practice of providing iron supplement for *in vitro* MRI has been adopted in most of the studies on metalloprotein MRI reporters to date with considerable benefit (Moore et al., 1998; Genove et al., 2005; Deans et al., 2006). However, from our experience we would also caution against over-interpreting data obtained with the help of iron supplement. The key point is that most iron supplement regimens bear no resemblance to the endogenous iron supply *in vivo* (In the majority of reports, the Fe dose from supplement was unphysiologically high); subsequently while positive *in vitro* results dependent upon supplement can confirm transgene function, it has limited predicative value of the usefulness of transgene as a reporter *in vivo* (especially when it has to rely solely upon much more limited endogenous iron supply in the form of circulating h-Tf). We found this out the hard way in a separate project where an artificial transgene showed great promise as a MRI reporter *in vitro* (with supplements), only to

turn out ineffective *in vivo* after devotion of considerable experimental efforts. Similar observation was reported in Deans et. al.(Deans et al., 2006) where positive results *in vitro* (with heavy iron supplement) turned out negative in transplant studies. A cautionary note on the risk of false positives associated with iron supplementation should be in place.

MRI

In discussing the application of iron supplements, we have cautioned against false positive from over-interpreting data based on iron supplement. This, however, does not necessarily translate into better predictability when supplements are removed. Just as there as scenarios of positive outcome *in vitro* turned negative *in vivo*; there are also instances where transgene produces insufficient MRI contrast *in vitro* (without supplement), but functioned effectively as reporter gene *in vivo*. This was the case with Genove et al.'s (Genove et al., 2005) study on a ferritin reporter, and has also been observed in our own studies on C6-Tfrc, in which R2 enhancement increased from 11% *in vitro* (barely significant) to 27% *in vivo*. (At the risk of getting ahead of ourselves, the same situation applied to ferritin transgenic ESCs as well, to be covered in Chapter III).

To understand these phenomena, it is important to note that in the case of metalloprotein reporters, MRI does not directly measure the transgenic protein product (this is different from the case of optic image of EGFP), but has to indirectly monitor transgene expression through induced changes in iron content/storage. Both accumulation of iron and redistribution of it in ferritin storage took considerable time (weeks or more) to have maximum impact on MRI contrast, and this could translate into a detection advantage of *in vivo* MRI of transplants over *in vitro* cell pellet studies especially when

conducted without iron supplement. Taken together, our findings caution that the outcomes of cell pellet MRI are not always consistent with *in vivo* MRI when cells from the same clonal line are subsequently used for transplant; the influence of multiple factors including iron access and time course of iron homeostasis should be taken into account to avoid both false positive and false negative interpretations.

In conducting MRI, our study focused on using T2 weighted sequences on high field strength MRI unit to probe metalloprotein functions. These choices are justified given (1) Increased iron content induced a much stronger decrease in T2 relaxation time than in T1 relaxation time, especially at low iron concentrations (Vymazal et al., 1996; Wood et al., 2004; Cohen et al., 2005), thus T2 weighted sequences are more sensitive than T1 weighted sequences in detecting transgene-induced changes in iron homeostasis; and (2) In both Tfrc and FTH transgenic cells, we will be measuring intracellular iron storage in the form of ferritin. Ferritin iron shows magnetic field-dependent R2 increases (Vymazal et al., 1992), thus the detection of transgene-induced MRI contrast will become easier as the MRI scanner goes up in field strength. Tellingly, while 4.7 T used in the current study is generally considered high strength (reserved mostly for research applications), so far it is also the lowest field strength on which ferritin transgene has been successfully applied as a MRI reporter *in vivo* (Cohen et al., 2005; Genove et al., 2005; Cohen et al., 2007).

It is worth pointing out that T2 weighted image based on spin echo sequence in the current study is actually not the most sensitive approach to detect ferritin-induced MRI contrast. In theory, T2* weighted image (using gradient echo sequences) would be more sensitive to metalloprotein based reporters because it reflects the combined effect of

three sources that lead to loss of phase coherence: spin-spin energy transfer, inhomogeneity of the magnetic field, and inhomogeneity of tissue samples (difference in magnetic susceptibility between adjacent tissues). In contrast, T2 weighted sequence only reflects loss of coherence due to spin-spin energy transfer. Metalloprotein reporters are expected to change the magnetic susceptibility of host cells, and the resulting difference in susceptibility between transplants and their environment can be more effectively exploited by T2* weighted sequences.

The situation was more complicated in practice, as T2* weighting can be both an additional source of contrast and an additional source of noise. Inhomogeneity of the magnetic field is especially problematic on high field strength scanners (like the 4.7 T in this study), and the transplants also suffered from undesirable local fluctuations (between transplants and skin, air, muscle etc.) in magnetic susceptibility. Both could significantly reduce the quality of T2* images. We collected some data with T2* weighting during our pilot studies and found they were too noisy to be of much value. However, it should be emphasized that with improved hardware, and/or when the transplant was placed in a more homogenous local environment (brain tissue is ideal for this purpose), T2* weighted sequence could be a powerful tool to improve the detection sensitivity of metalloprotein-based MRI contrast.

Finally, in the current study MRI was essentially used to probe changes in iron homeostasis. While it has great advantage in being non-invasive, its sensitivity and reliability in measuring iron changes are not comparable to more specialized *in vitro* Fe assays. MR contrast alone does not constitute sufficient proof of transgene function, nor does it reveal whether the contrast was mediated through change in iron homeostasis. We

thus consider post-mortem iron assays (like ICP-OES) on tumor explant samples, along with confirmation of *in vivo* transgene protein expression, as indispensable components of experimental design to establish a more convincing link between transgene expression and their function as MRI reporters.

Theoretical Considerations

Our studies on Tfrc and FTH transgenesis in common cell lines, first and foremost, provided support for the iron homeostasis model of metalloprotein MRI reporters. As predicted, expression of FTH, free from endogenous regulatory influences (removal of 5' IRE sequences), did lead to compensatory up-regulation of Tfrc and changes in intracellular iron content. Similarly, expression of Tfrc transgene free of IRE directly translated into increased levels of Tfrc protein and greatly enhanced iron uptake both *in vitro* and *in vivo*. And both Tfrc and FTH transgenesis led to sufficient changes in iron homeostasis detectable with *in vivo* MRI.

Since this study represented the first parallel comparisons between Tfrc, FTH and their co-expression, it provided an opportunity to experimentally determine the best candidate among them for applications as a reporter gene. And in the process we also came across unexpected findings that pointed to prior misconceptions. The followings are summaries of each candidate:

Tfrc as MRI reporter

In vivo MRI on Tfrc transgenic C6 transplants (both C6-Tfrc and C6-Combined without induction) indicated that expression of Tfrc led to significant MRI contrast

(increase in R2 relaxation rate). The changes in relaxivity were corroborated by post-mortem analysis showing significant increase in iron content of transplants that overexpressed Tfrc. Our findings suggested that Tfrc could function as an MRI reporter without external supplement of contrast agent.

As noted in the introduction, the efficacy of Tfrc as an MRI reporter (without contrast agents) is a controversial matter. First proposed by Koretsky et al. and demonstrated in mouse fibroblast transplants (Koretsky et al., 1996); Tfrc was initially thought of a natural candidate for MRI reporter for its role in iron uptake. However, subsequent characterization from Weissleder's group in 9L carcinoma cells concluded that, without supplement of contrast agent, Tfrc expression alone could not produce sufficient MRI contrast either *in vitro* (Moore et al., 1998) or *in vivo* (Weissleder et al., 2000). Instead, they sought to utilize transferrin coupled with monocrystalline iron oxide nanoparticles (Tf-MION) to probe expression of engineered Tfrc, and were successful with that approach. (Weissleder et al., 2000) (Note in this case, Tfrc-mediated MRI contrast is no longer based on iron homeostasis, but on a receptor-ligand delivery of contrast agent). These early efforts doubtlessly inspired subsequent studies and demonstrations of ferritin as an MRI reporter, which did not rely upon administration of external contrast agents *in vivo* (Cohen et al., 2005; Genove et al., 2005; Cohen et al., 2007), and led to the prevailing view that ferritin makes a more effective reporter gene than Tfrc (Cohen et al., 2005; Gilad et al., 2007a).

Our findings suggest a somewhat different scenario: Tfrc, like FTH, was capable of producing MRI contrast without supplement both *in vitro* and *in vivo*, and the MRI contrast from the two reporter genes was comparable. We are confident about this

position because (1) The earlier concept of "ferritin advantage over Tfrc" was not based on solid empirical support from parallel comparisons, but inferred from studies with critical differences in experimental settings, notably field strength of MRI (negative Tfrc was from 1.5 T, while positive ferritin was from 4.7 T and up). Given the field-strength dependency of R2 and the fact that Weissleder et al. (Weissleder et al., 2000) did confirm iron content increase in Tfrc transgenic tumors, the outcome of Tfrc transgenesis could have been different following a different experimental design. In our studies experiments on Tfrc and FTH transgenic cell lines were conducted with matching conditions along each step and offered a more rigorous basis for comparison. (2) The "comparable" observation also makes more logical sense when one considers that ferritin and Tfrc transgenesis essentially tapped the same mechanism of iron homeostasis for MRI contrast, and expression of either one will inevitably lead to compensatory change in the other. So it is our conclusion that Tfrc was capable of reporter gene function in an *in vivo* tumor transplant model independent of contrast agent supplement, and its effectiveness was comparable to that of FTH transgene at least under experimental conditions employed in the current study.

FTH as MRI reporter

Findings on C6-FTH transplants suggested that expression of FTH led to significant MRI contrast (increase in R2 relaxation rate). This was consistent with recent publications (Cohen et al., 2005; Genove et al., 2005; Cohen et al., 2007) and added further support to FTH as a molecular MRI reporter. Our *in vivo* experimental design was closely modeled after the first successful study on FTH (Cohen et al., 2005), matching its

choice of cell model (C6 glioma line), animal model (CD-1 nude mice), MRI hardware (4.7 T) and imaging sequence (multi-echo T2). This practice was aimed at minimizing possible confounds. The results from the two studies were closely matched except for our experiments recorded a more significant increase in R2 accompanied with a moderate reduction in transplant growth rate, both likely outcomes of variation in transgene expression levels.

As previously discussed, the relative effectiveness of Tfrc and FTH as MRI reporters was of considerable interest; and as far as observations with transgenic C6 glioma lines go, changes in R2 from the two transgenes were about the same. From a theoretical perspective, the matching contrast could be a matter of coincidence as the relative "effectiveness" would be dependent upon factors like levels of transgene expression, and to compare Tfrc expression with FTH expression is like comparing apples to oranges. From a practical perspective, however, it does serve a useful guidance suggesting that, when incorporated into the same vector and targeted to the same cells, with matching transduction, selection, transplantation and visualization protocols, FTH was on par with Tfrc in the best MRI contrast they can achieve.

The observation that, comparing to Tfrc, FTH was able to achieve similar MRI contrast with less iron accumulation was also of interest. Prior *in vitro* characterization of ferritin suggested that while ferritin relaxivity per iron was constant when iron loading factor was high, significantly higher relaxivity per iron was observed at low iron loading factor. (I underlined per iron to avoid confusion because relaxivity is still higher in the high iron condition. The real implication is when the same amount of iron is distributed in greater amounts of ferritin, the resultant relaxivity would be higher than if the same

amount of iron is distributed in less ferritin proteins) (Vymazal et al., 1996; Vymazal et al., 1998). This has important relevance to application of ferritin as an MRI reporter because introduction of ferritin as a transgene is expected to significantly reduce the iron loading factor of intracellular ferritin, as in Cohen's proposition (Cohen et al., 2005) that "changes in the expression of apoferritin and redistribution of iron could alter MR contrast even in the absence of changes in total iron content". In actual transplant studies ferritin transgenesis would simultaneously induce increased iron uptake and redistribution of iron into more ferritin proteins *in vivo*, and the impacts of these two mechanisms on relaxivity would be hard to separate. Still, the loading factor model offers the most logically consistent explanation for the observation that FTH transgenesis achieved comparable MRI contrast with less iron increase.

Also consistent with reduced iron increase through FTH transgenesis was the observation that FTH-induced Tfrc upregulation was prominent in culture but reverted to baseline level after weeks of proliferation *in vivo*. This was indicative of rebalancing of iron homeostasis and suggested effective endogenous regulatory control over Tfrc was still in place (with FTH transgenesis) to promptly modulate iron uptake; potentially this would also grant FTH transgene a safety advantage over its Tfrc counterpart because in the event of Tfrc transgenesis, iron uptake would be mostly un-regulatable and pose greater risk of excessive LIP mediated toxicity.

Combinatory reporter

The results from Tfrc/FTH combination were most unexpected. As detailed in the introduction, the original proposition from Deans (Deans et al., 2006) suggested co-

expression could be advantageous over single transgene approaches, "such as the ability to decrease cellular toxicity while achieving effective cellular contrast." The Deans study fell short of providing empirical support for the claim of comparative advantage. When we were finally able to test the hypothesis experimentally, co-expression appeared to be not particularly effective in further enhancing MRI contrast, and definitely not beneficial to cell viability.

In terms of MRI contrast, Tfrc/FTH combination did not reliably generate superior MRI contrast over Tfrc-only condition (both *in vitro* and *in vivo*, induced expression of FTH on top of Tfrc overexpression produced slight increases in R2 that did not reach statistical significance). The apparent lack of enhancement from additional FTH expression is open to different interpretations; we tend to believe the slight positive trend from co-expression was real, just not of sufficient efficacy to be of practical significance. And we will not rule of the possibility that further increase in the level and duration of transgene expression (especially of FTH) could make the contrast enhancement from co-expression more significant; however, in light of potential toxicity (discussed below), this option would not be particularly worthwhile to pursue in stem cell research.

The reduced viability from Tfrc/FTH came as a surprise, not the least because reduction of toxicity was originally cited as the major advantage of co-expression approach, and it made intuitive sense for additional FTH expression to be protective. Having ruled out possible confounds and confirmed that toxicity was indeed linked to co-expression, the key to understand this unexpected phenomenon can be traced back to a flaw in the logic of Deans' original proposition (Deans et al., 2006). They argued that single gene-induced fluctuation in LIP and subsequent compensatory changes were

stressful to the cells, and instead of letting the transgene perturb the LIP and induce the compensatory up-regulation to restore iron balance, co-expressing both Tfrc and FTH would maintain the balance in the first place, which was supposed to be beneficial to cell viability. The problem is, by expressing IRE-free Tfrc and FTH together, a co-expression approach will effectively deprive the host of its endogenous capacity to regulate LIP through the IRP system. And the new "balance" will be dictated by the relative expression efficiency of viral vectors carrying the two transgenes, not necessarily at optimal levels for cell viability (a possibility that Deans and colleagues recognized but downplayed in the original proposition). It turned out that the new un-regulatable balance was a lot more toxic to the host than expected. Without delving into philosophical discourse on the virtue and vice of regulation, suffice to say in this case it is best for the transgenic cells to maintain at least partial control over its iron balance.

Choice for ES cells

When it finally comes to choose an MRI reporter gene for ESCs, the Tfrc/FTH combination was first ruled out due to its clear risk of toxicity. Between Tfrc and FTH, both were relatively safe transgenes and were similarly effective in inducing R2 relaxivity changes. However, there are subtle but important differences between Tfrc and FTH reporters to make one more suited to certain applications than the other. Focusing on iron uptake, Tfrc-induced intracellular iron uptake is more immediate and of greater magnitude. And as a receptor protein, Tfrc can be probed with external administration of Tf-bound contrast agent. These are desirable features if one wishes to make more prompt observation of transgene-induced changes.

Transgenic FTH, on the other hand, was able to achieve comparable MRI contrast with less iron accumulation, and iron uptake through Tfrc remains regulatable with FTH transgenesis. On top of these, ferritin has a well established role in protection against ROS damage by buffering against excessive LIP (Arosio and Levi, 2002). Together, these translate into potential safety advantages of FTH over Tfrc. Since safety would be the top priority in applications of cell-based therapies, with comparable efficacy to Tfrc, we conclude that FTH makes the best candidate MRI reporter for introduction into ESCs.

Figure II-1. Transferrin Receptor and Ferritin

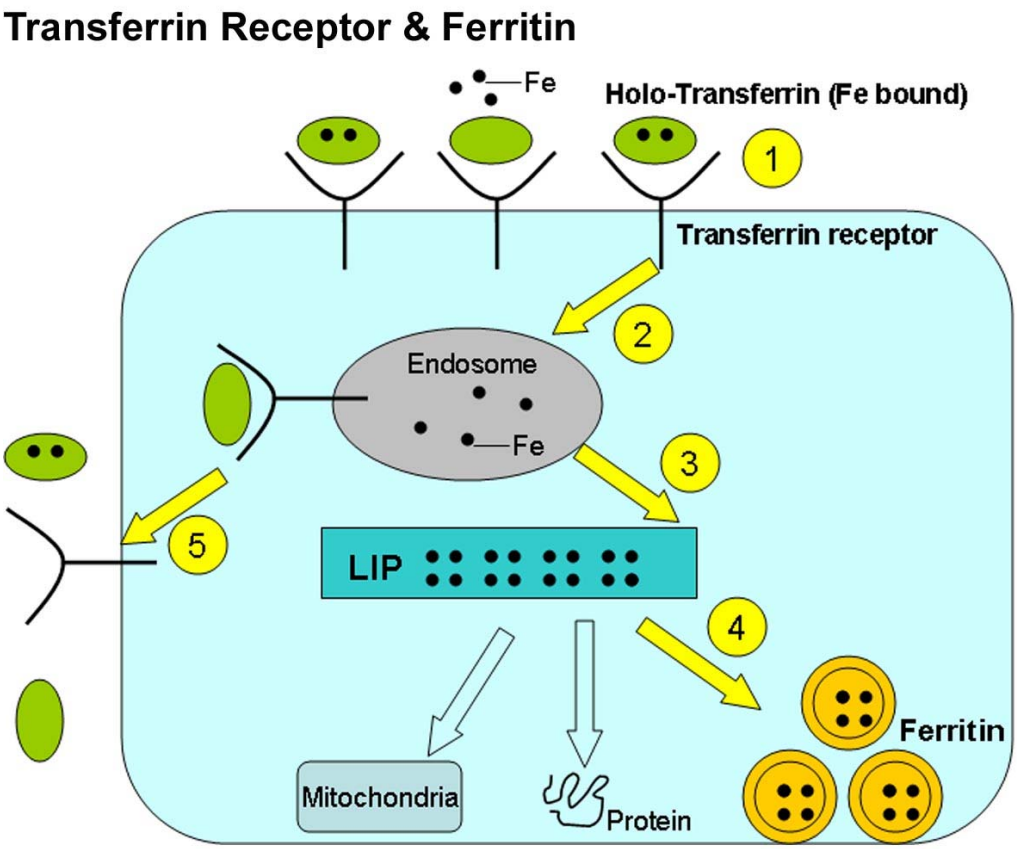

Figure II-1. Transferrin receptors mediate iron transport into cells that eventually store iron in ferritin-bound form. (1) Circulating holo-transferrin binds to transferrin receptor (2) Transferrin-Transferrin Receptor complex is internalized into the cell and fuses with endosome, where iron is released in an acidic environment. (3) Iron transported into the cytoplasm and become part of labile iron pool. (4) Labile iron pool interface between iron in active function (diverted to mitochondria, protein etc.) and in storage form, ferritin. Ferritin incorporates excessive iron from LIP into its core as ferrihydrite crystals. (5) Apo-transferrin and transferrin receptor will be transported back to cell surface to restart the cycle.

Figure II-2. IRP and IRE interactions

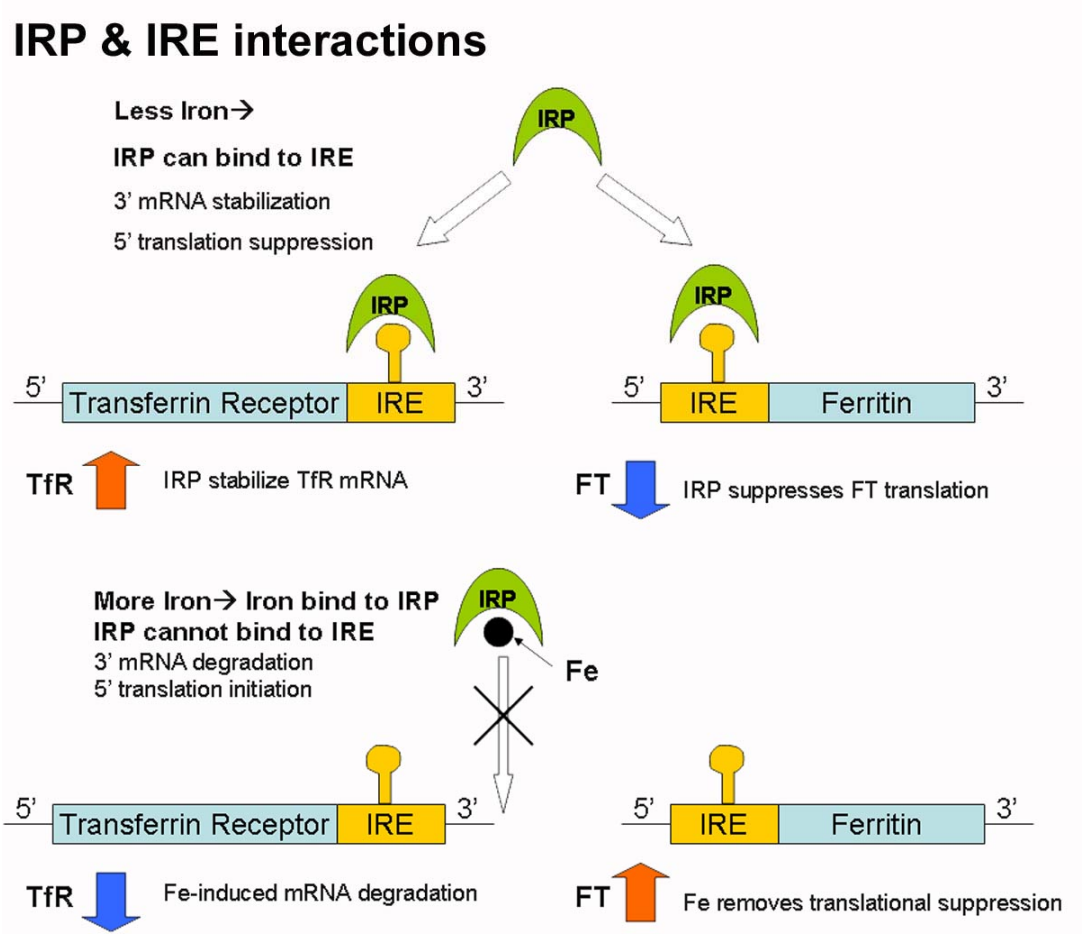

Figure II-2. Iron Regulatory Protein interacts with Iron Responsive Element to regulate iron homeostasis at posttranscriptional level. Binding of IRP to 5' IRE (example: ferritin) suppresses protein translation, while binding to 3' IRE (example: transferrin receptor) stabilizes mRNA to enhance protein expression. Consequently, in the event of iron deficiency, IRP binds to IRE on both Tfrc and FT mRNA to increase Tfrc expression and decrease FT translation; while in the event of iron excess, iron-bound IRP loses its capacity to bind to IRE which leads to decreased Tfrc expression and increased FT translation.

Figure II-3. Changes in iron regulation in response to transgenesis

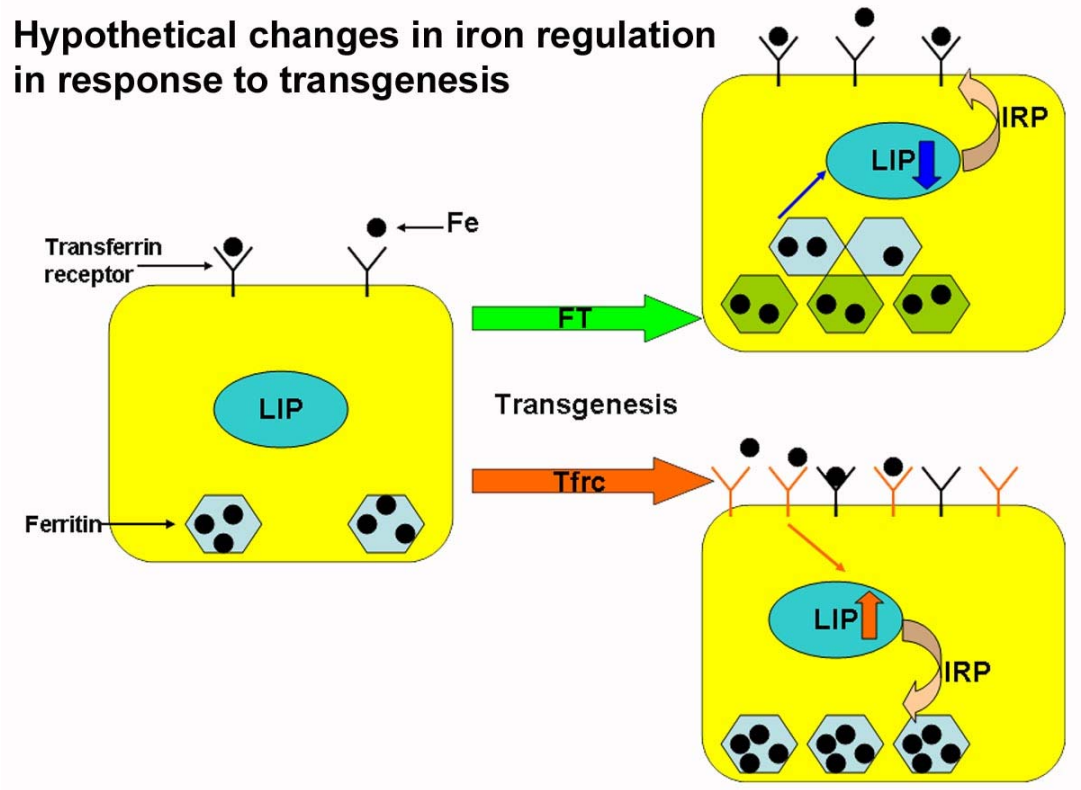

Figure II-3. Intracellular iron content and distribution are expected to change in response to metalloprotein transgenesis. Introduction of ferritin transgene is expected to divert more iron into storage form, decrease LIP, and induce compensatory increases in iron uptake. Introduction of transferrin receptor transgene is expected to directly increase iron uptake, increase LIP, and induce compensatory increases in iron storage. Both approaches are expected to lead to increases in cellular iron content, though the extent of iron accumulation and pattern of iron distribution will likely be different.

Figure II-4. Schematic of constitutive expression lentiviral vectors

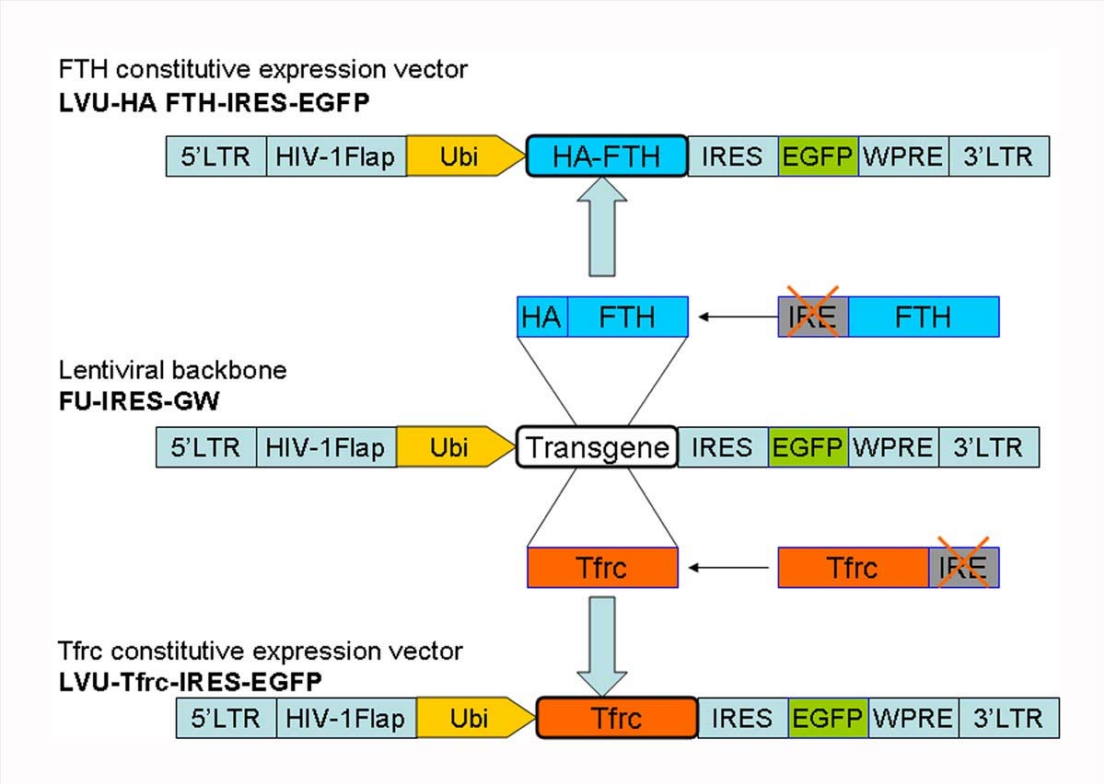

Figure II-4. Lentiviral vector FU-IRES-GW is a bicistronic expression vector that constitutively expresses transgene of interest under the ubiquitin promoter and EGFP linked by IRES sequence. Human FTH cDNA was PCR modified to remove 5' IRE sequence and tagged with HA sequence before insertion into the multiple cloning sites of FU-IRES-GW to create vector LVU-HA-FTH-IRES-EGFP that constitutively expresses FTH and EGFP. Similarly, IRE sequence was removed from 3' Human Tfrc cDNA through restriction enzyme digestion before insertion into the multiple cloning sites of FU-IRES-GW to create vector LVU-Tfrc-IRES-EGFP that constitutively expresses Tfrc and EGFP.

Figure II-5. Schematic of inducible expression lentiviral vector

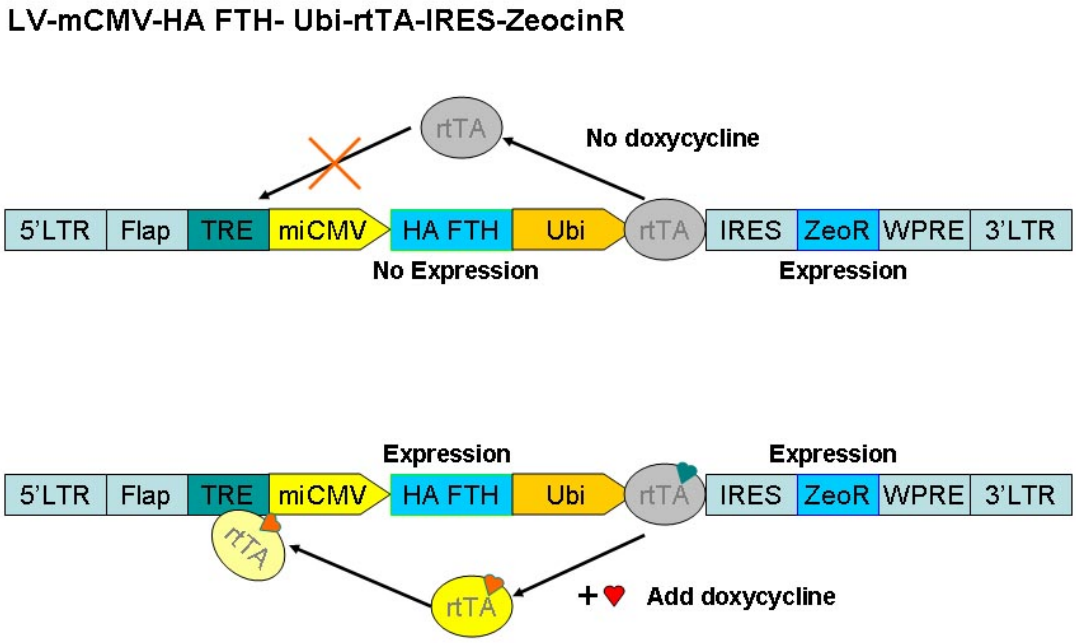

Figure II-5. Lentiviral vector LV-mCMV-HA-FTH- Ubi-rtTA-IRES-ZeocinR expresses HA tagged FTH under miCMV promoter and its expression is under TetOn inducible control: Only in the presence of doxycycline (synthetic tetracycline), reverse tetracycline Transactivator (rtTA) can bind to Tetracycline Response Element (TRE) to initiate FTH transgene expression. While the expression of selection marker ZeoR is linked to ubiquitin promoter by IRES and not under TRE-rtTA control, it enables Zeocin selection independent of doxycycline induction.

Figure II-6.

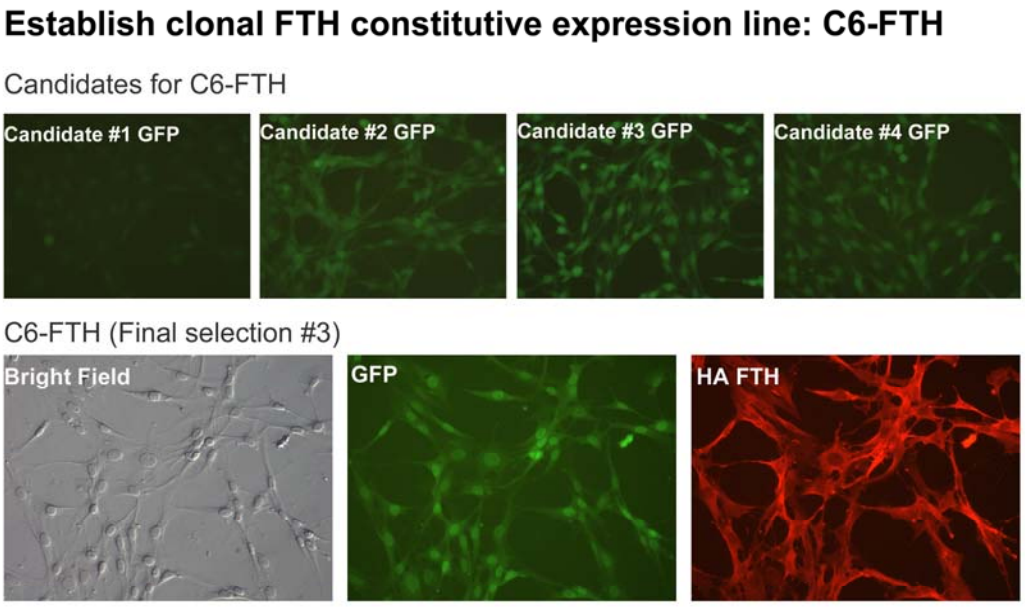

Figure II-6. Establishment of FTH constitutive expression line: C6-FTH

Multiple clonal lines were established through pLVU-HA FTH-IRES-EGFP transduction of C6 glioma cells. 4 clones with varying GFP expression level are shown here and candidate #3 among them with the highest transgene expression was chosen as C6-FTH for further characterization.

Figure II-7.

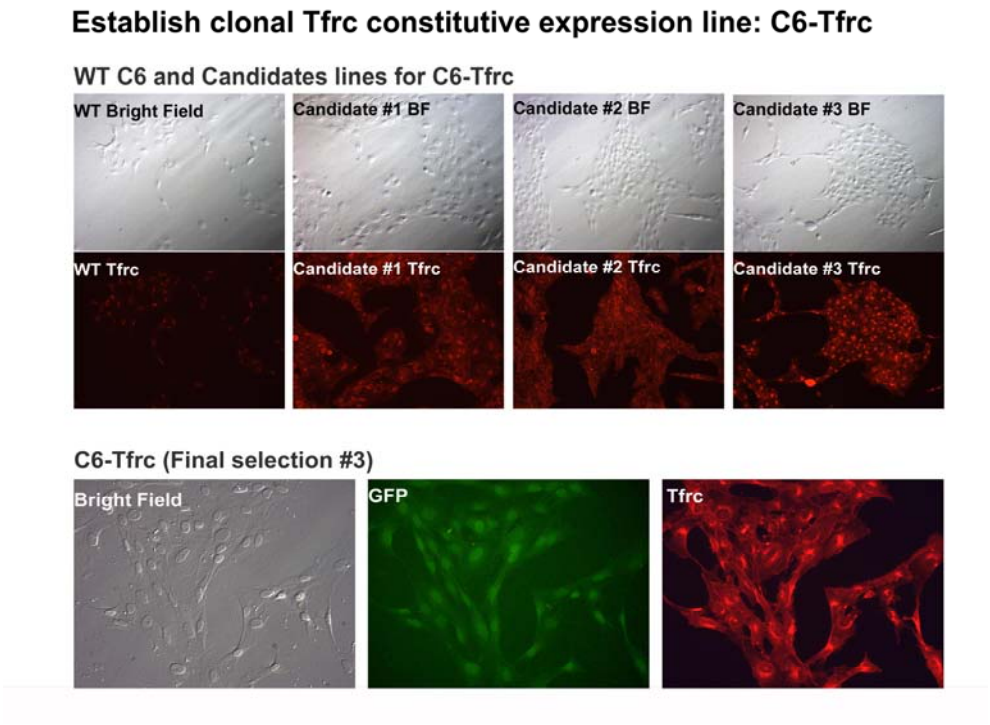

Figure II-7. Establishment of Tfrc constitutive expression line: C6-Tfrc

Multiple clonal lines were established through pLVU-Tfrc-IRES-EGFP transduction of C6 glioma cells. 3 clones with varying Tfrc expression level are shown here along with WT C6 control. Highest Tfrc transgene expression level was determined by pair-wise comparisons of Tfrc ICC under matching conditions. Candidate #3 was chosen as C6-Tfrc for subsequent studies.

Figure II-8.

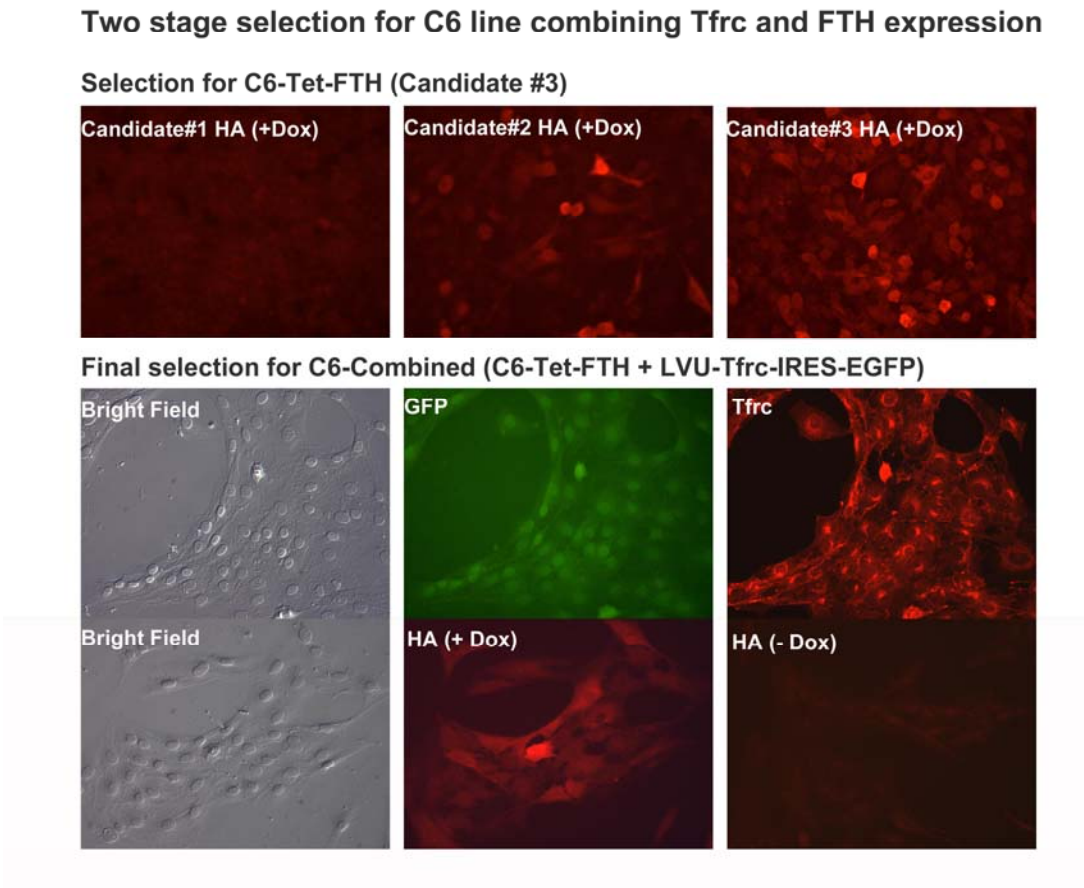

Figure II-8. Establishment of Tfrc/FTH co-expression line: C6-Combined

C6-Combined line was established in two phases. First, pLV-mCMV-HA FTH-Ubi-rtTA-IRES-ZeocinR was used to transduce C6 glioma cells to establish candidate lines that express FTH in response to Tet/Dox induction, and the line with strongest induced FTH expression was chosen as C6-Tet-FTH. Subsequently, C6-Tet-FTH was transduced with pLVU-Tfrc-IRES-EGFP to introduce Tfrc overexpression and a high expression clone was chosen as the Tfrc/FTH co-expression line: C6-Combined. C6-Combined is GFP positive, constitutively expresses human Tfrc, and will co-express HA tagged FTH under Tet/Dox induction.

Figure II-9.

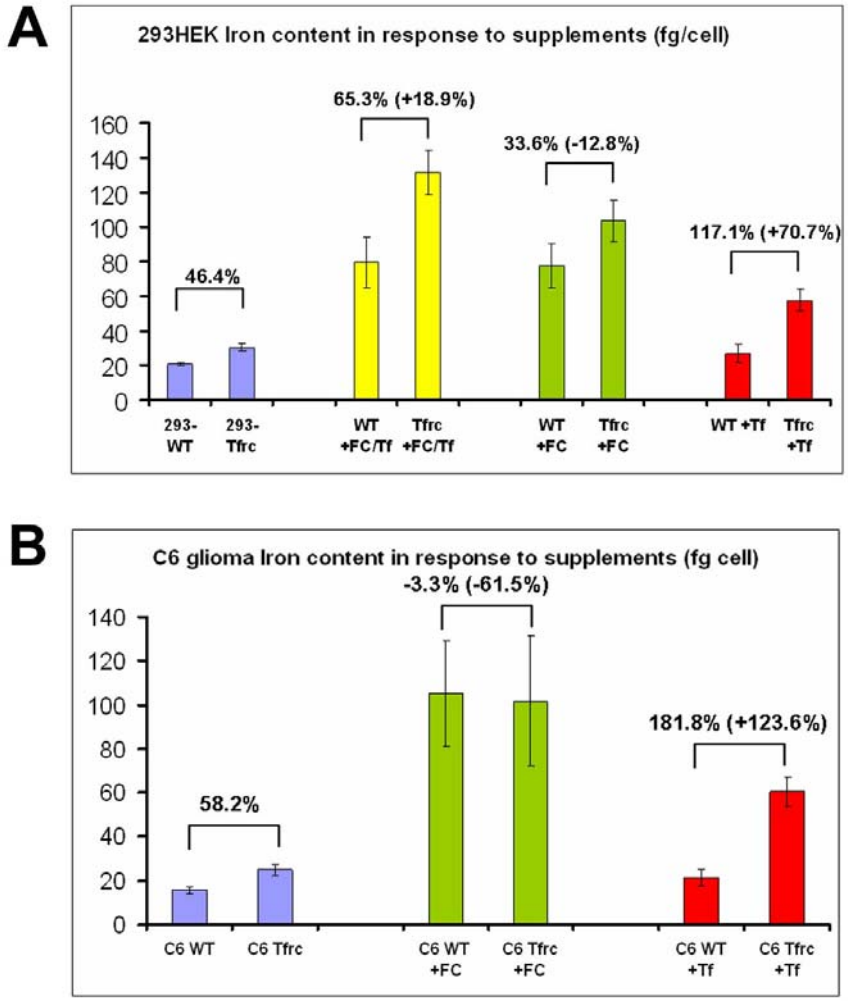
A
293HEK Iron content in response to supplements (fg/cell)
65.3% (+18.9%)
33.6% (-12.8%)
117.1% (+70.7%)
46.4%
160
140
120
100
80
60
40
20
0
293-WT
293-Tfrc
WT +FC/Tf
Tfrc +FC/Tf
WT +FC
Tfrc +FC
WT +Tf
Tfrc +Tf
B
C6 glioma Iron content in response to supplements (fg cell)
-3.3% (-61.5%)
181.8% (+123.6%)
58.2%
140
120
100
80
60
40
20
0
C6 WT
C6 Tfrc
C6 WT +FC
C6 Tfrc +FC
C6 WT +Tf
C6 Tfrc +Tf

Figure II-9. Influence of cell types and iron supplement choices on cellular Fe content

A) Comparisons between WT 293HEK and 293-Tfrc cell iron content (measured by O-phenanthroline method) in response to different forms of iron supplement. The baseline cellular iron content in 293-Tfrc was 46.4% higher than 293-WT cells without iron supplement. Iron supplement, irrespective of form, significantly increased total iron content. Co-supplement of Ferric citrate (FC 200uM) and holo-transferrin (h-Tf 1mg/ml) over 72 hrs increased 293-Tfrc iron content to a high of 131.3 fg/cell, 65.3% higher than WT controls. It was later revealed that 293 cells responded differently when FC and h-Tf were separately supplemented; FC reduced the Fe difference between WT and 293-Tfrc cells to 33.6% while holo-transferrin increased it to 117.1%.

B) Difference in selectivity to iron supplements was even more pronounced in C6 glioma cells. The baseline iron content difference without supplement was estimated at 58.2%, supplement with FC completely obliterated the distinction while h-Tf supplement amplified the difference to 181.8%.

Figure II-10.

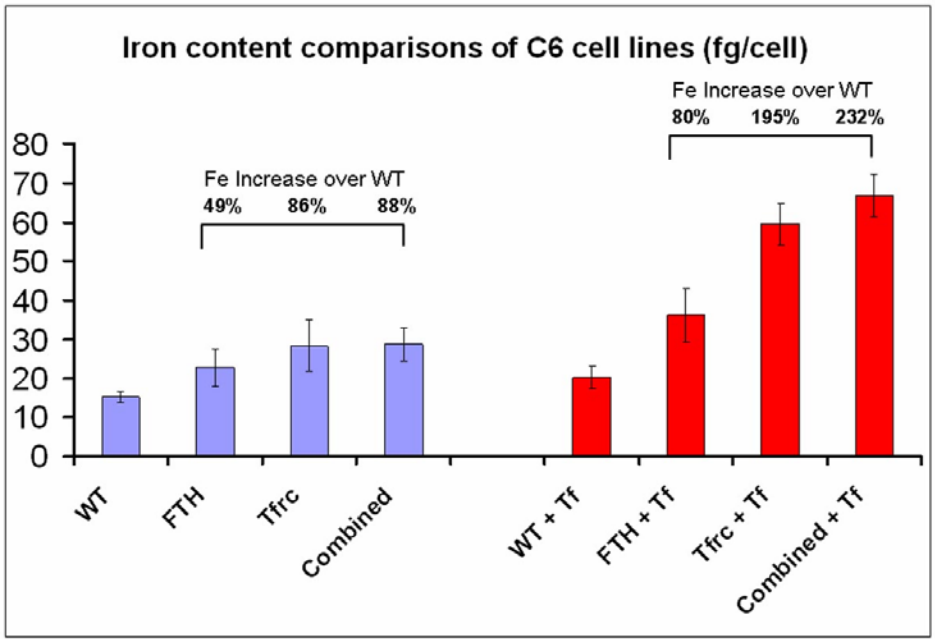

Figure II-10. Comparisons of iron contents between C6 cell lines

Iron content of C6 cell lines under the influence of metalloprotein transgenes (WT=wild type, FTH=FTH overexpression, Tfrc=Tfrc overexpression, Combined= Tfrc overexpression + inducible FTH expression) was determined by o-phenanthroline iron absorbance assay. (Note that Tfrc condition here came from C6-Combined without induction to exclude genetic background differences when comparing to co-expression condition.) Both FTH and Tfrc transgenesis increase iron cellular content, with greater increase under Tfrc overexpression condition. Comparing to Tfrc expression alone, co-expression of Tfrc/FTH had positive but not significant influence on iron content. Iron supplement in the form of h-Tf significantly amplified transgene-mediated increases in cellular iron, without altering the WT<FTH<Tfrc<=Combined relationship of Fe content.

Figure II-11.

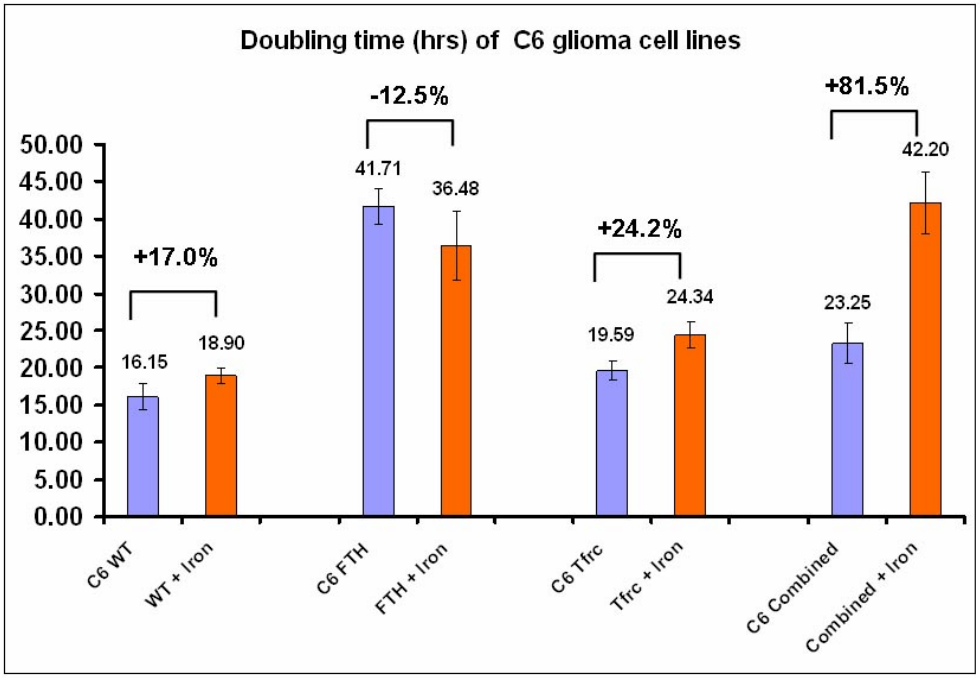

Figure II-11. Growth rate of C6 cell lines and their response to iron challenge

Growth rate of four C6 cell lines of interest: WT C6, C6-FTH, C6-Tfrc, and C6-Combined (+Dox induction) were estimated by cell count and presented here as doubling times. Note that variations in doubling time between clonal lines may be attributable to factors independent of the safety of transgenes. In response to a moderate dose of iron challenge (2X Chemically defined iron supplement, Fe=0.54ug/ml), all conditions showed reduction in growth rate except for C6-FTH, which slightly accelerated its growth rate in response to iron supplement.

Figure II-12.

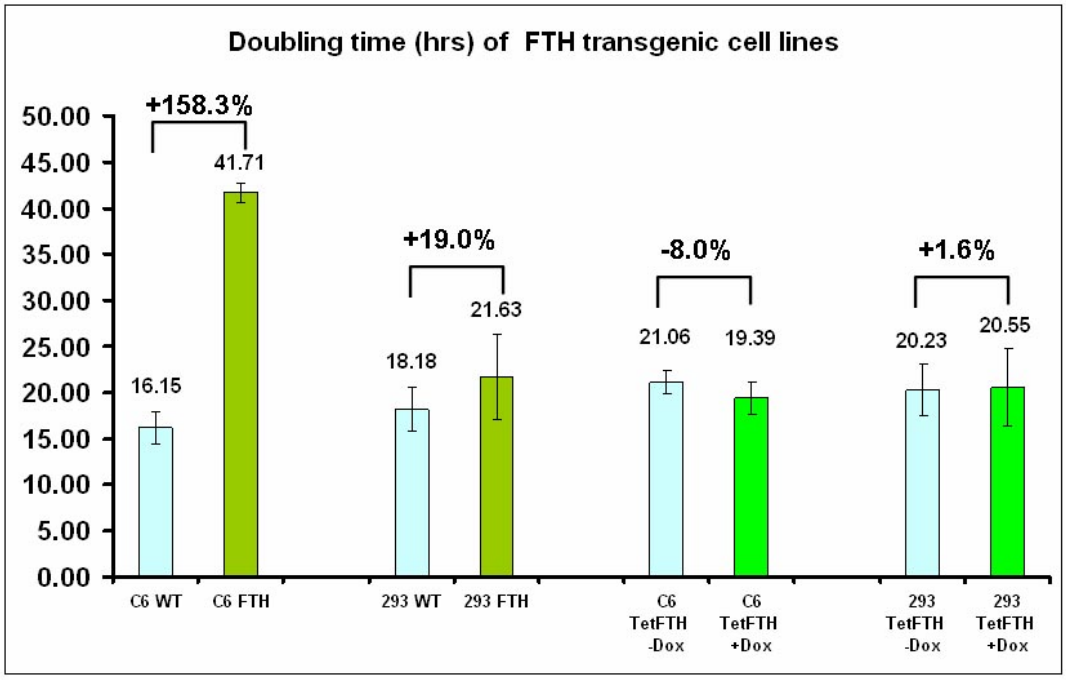

Figure II-12. Growth rate of C6 and 293 cells in response to FTH expression

The growth rate of clonal transgenic cell lines can be idiosyncratic, as shown by two pairs of comparisons of doubling times with corresponding controls: between C6-FTH and WT C6 (158.3%), and between 293-FTH and WT 293 (much more moderate difference of 19%). More reliable indicators of FTH transgene influence may be derived from induced expression of FTH within the same cell line. As Dox On/ Dox off comparisons in both C6-Tet-FTH and 293-FTH revealed, moderate FTH expression had no significant growth slowing effect on host cells; though it is entirely possible that further increases in expression level could reduce proliferation as in C6-FTH.

Figure II-13.

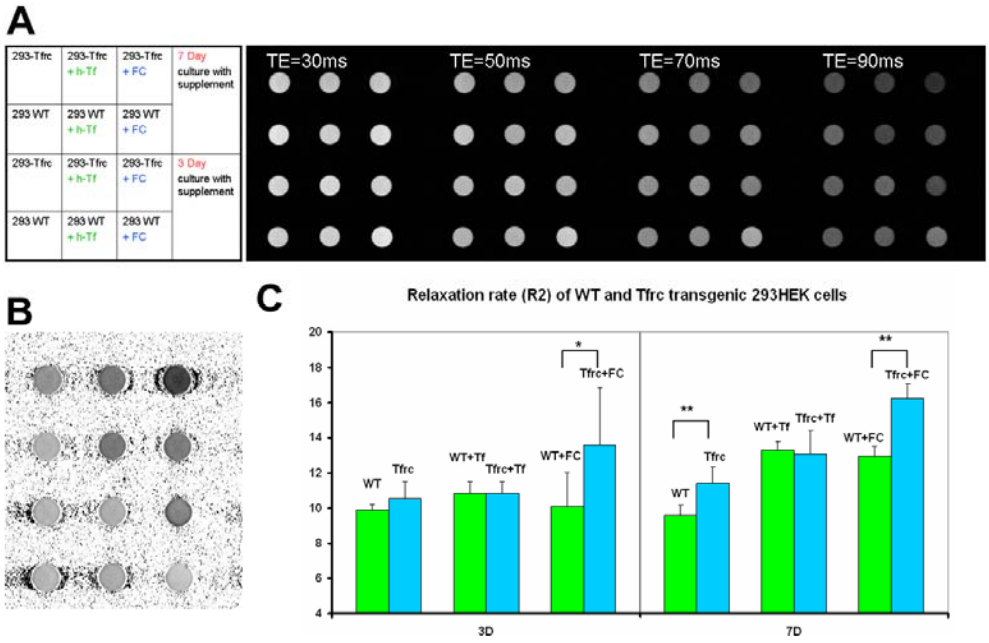

Figure II-13. *In vitro* MRI of 293HEK cell pellets

A) Left panel, treatment conditions of cell pellets. WT 293 and 293-Tfrc cells after either 3 or 7 days of iron supplement regimens (no supplement, holo-transferrin or ferric citrate). T2 weighted images (TR=2 s, TE=30, 50, 70, 90 ms) of these samples are presented in the right panel. Note that MRI contrast was more pronounced at longer TE times.

B) R2 relaxation rate map calculated for the same samples with T2 images of multiple TEs (TR=2 s, TE=20-90 ms, with 10 ms increment).

C) Chart representing the R2 values of cell pellets. Note that significant differences in R2 between 293-Tfrc cells and their WT controls were observed after longer culture duration (7 days) and with FC as iron supplement.

Figure II-14.

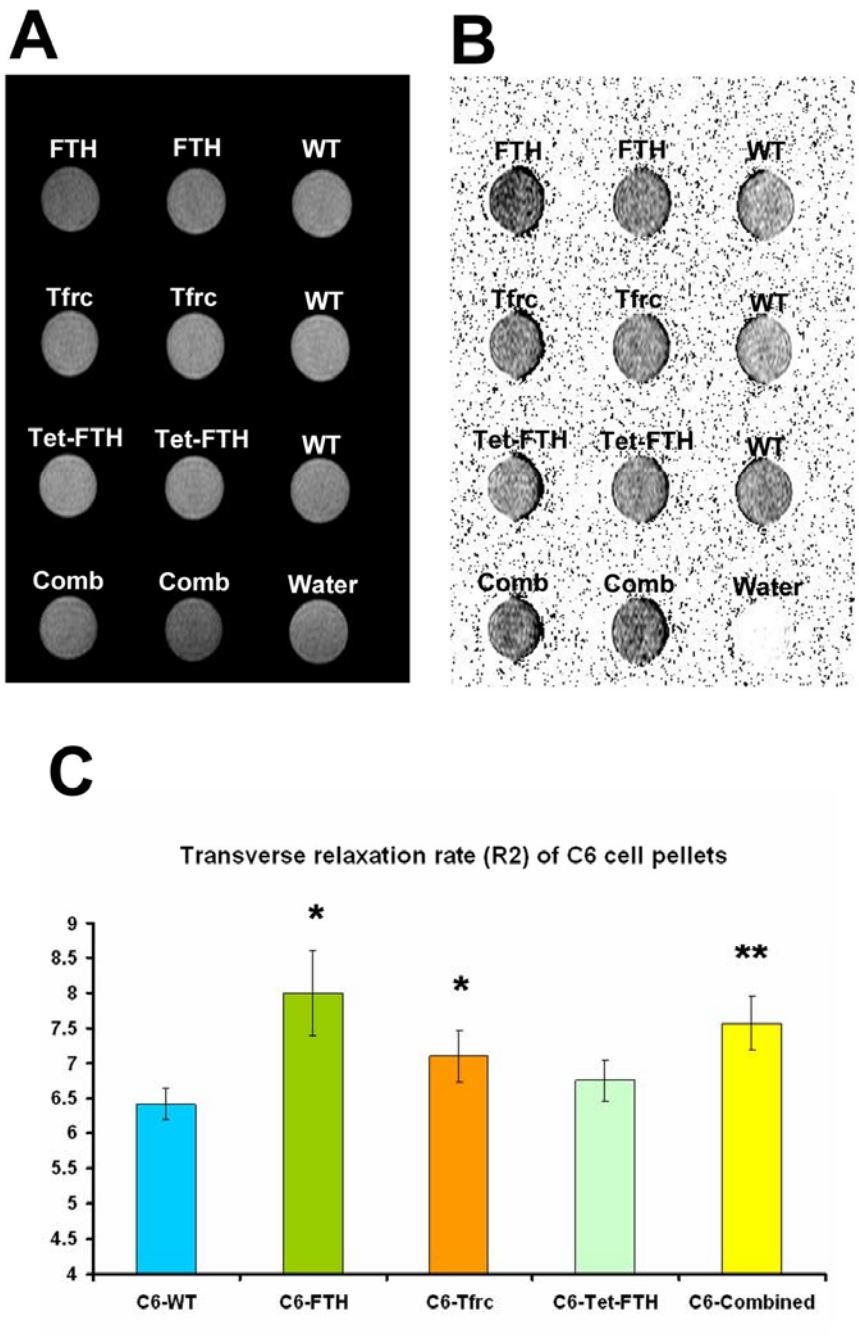
A
FTH
FTH
WT
Tfrc
Tfrc
WT
Tet-FTH
Tet-FTH
WT
Comb
Comb
Water
B
FTH
FTH
WT
Tfrc
Tfrc
WT
Tet-FTH
Tet-FTH
WT
Comb
Comb
Water
C
Transverse relaxation rate (R2) of C6 cell pellets
9
8.5
8
7.5
7
6.5
6
5.5
5
4.5
4
*
*
**
C6-WT
C6-FTH
C6-Tfrc
C6-Tet-FTH
C6-Combined

Figure II-14. *In vitro* MRI of C6 glioma cell pellets

A) T2 weighted image (TR=5s, TE=80ms) of C6 cell pellets from different genetic backgrounds (WT= WT C6, FTH= C6-FTH, Tfrc=C6-Tfrc, Tet-FTH=C6-Tet-FTH and Comb=C6-Combined)

B) R2 map calculated from T2 images with multiple TEs (TR=5s, TE=20-80 ms, with 20 ms increment)

C) Chart representing the R2 values of C6 cell pellets. Note that significant differences in relaxation rate were observed with both FTH and Tfrc overexpression. Inducible expression of FTH had positive but not statistically significant influence on R2 both in C6-Tet-FTH vs. WT C6 and C6-Combined vs. C6-Tfrc comparisons.

Figure II-15.

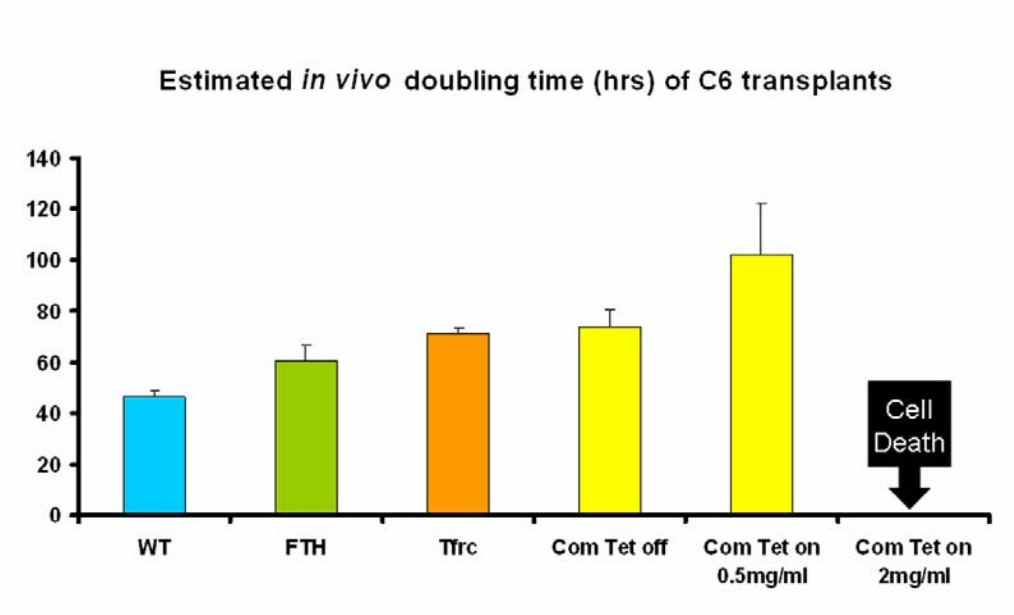

Figure II-15. Growth rate of C6 transplants *in vivo*

In vivo growth rate of C6 transplants was calculated from weekly changes in tumor volume (based on MR image) and quantified in this chart as doubling times. Note that the growth rate of C6-FTH transplants was faster *in vivo* than transplants overexpressing Tfrc (C6-Tfrc and C6 Combined without induction). Induced expression of FTH (Dox 0.5 mg/ml in drinking water) on top of Tfrc expression reduced the growth rate in C6-Combined transplants, and was clearly toxic to the transplants at higher induction dosage (Dox 2mg/ml). Dox induction itself was not toxic, and had no impact on growth of C6-Tfrc transplants.

Figure II-16.

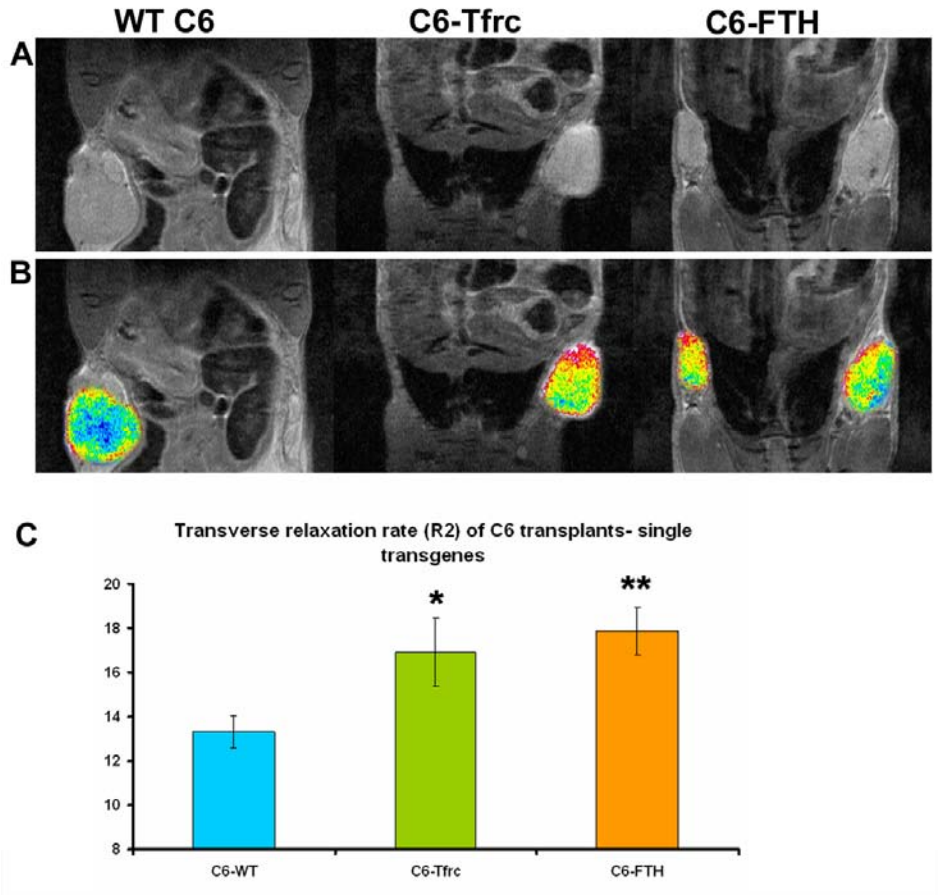

Figure II-16. *In vivo* MRI of C6 transplants carrying single transgenes

A) Representative T2 weighted images of tumor transplants of different origins in CD-1 nude mice (TR=5s, TE=20ms).

B) R2 map of the same tumors calculated from T2 images with multiple TEs (TR=5s, TE=20, 40, 60 and 80ms) overlaid with anatomical image.

C) Average R2 relaxation rate of each condition (n=3) is presented in this chart. Note that both Tfrc and FTH overexpression significantly increased R2 in transgenic C6 transplants.

Figure II-17.

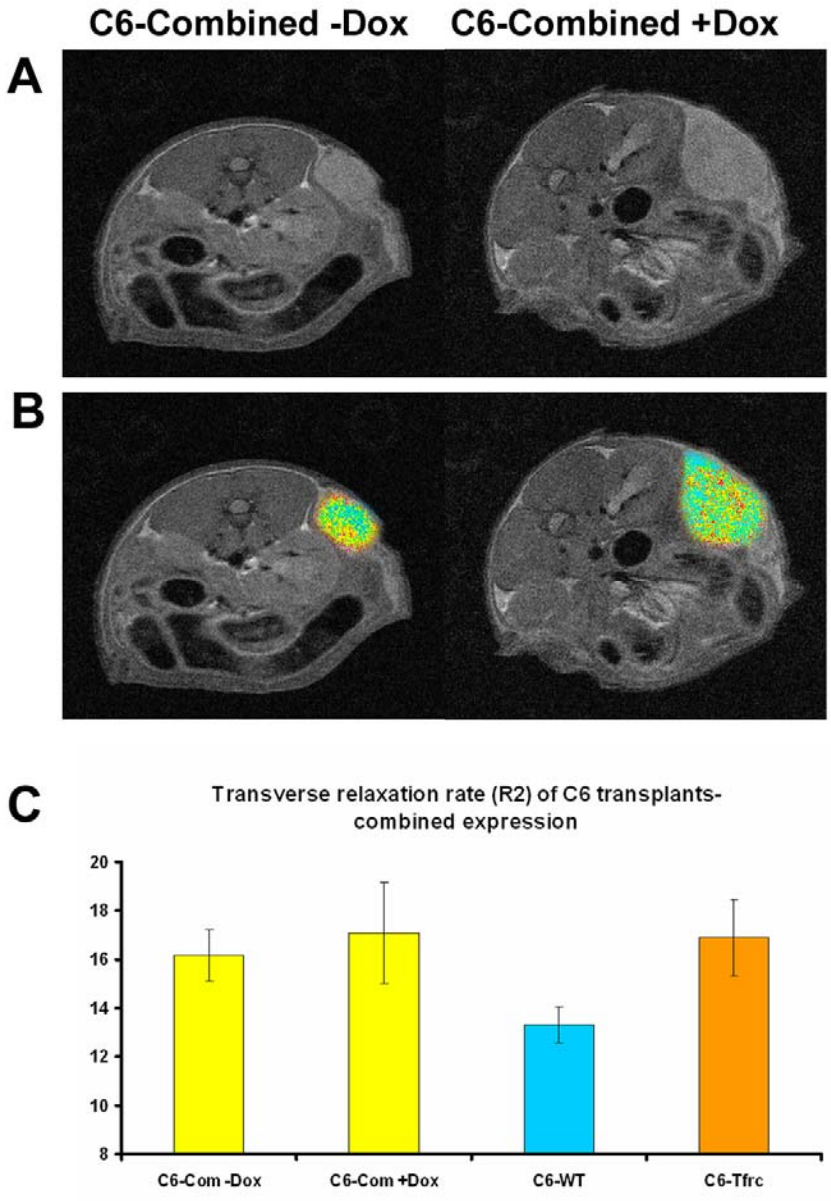
C6-Combined -Dox
C6-Combined +Dox
A
B
C
Transverse relaxation rate (R2) of C6 transplants-combined expression
20
18
16
14
12
10
8
C6-Com -Dox
C6-Com +Dox
C6-WT
C6-Tfrc

Figure II-17. *In vivo* MRI of C6-Combined transplants

A) Representative T2 weighted images of C6-Combined transplants at week 2 (pre-induction) and week 3 (post-induction) in CD-1 nude mice (TR=5 s, TE=20 ms).

B) R2 map of the same tumors calculated from T2 images with multiple TEs (TR=5 s, TE=20, 40, 60 and 80 ms) overlaid with anatomical image.

C) Average R2 relaxation rate of each condition (n=3) is presented in this chart. Note that induction of FTH expression on top of Tfrc overexpression (C6-Combined+ Dox) did not have statistically significant influence (p=.60) on R2 when compared to its pre-induction conditions (C6-Combined –Dox). Without induction, C6-Combined is functionally equivalent to C6-Tfrc and the two lines recorded similar relaxation rates. R2 value of C6-WT and C6-Tfrc were added as a reference.

Figure II-18.

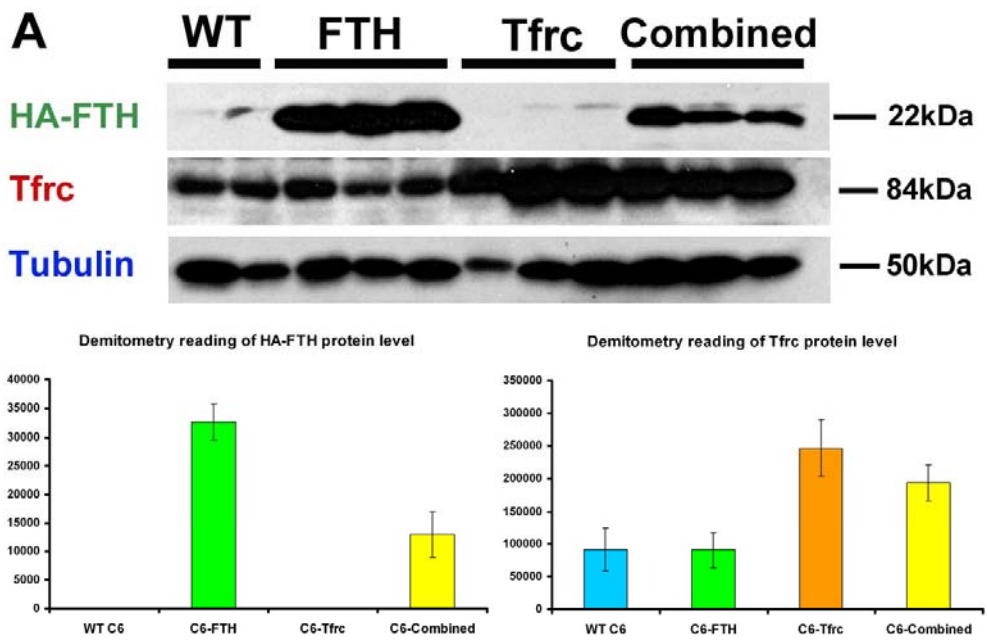
A
WT
FTH
Tfrc
Combined
HA-FTH
Tfrc
Tubulin
22kDa
84kDa
50kDa
Demitometry reading of HA-FTH protein level
40000
35000
30000
25000
20000
15000
10000
5000
0
WT C6
C6-FTH
C6-Tfrc
C6-Combined
Demitometry reading of Tfrc protein level
350000
300000
250000
200000
150000
100000
50000
0
WT C6
C6-FTH
C6-Tfrc
C6-Combined

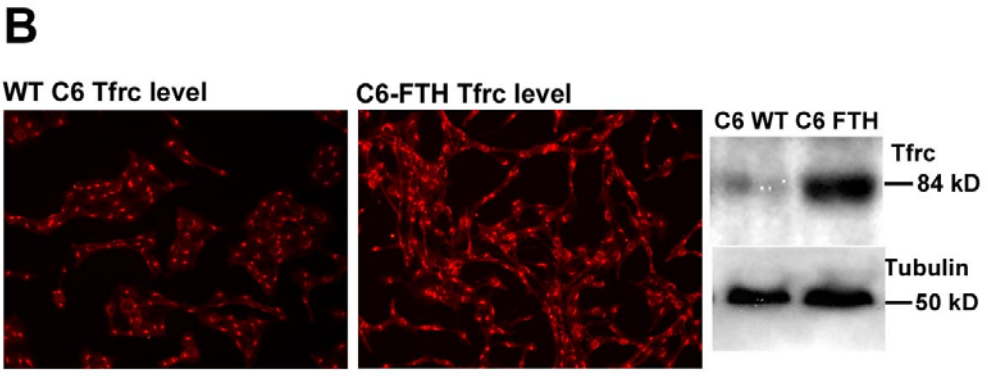
B
WT C6 Tfrc level
C6-FTH Tfrc level
C6 WT C6 FTH
Tfrc
84 kD
Tubulin
50 kD

Figure II-18. Post-mortem analysis of protein expression

A) Western blot of tumor explants of WT C6, C6-FTH, C6-Tfrc and C6-Combined, using antibody against HA tagged for detection of FTH transgene expression and antibody against Tfrc for detection of Tfrc of both endogenous and transgenic origins. FTH western confirmed the transgene expression in both C6-FTH (constitutive) and C6-Combined (induced). Note that higher FTH expression level was achieved in C6-FTH than C6-Combined with one week of Dox induction (0.5 mg/ml) with 152.2% difference estimated by densitometry. Significant increase of Tfrc expression was confirmed in C6-Tfrc and C6-Combined lines, both constitutively expressed Tfrc transgene. Curiously, C6-FTH did not show significant Tfrc upregulation in tumor explants as compared to WT controls.

B) When it came to Tfrc level in C6-FTH line, the *in vitro* picture was quite different from that *in vivo***.** With ICC, C6-FTH cell culture did show elevated level of Tfrc expression when compared to WT C6 in parallel; and western blot using samples from *in vitro* cell culture confirmed significant Tfrc upregulation in response to FTH expression.

Figure II-19.

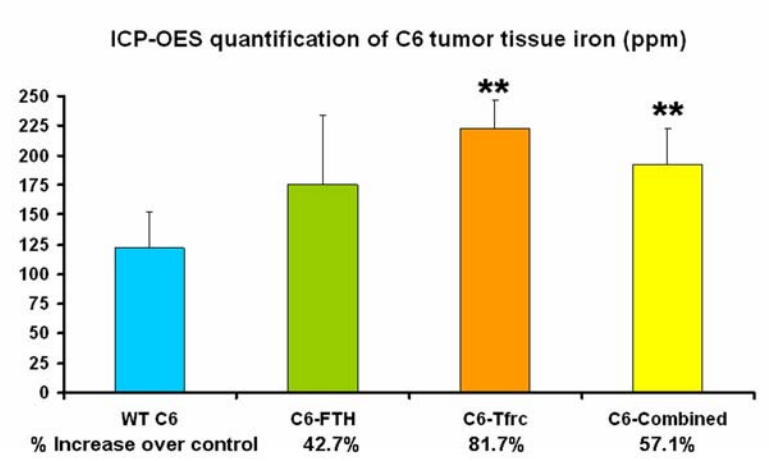

Figure II-19. Post mortem analysis of transplant iron content

Tumor samples (n=4 for each condition) from C6 transplants were processed to dry powder and iron content quantified using ICP-OES method and reported here as parts per million (ppm) of tissue dry weight. As expected, transplants carrying Tfrc transgenes (C6-Tfrc and C6-Combined) showed substantial increases in iron content over WT controls. C6-FTH transplants showed more moderate iron content increase, presumably through compensatory mechanisms to maintain iron homeostasis.

Chapter III

Monitoring mESCs with FTH Transgenic Reporter

3.1 Introduction

Earlier experimental efforts on C6/293HEK cells (covered in Chapter II) led to the identification of FTH as the preferred candidate for MRI reporter gene, and provided valuable references for improving experimental design/ methods. Confirmation of metalloprotein function in common cell lines was encouraging and set the stage for exploring the possibility of monitoring transgenic ESCs *in vivo* with molecular MRI reporters.

A FTH-ESC combination has its obvious appeals. So far, MRI tracking of stem cells has heavily relied upon *ex vivo* pre-labeling of stem cells with magnetic nanoparticles (mostly SPIOs), which can be internalized by the cells to generate strong MRI contrast on T2 and T2* weighted images (Arbab et al., 2004; Bulte and Kraitchman, 2004; Arbab et al., 2005; de Vries et al., 2005; Arbab et al., 2006; Zhu et al., 2006). SPIOs have large magnetic moments and are ideally suited for tracking transplants at the cellular level over the short term. However, for imaging studies requiring monitoring changes at the molecular level, and/or over the long term, the nanoparticle pre-labeling approach is inadequate. Here, a molecular MRI reporter introduced into ESCs could provide a viable imaging alternative as it holds at least two unique potentials: 1) unlike SPIO labeling, transgene-based reporters are expected to be much less susceptible to signal loss through cell divisions and are uniquely suited for longitudinal monitoring of stem cell transplants over extended periods; and 2) expression of reporter genes can be linked to that of therapeutic genes, effectively linking stem cell-based gene therapy to *in vivo* imaging of stem cells.

Despite what we have learnt, there are still considerable uncertainties when it comes to the viability of a FTH-ESC combination. For the current study, our focus has changed from confirmation of metalloprotein function to examining the applicability of combining MRI reporters with cell based therapy. This, coupled with unique properties of ESCs, poses some additional challenges: 1) Transgene expression: Transgenesis in ESCs tends to be of lower efficiency, and long-term transgene expression is prone to methylation-mediated silencing (Cherry et al., 2000). 2) Viability: Most MRI reporter genes to date are involved in the critical cellular process of iron regulation. Even ferritin, with the best safety profile among them, has been shown to significantly slow cell proliferation rate in certain cell models (Picard et al., 1996; Cozzi et al., 2000; Arosio and Levi, 2002); whether introducing FTH into ESCs will impair cell viability remains an open question and is likely to be species dependent. 3) Pluripotency: One of the major appeals of ESCs to regenerative medicine is their potential to differentiate into any type of cells in the adult organism and it remains unexplored whether the introduction of a metalloprotein transgene into ESCs will impair differentiation potential overall or that of specific lineages. 4) Function: Despite strong evidence that high FTH expression could function effectively in C6 cells, it is unknown how much of this will remain true with reduced transgene expression levels; and it is highly likely for FTH expression in ESCs to be lower than that of C6-FTH due to the dual influences of transgene inefficiency and the priority to preserve viability/pluripotency in ESCs. Thus, the key to FTH-ESC success lies in a proper balance between ESC compatibility and MRI reporter function.

The best way to address these uncertainties, as always, is through careful experimental efforts. Our strategy to study the feasibility of FTH-ESC is as following: 1)

Choose mouse embryonic stem cell (mESC) as the experimental model. Studying mESCs may not be as exciting as studying human ESCs, however, mESCs are comparatively easier to maintain in culture and proliferation quickly (doubling time of 12 hrs), making sample collection more accessible for all the characterizations. Mouse, as opposed to human ESCs are also more malleable to genetic modification, and both human ferritin and human transferrin transgenes are known to function in murine cells. All these features of mESC make them ideal for our exploratory efforts. 2) Use lentiviral transduction to achieve stable expression and avoid transgene silencing in mESCs. Lentiviral transduction is the method of choice for stable transgenesis in mESCs (Pfeifer et al., 2002; Ma et al., 2003), and the FUGW (Lois et al., 2002) derived lentiviral vector currently in use has been proven highly effective in transducing ESCs (Ivanova et al., 2006) as well creating transgenic animals (Yang et al., 2008). 3) Instead of selecting the highest expression lines, choose clonal cell lines that combine good viability (growth and morphology) and stable expression.

Once the appropriate cell lines are established, they will be subjected to characterizations typical of MRI reporter studies, including gene expression, viability, iron content, *in vitro* and *in vivo* MRI; along with pluripotency tests to confirm that the transgenic cell lines have retained their stem cell properties. The experiments will enable us to determine whether MRI reporter genes could simultaneously achieve function and compatibility in ESC hosts to warrant future applications.

3.2 MATERIALS AND METHODS

Construct Design

Lentiviral vector pLVU-HA-FTH-IRES-EGFP (pLVU-HFG) derived from FUGW was constructed to introduce FTH transgene into mESCs. It constitutively expresses HA tagged FTH (with IRE removed) under the ubiquitin promoter and co-expresses IRES linked EGFP. Details on the construction of this vector were provided in Chapter II methods section (Figure II-4).

Maintenance of mES Cells

mESCs (line AB2.2, i.e. WT-mESC) were cultured in mESC maintenance medium composed of Dulbecco's modified Eagle's medium (DMEM; Invitrogen) supplemented with 15% fetal bovine serum (FBS; Hyclone), 1 mM glutamine (Invitrogen), 0.1 mM β-mercaptoethanol (Sigma) and 1000 IU/ml of human recombinant leukemia inhibiting factor (hLIF; Chemicon). Medium was changed daily and mESCs passaged every two days at 1:10 to 1:15 ratio. On the day of passage, mESCs were treated with 0.05% trypsin-EDTA and dissociated into single cells before seeding onto mitomycin-C inactivated mouse embryonic fibroblast (MEF) feeder layers.

Establishment of Clonal Transgenic mESC Lines

Bicistronic lentiviral vector pLVU-HFG which constitutively expresses IRE-free human FTH and EGFP was used to establish clonal transgenic mESC lines. Lentivirus was generated by co-transfecting pLVU-HFG with packaging plasmid pΔ8.9 and envelope vector pVSV-G into 293FT packaging cells (Invitrogen). Culture medium was collected 48 hrs post transfection. mESCs were passaged as single cells and seeded at low densities onto inactivated MEFs. Once the cells attach, the medium was changed to

freshly collected VSVG-LVU-HFG containing mESC medium supplemented with polybrene (8μg/ml) and cultured overnight. The following day viral medium was replaced with mESC medium and 48 hrs after transduction positive colonies were selected manually based on EGFP expression. Each positive colony was passaged as single cells onto individual 35 mm culture plates with MEFs and the process was repeated if necessary until clonal transgenic lines were established. One transgenic mESC line that has maintained stable and the highest level of FTH expression was chosen for the current study and named HFG-mES.

Cell Growth

Cell growth rate was estimated as doubling time based on cell counts. Specifically, $1x10^4$ per cm^2 of WT-mES and HFG-mES cells were seeded as single cells onto gelatin-coated plates with inactivated MEF feeder layers. mESCs were cultured following the maintenance protocol with daily medium changes. After cell attachment, mESCs were harvested and counted at three different time points during their exponential growth phase (21, 49 and 74 hrs). For each time point, data were averaged from three replicates.

Differentiation of mES Cells

Neuronal differentiation of mESCs followed the five stage differentiation protocol previously described with minor modifications (Okabe et al., 1996; Lee et al., 2000). Briefly, mESCs were cultured on MEF feeders in mESC medium to maintain them in an undifferentiated state. To initiate differentiation, mESCs were suspended as single cells in mESC medium without LIF at a concentration of $1.5x\ 10^5$ cells/ml and transferred to

non-adherent plates for embryoid body (EB) formation. After four days, EBs were transferred to adherent cell culture dishes, allowed to attach overnight and medium switched to serum-free ITSFn (insulin/transferrin/selenium/fibronectin) medium (DMEM/F12 medium supplemented with 10 ul/ml ITSFn) to select for neural progenitor cells (NPCs). After eight days in ITSFn medium, expansion of nestin positive NPCs was initiated by switching ITSFn medium to N2 medium (DMEM/F12 medium + 10 ul/ml N2 supplement) supplemented with basic fibroblast growth factor (bFGF 20 ug/ml). The expansion phase lasted for four days, at the end of which bFGF was removed from N2 medium to initiate neuronal differentiation. The last differentiation stage lasted for six to ten days.

Western Blot

Tumors explants were dissected immediately post euthanization and stored at -80 °C for protein assays. Samples were lysed in RIPA buffer with protease inhibitor cocktail and homogenized with a sonicator. Protein concentration was determined by Bradford assay (Bio-Rad) and equal amounts (30 μg) of proteins from each sample were loaded into15% SDS polyacrylamide gel and separated by electrophoresis. Proteins were transferred onto a PVDF membrane (Millipore) using Bio-Rad's transblot, the membranes were blocked for 3 hrs in 5% milk in TBST, and incubated overnight at 4°C with monoclonal HA antibody (1:1000 Chemicon) and monoclonal Tfrc antibody (1:1000 Zymed), followed by 45 minutes incubation with horseradish peroxidase (1:10000, Jackson Immunoresearch) at room temperature. Proteins were visualized with

Amersham ECL kit (Amersham) and quantified using densitometry with Photoshop and ImageJ programs.

Teratoma formation

Teratoma formation of HFG-mES cells was confirmed by two subcutaneous (s.c.) inoculations of $1x10^6$ HFG-mES cells into severe combined immunodeficiency (SCID) mice. At day 30 post inoculation animals were euthanized and tumors removed, paraffin embedded, sectioned at 8 μm and stained with hematoxylin-eosin (H&E) for histological characterizations.

***In vitro* Magnetic Resonance Imaging**

WT vs. FTH mESC comparison—WT-mESCs and HFG-mESCs (full confluence in 10 cm culture plates for each sample) were collected after 3 PBS washes, 0.05% trypsin-EDTA treatment, and pelleted in 96 well PCR tubes at 1000 rpm. MRI of cell pellets was performed on a 4.7-Tesla horizontal bore (33 cm) MRI scanner (Oxford Magnet Technology, Oxford, UK), interfaced to a Unity INOVA console (Varian, Palo Alto, CA, USA). Using T2 weighted FSE sequence with TR of 5000 ms multiple effective TE between 20 to 100 ms, four averages, matrix 256 x 256, FOV 40 mm x 70 mm, slice thickness 0.5 mm and a gap of 0.15 mm. Multi-echo images of slices cutting through the center of cell pellets across samples were used for calculating R2 maps using MRI analysis calculator plugin of ImageJ.

SPIO vs. FTH comparison—SPIO Cell labeling was performed on WT-mESCs labeled with 13 nm magnetic iron oxide nanoparticles (Ocean Nanotech). Each condition

has 3 million WT-mESCs co-incubated with SPIO in culture medium for 2 hrs before the medium was removed and cells evenly re-suspended in agarose gel (500 ul). Concentrations of SPIOs were 0.25 mg/ml for standard (undiluted) condition, followed by serial dilutions (1/2, 1/4, 1/8, 1/16, 1/32, 1/64, 1/256, 1/1024) down to 0.24 ug/ml for 1/1024 dilution. HFG-mES cell samples were similarly prepared without SPIO or any other iron supplement in culture medium. T2 weighed MRI was performed on a 3T unit (Siemens) with FSE sequence (multi-TE points using TR of 2 s, 15 TE values: 10-150 ms with a 10 ms increment). Images were processed and R2 values of each sample were calculated using ImageJ.

In vivo Magnetic Resonance Imaging

CD-1 nude mice (n=4) were chosen for *in vivo* MRI study. Following a within subject design, $3x10^6$ WT-mESCs and HFG-mESCs were inoculated subcutaneously into opposite flanks of each mouse to facilitate direct comparison. Tumor growth was monitored daily and first MRI scans were performed on day 14 post transplant when tumor diameters reached 7-10 mm range, with repeat scans on three remaining mice from the same group performed on day 21.

For imaging of animals, mice were scanned using a 4.7T MRI scanner, interfaced to a Unity INOVA console. Animals were placed in a custom-built volume coil (5 cm ID, 8 cm long) and anesthetized using 2% isoflurane delivered via a mask throughout the MRI experiments. A set of survey images was obtained using T2 weighted FSE imaging sequence with TR of 5000 ms and TE of 20 ms. This is followed by high resolution images of selected FOV covering the full extent of tumors with T2 weighted FSE

sequence with TR of 5000 ms and multiple effective TE of 20, 40, 60, 80 ms, matrix 256 x 256. Typically, FOV of 40 mm x 70 mm, slice thickness of 0.5 mm and a gap of 0.15 mm were used. Care was taken to maintain the same animal positions and same imaging parameters across different scan sessions. Multi-echo images of slices cutting through the center of tumors across samples were used for calculating T2 maps using MRI analysis calculator plugin of ImageJ.

Histology and Immunohistochemistry

For *in vitro* characterization, cell cultures at both undifferentiated stage and multiple stages during neuronal differentiation were fixed in 4% paraformaldehyde for 15 minutes followed by thorough washes. Samples were then incubated overnight with the following primary antibodies: monoclonal Octamer-4 (Oct-4, 1: 250 Santa Cruz), monoclonal stage-specific embryonic antigen-1 (SSEA-1, 1:200 Chemicon), monoclonal nestin (1:500 Chemicon), monoclonal beta III-tubulin (1:250, Chemicon), rabbit polyclonal tyrosine hydroxylase (1: 500, Chemicon), monoclonal human ferritin heavy chain (rH02, 1:200 Ramco Lab) and monoclonal HA antibody (1:1000 Chemicon), followed by incubation with secondary antibodies conjugated with appropriate flurochromes. All the antibodies used in the experiment have confirmed specificity from prior testing in the lab.

To confirm transgene expression in cell transplants, animals were euthanized upon completion of MRI scan. Tumor tissues were removed and cryostat sectioned at 20 μm followed by fluorescence microscopy of EGFP expression and confirmation of HA tagged FTH expression with monoclonal HA antibody (1:1000 Chemicon).

Determination of iron content

Snap frozen WT and FTH transgenic tumor samples were sent to CAIS/Chemical Analysis Laboratory at University of Georgia for Inductively Coupled Plasma-Optical Emission Spectroscopy (ICP-OES) analysis (20 elements) and Inductively coupled plasma mass spectrometry (ICP-MS) to determine Fe content normalized to tissue dry weight.

Statistical Analysis

Data were presented as mean ± SD. Two-tailed *t* test was used in data analysis with $p<.05$ considered statistically significant (The assumption of normal distribution was met and allows the use of Student's T test). All experiments have at least three replicates.

3.3 Results

Establishment of FTH transgenic mESC lines

Culture medium containing lentivirus LVU-HFG (prepared from co-transfection of pLVU-HFG and packaging plasmids of 293FT cells) was used to transduce WT mESCs seeded as single cells. The transduction was of sufficient efficiency that we were able to obtain a number of EGFP positive colonies. Impaired viability could be readily identified in some transgenic clones (usually high expression clones judging from EGFP expression), which had distorted morphology or arrested growth. We selected only the transgenic lines that retained normal morphologies and fast proliferation rates. Among the clones selected, some lost transgene expression upon subsequent passages. Eventually

we were able to identify one clonal line with normal morphology, fast growth rate and maintained homogenous, stable transgene expression over 20 passages; this FTH transgenic mESC line was named HFG-mES for subsequent studies (Figure III-1). The selection criterion for HFG-mES was notably different from the highest expression-only approach we adopted with C6 glioma cells, and in our opinion more appropriate for the study of transgenic ESCs.

While the establishment of cell line HFG-mES was relatively smooth, we were prepared for less ideal scenarios as well. Two potential challenges considered were: 1) poor transduction efficiency, which can be improved with high-titer lentivirus prepared from larger scale transfection of packaging cells and subsequent concentration of viral particles; 2) strong FTH toxicity in mESCs. If toxicity is high, an inducible transgene expression system should replace the constitutive expression vector. With an inducible system, transgene expression can be turned off/on during critical stages like initial selection or neuronal differentiation to reduce the negative impact of transgene expression. Using lentiviral vector pLV-mCMV-HA FTH- Ubi-rtTA-IRES-ZeocinR (the same vector used in creating C6-Tet-FTH) we also established mESC lines that inducibly express FTH: mES-Tet-FTH.

Eventually we chose HFG-mES (constitutive) over mES-Tet-FTH (inducible) to focus our experimental efforts. This decision was largely due to concerns of insufficient transgene expression: As observed in C6 glioma cells, our pilot study suggested inducible expression of FTH (under the miCMV promoter) was also less robust than constitutive expression (under the ubiquitin promoter) in mESCs; and transgene expression in mESCs was considerably lower than those achievable in C6 cells to start with. Thus there was a

genuine concern that relying upon inducible expression in mES-Tet-FTH would lead to increased risk of false negatives (rejection of transgene function due to insufficient expression). This, together with the fact that FTH overexpression has shown good compatibility with host ESCs throughout the experiment, led us to choose HFG-mES as the cell model of choice.

In vitro growth rate

To examine whether FTH transgenesis negatively impacted mESC proliferation, same number of WT and HFG-mES cells were seeded simultaneously into separate plates, cultured under standard conditions, and quantified at multiple time points during exponential growth phase. The doubling times were estimated at 12.25 hrs for HFG-mES line and 12.15 hrs for WT mESCs, the difference was not statistically significant ($p=0.236$). This suggested that continuous expression of moderate levels of FTH had no detrimental effects on mESC growth (Figure III-2).

Early stem cell markers and neuronal differentiation

One major concern about introducing a reporter gene into ESCs is whether it will disrupt pluripotency. Three methods were adopted to evaluate the effect of constitutive FTH expression on HFG-mESC pluripotency: expression of stem cell markers, neuronal differentiation and teratoma formation.

Early stem cell marker characterizations were performed on undifferentiated HFG-mESCs maintained in standard mESC culture. HFG-mES cells were positive for alkaline phosphatase; elevated expression of this enzyme is associated with

undifferentiated pluripotent stem cells (Thomson et al., 1995; Thomson et al., 1998). HFG-mES cells were also immunoreactive for Oct-4, a transcription factor essential in maintaining pluripotent stem cells in the undifferentiated stage (Nichols et al., 1998; Niwa et al., 2000); as well as SSEA-1, which is specifically expressed in murine ESCs Solter and Knowles, 1978). For all the stem cell markers we examined, HFG-mES cells had the same positive immunostaining results as WT mESC controls (Figure III-3 A).

Neuronal differentiation of HFG-mES cells was carried out following the five stage differentiation protocol previously described by the McKay group (Okabe et al., 1996; Lee et al., 2000). The rationale behind the McKay neuronal differentiation protocol was to first initiate differentiation by embryoid body formation (with potential to differentiate into all three germ layers), which was followed by culture in ITSFn medium to eliminate non-neural lineage cell types, at the end of this selection phase surviving cells mostly became nestin-positive neural progenitor cells. Neural progenitor cells are then expanded in medium optimized for neuronal culture (N2 medium) supplemented with cytokines (bFGF); at the final stage removal of bFGF is used to induce progenitor cells to differentiate into more mature neurons (beta-tubulin III positive). Following this protocol, HFG-mES cells were successfully induced to undergo transitions from embryoid bodies to neural progenitor cells to mature neurons (Figure III-3 B), without morphologic or temporal differences in differentiation to those of WT-mESCs. Some neurons were also positive for tyrosine hydroxylase activity (only a small proportion, <10%, because we did not supplement additional cytokines of SHH (sonic hedgehog) and FGF8 (Fibroblast growth factor 8) that promote midbrain terminal neuronal differentiation). All the differentiated cells were HA positive at the final stage, suggesting

transgene expression has been stably maintained during the neuronal differentiation process (Figure III-3 B).

It should be emphasized that while ESCs have the potential to differentiate into any cell type of the adult body, here we have focused on only one cell type (mature neuron) of one lineage (ectoderm) out of numerous possibilities. The positive outcome in our neuronal differentiation experiment was more of a testimony that FTH transgenic mESCs can be as effectively differentiated as WT-mESCs under a standard protocol, rather than intended as a complete proof of pluripotency.

Teratoma formation

A teratoma is a (benign) tumor with differentiated cellular components from all three germ layers. Under experimental conditions, teratoma can result from inoculating pluripotent stem cells into (often, but not necessarily) immuno-compromised hosts, a practice that traces back to initial establishment of ESC lines (Evans and Kaufman, 1981; Martin, 1981; Thomson et al., 1995; Thomson et al., 1998). Since it is unrealistic to prove pluripotency by differentiating an ESC line *in vitro* into all known cell types, teratoma formation was often accepted instead as the gold standard assay. For further confirmation of transgenic mESC pluripotency, HFG-mES cells were inoculated subcutaneously into SCID mice and allowed to proliferate and differentiate. Tumors were removed 30 days after transplant and examined histologically. H&E staining indeed revealed tissue types representing all three germ layers: neural epithelium and squamous epithelium (with keratin deposition) of ectoderm, cartilage and striated muscle of mesoderm, together with ciliated epithelium and gut epithelium of endoderm (Figure III-

4). These teratoma provided strong evidence of HFG-mESC pluripotency, though it should be acknowledged that they still fall short of providing absolute proof of pluripotency, which would require germline transmission and production of chimeras.

It is worth pointing out that while both Nude mice and SCID mice are immuno-compromised, allow fast proliferation of mESC transplants, and have both been used in previous teratoma formation studies (Toomey et al., 1997), our experience suggested that SCID mice were considerably more conducive to differentiation of HFG-mES transplants than CD-1 Nude. Our recommendation would be to use Nude mice for *in vivo* MRI studies (easier to monitor transplant growth and better resistance to pathogens), and SCID mice for teratoma formation.

Iron content

Estimation of cellular iron content by O-phenanthroline method suggested that mESCs contained much lower Fe per cell (about 6 fg/cell) than their 293HEK (22 fg/cell) or C6 glioma (15 fg/cell) counterparts. This posed some challenges as such measurements approached the lower threshold of accurate quantification using O-phenanthroline absorbance and we experienced considerable variations between measurements. Without iron supplement, the difference between WT and HFG-mES cells was estimated at 37%, or 2.46 fg/cell ($p=0.29$); supplement with Chemically Defined Iron Supplement (CDIS, to final medium Fe concentration at 0.54 ug/ml) over 4 days increased Fe content in HFG-mES cells to 12.2 fg/cell, twice that of control level ($p=0.01$) (Figure III-5).

In vitro MRI

When *in vitro* MRI was performed on WT and HFG-mES cell pellets (collected from culture without iron supplement) on a 4.7T unit with T2 weighted FSE sequences (TR=5s, TE=20, 40, 60, 80ms), no significant difference between R2 relaxation rates was observed. The negative outcome was most likely due to the limited detection sensitivity of *in vitro* MRI to contrast between low-iron samples. Iron supplement in the form of CDIS (Fe 0.54ug/ml) over 3 days brought the MRI contrast between transgenic and WT samples to detectable levels, with estimated R2 of 5.3 for HFG-mES cells and 4.4 for their WT controls (p=0.01 Figure III-6). Note that our prior experience with high FTH expressing cell lines (C6-FTH) suggested MRI contrast were detectable *in vitro* without iron supplement. So higher FTH expression levels helped assay cell pellets by MRI *in vitro*; though the *in vivo* situation (as we will soon discuss) proved more complicated.

As previously discussed, iron supplement is a convenient way to amplify contrast and demonstrate reporter gene function *in vitro*, but its predictive value of the actual reporter utility *in vivo* is questionable at best. Supplements often create artificially high iron conditions that are unattainable *in vivo* and can lead to false positives. While we have avoided excessive iron supplement *in vitro* so that the finding would bear greater relevance, the final verdict on whether FTH could be an effective MRI reporter can only come from *in vivo* characterizations.

In vivo MRI

To validate the function of FTH as an MRI reporter in ESCs *in vivo*, WT and HFG-mES cells were grafted into CD-1 nude mice (n=4) following a within subject

design with each mouse receiving WT-mES and HFG-mES transplants subcutaneously onto opposite flanks. Tumor growth was monitored daily. On day 14 post transplant when average tumor diameter reached 8 mm, the first *in vivo* MRI on a 4.7T unit with T2 weighted FSE sequences (TR=5000 ms, effective TE= 20, 40, 60, 80 ms) was performed on all four mice. Care was taken in selection of image slices to cover the full extent of transplants on both sides. Measurements of MRI signal decay at multiple TE points showed significantly (p=0.038) decreased T2 relaxation time in transgenic mESC transplants overexpressing FTH (Figure III-7 A-C), with a corresponding increase in R2 transverse relaxation rate (R2=1/T2) of 15% between WT (R2=14.5 s-1) and FTH transgenic transplants (R2=16.6 s-1) (Fig. III-7 G). One week later, repeat scans were performed with the same parameters on three remaining mice from the original group, again with significant (p=0.019) decrease in T2 relaxation time in transplants of HFG-mES origin (Figure III-7 D-F). An average 28% increase in R2 was observed in FTH transgenic transplants (R2=18.1 s-1) as compared to WT-mESCs (R2=14.1 s-1) (Figure III-7 G). This suggested that FTH transgene expression could induce significant MRI contrast *in vivo* relying only on endogenous iron supply, meeting the functional requirement as an MRI reporter. Further amplification of MRI contrast between weeks 2 and 3 also suggested that rebalancing of iron homeostasis was ongoing 21 days post-transplant, and if this was indeed the case, we would also expect to detect active compensatory changes (i.e. Tfrc upregulation) in post-mortem analysis.

In vivo proliferation

The decision to follow a within subject design was made possible by the comparable proliferation rate of WT-mESC and HFG-mESC *in vitro*. Monitoring transplant growth suggested similar proliferation rates for the two lines were maintained *in vivo*: Throughout the experimental period, both WT-mESCs and HFG-mESCs transplants maintained similar growth rate as measured by tumor size based on MR image. On day 14 average tumor diameters measured at 8.3 ± 1.06 mm for WT-mESC and 9.1 ± 1.53 mm for HFG-mESC transplants, on day 21 the measurements were 15.0 ± 2.71 mm (WT-mESC) and 16.9 ± 4.09 mm (HFG-mESC) respectively, with no sign of negative impact on cell survival from ferritin expression ($p=0.266$ on day 14; $p=0.215$ on day 21; Figure III-8B). This additional evidence *in vivo* over an extended period of time provided further support that moderate FTH expression was not toxic to mESCs. A typical pair of tumor explants from the same animal is shown in Figure III-8A along with fluorescence images to distinguish WT and transgenic tumors.

Post mortem analysis

Post mortem analysis was conducted to probe transgene expression and iron content changes *in vivo*. Tumor samples were sectioned at 20 μm and immunostained with antibody against HA; homogenous transgene expression was confirmed with fluorescence microscopy of HA and EGFP (Figure III-9). Images of WT-mESC tumors were taken in parallel with the same settings, and were shown to be fluorescence negative to rule out autofluorescence concerns often associated with tumor sections.

To evaluate the impact of FTH expression on iron regulation, the expression levels of both Tfrc and HA-tagged FTH were determined by western blot. HA tagged

FTH expression was confirmed in all the transgenic transplants and was absent in all WT ones. Significant up-regulation of Tfrc in HFG-mES tumors, with an average increase of 70% (170% ± 17.8%) over WT-mESC as estimated by densitometry, was also observed. (*In our manuscript published in Tissue Engineering, the increase was conservatively estimated at 35%, cross-examination using multiple software packages suggests70% increase is a more accurate estimate.) (Figure III-10). This not only confirmed compensatory Tfrc upregulation as the iron homeostasis model would predict, but also suggested that iron rebalancing was still ongoing 3 weeks post transplant, consistent with our hypothesis based on *in vivo* MRI outcome and helped to explain the increase in MRI contrast between week 2 and week 3 imaging sessions.

Iron content of both control and FTH transgenic tissue samples was quantified using ICP-OES (performed by UGA chemical analysis lab). An average 80% ($p=0.029$) increase in iron content normalized to tissue dry weight was found in transgenic mESC transplants (Fe 226.9 ppm) when compared to that of control samples (Fe 126.1 ppm). The UGA chemical analysis lab also performed ICP-MS, a highly sensitive mass spectrometry measurement of metal content, on the same tumor samples. It turned out that the parts-per-trillion sensitivity of ICP-MS was actually a liability for such measurement and the iron content could only be quantified after multiple rounds of dilutions, with considerable variations between samples. Pooled average iron contents (sum of total iron divided by total weight) of WT-mESC and HFG-mESC tumors were estimated by ICP-MS as Fe 157.5 ppm and 303.1 ppm respectively, a 92.4% increase (Figure III-11). Both measurements confirmed compensatory iron increase in response to FTH expression, and offered similar estimates of the extent of changes. These findings

further corroborated MRI and western blot results in support of the hypothesis that FTH could function as an MRI reporter through its influence on iron homeostasis.

3.4 DISCUSSION

FTH-mESC combination was safe and effective

To become a useful tool for stem cell research and therapy, a transgenic MRI reporter is expected to meet the criteria of compatibility and functionality in host cells. Our characterizations of mESCs constitutively expressing FTH suggest a proper balance can be found in a ferritin-ESC combination to achieve both.

Host compatibility encompasses the concerns of both viability and interference with pluripotency and differentiation, and our findings support ferritin as a safe MRI reporter in both aspects. The growth rate of HFG-mES cells closely matched that of WT-mESC controls both *in vitro* (under standard ESC culture conditions) and *in vivo* (as cell grafts in nude mice). Previous study of FTH overexpression in HeLa cells found it induced an iron-deficiency phenotype with significantly reduced cell growth, which was reversible by incubation in iron-supplemented medium (Arosio and Levi, 2002). And similar observations were made in C6-FTH, a glioma cell line constitutively expressing high levels of human FTH. In the ESC study, however, overexpression of FTH transgene did not reduce cell growth, even without iron supplement. This by no means contradicted previous findings as the different outcomes most likely reflected variations in transgene expression levels between cell models. Instead of suggesting FTH safety under any

conditions, our findings should be interpreted as feasibility of maintaining sufficient level of FTH expression (for reporter function) in ESCs without impairment of cell growth.

Less was known about the relationship between FTH expression and ESC pluripotency, as the current study constitutes the first attempt at ferritin reporter gene-ES cell combination. Under standard culture conditions, HFG-mESC matched WT-mESC controls in early stem cell marker expression patterns associated with undifferentiated stem cell status. HFG-mESC also successfully underwent neuronal differentiation following standard protocols and passed a critical pluripotency test of teratoma formation. Together, this evidence provided strong support that FTH overexpression does not interfere with stem cell pluripotency. Currently, we cannot speculate on how pluripotency might respond to much higher levels of FTH expression; neither do we consider that further increase in transgene expression would be of much benefit for future applications of this reporter. Taken together, under the current design FTH has been constitutively and stably expressed throughout the experiments with mESC growth and pluripotency intact, thus we assert with confidence that moderate FTH expression is compatible with mESC biology.

As for reporter function, it turned out that moderate level FTH expression was quite effective as a MRI reporter gene in ESCs. On a high field strength (4.7T) unit with T2 weighted sequences we observed up to 28% increase in R2 relaxation rate from transgenic mESC transplants, which is comparable to or greater than the R2 changes from previous reports on murine ferritin transgene expression under the same field strength, with estimates in the 10%-25% range (Cohen et al., 2005; Cohen et al., 2007). MRI contrast from mESC transplants was accompanied by significant iron regulatory changes,

estimated at 70% up-regulation in Tfrc expression and 80% increase in iron content, which was remarkable given no noticeable change in cell growth or pluripotency was observed.

Also of interest was that, despite dramatic differences in FTH expression levels, the results from HFG-mES transplants were fairly similar to those of C6-FTH transplants. At the beginning of our mESC study, our greatest concern was that lower FTH expression level in stem cells (to ensure host compatibility) would render the transgene functionally ineffective. This scenario did not materialize and a few factors may have contributed: 1) *in vivo* metalloprotein reporter function relies on endogenous iron supply, which could be a limiting factor on the maximum level of contrast/iron increase achievable; and 2) in the case of FTH transgenesis, endogenous iron regulatory control was still active and responsive to LIP levels, which limits further iron accumulation once homeostasis was achieved. We postulate that while variations in transgene expression level may have a significant impact when the duration of transgene expression was short or under external iron supplement (like the case with *in vitro* MRI of cell pellets), its impact would be much reduced *in vivo* when extended expression periods allow more complete rebalancing towards equilibrium and when the transplant relies upon endogenous supply as the sole iron source.

This framework could explain the different observations made of C6-FTH and HFG-mES: While high FTH expression (in C6-FTH) could readily bring about the typical overexpression phenotype *in vitro* including higher Tfrc levels, higher cellular iron content, reduced growth rate, and positive MRI signal of cell pellets; the *in vitro* picture with lower FTH expression (in HFG-mES) was quite different. No significant

Tfrc upregulation or Fe increase (positive trend but not statistically significant), no growth inhibition, and no MRI signal unless amplified by iron supplement. However, when transplanted *in vivo* over a 3 week period to allow sufficient time for regulatory rebalancing with the same access to iron, both conditions achieved similar levels of iron increase and comparable MRI contrast.

Still, higher expression did seem to impact the speed of achieving a new iron homeostasis. In C6-FTH transplants, the major rebalancing was presumably completed by week 3, as Tfrc was back to baseline levels in tumor explants suggesting a semblance of iron balance was in place. Comparing this with the low expression HFG-mES transplants, in which MRI contrast continued to increase between weeks 2 and 3, and Tfrc was still up-regulated in tumor explants, suggesting rebalancing was not complete at 3 weeks. The implication was, in the *in vivo* environment, further increase in FTH expression would likely facilitate earlier detection of reporter, but its effect on increasing the maximum level of MRI contrast or Fe content was questionable.

Taken together, our findings suggest that FTH reporter gene can function as effectively in mESCs as in other cell models, and does so at an expression level that is compatible with both host viability and pluripotency.

Limitations and applications

While the success with FTH-mESC combination is encouraging, we also wish to stress that there are many existing and potential limitations with the use of MRI reporters, and we should avoid being overly optimistic in contemplating its future applications. Some of the concerns are discussed below:

One concern is the impact of long term transgene expression. Despite strong evidence in support of ferritin's safety from earlier studies (Picard et al., 1996; Cozzi et al., 2000; Arosio and Levi, 2002) as well as our own observations, caution should be exercised when generalizing these claims over longer time frames. Kaur and colleagues (Kaur et al., 2003) observed in a ferritin transgenic mice model that ferritin expression over the short term protected against MPTP toxicity, however, prolonged expression beyond 8 months saturated the storage capacity of ferritin and increased susceptibilities to neurotoxins in aging mice (Kaur et al., 2007). Currently, there is no telling whether careful calibration of ferritin expression level in ESCs could avoid this long term susceptibility (though the Tfrc levels returning to baseline in 3 weeks in C6-FTH was encouraging). One alternative that could address this long-term toxicity concern is to adopt an inducible system, which could also be used to its advantage to answer some questions raised in the study that cannot be addressed with the current experimental design, like whether further increase in reporter gene expression levels might impair ESC pluripotency. We wish to stress while the current study adopted a constitutive expression system mostly due to expression level concerns, an inducible system would be preferable in the majority of instances with reporter genes for improved safety and flexibility.

Delay in signal onset is another concern. Ferritin reporter function is dependent upon regulatory changes in iron homeostasis, and the rebalancing process might require days or even weeks before becoming capable of generating sufficient MRI contrast. This translates into a (potentially substantial) delay between the onset of transgene expression and the detection of reporter, influenced by factors like expression levels and iron supply

to local tissues. For measurements that seek immediate detection of reporter gene expression, a metalloprotein based reporter system may not be the best choice.

The greatest obstacle to applications of the ferritin reporter, in our opinion, is its lower detection sensitivity comparing to artificial magnetic nanoparticles. As reviewed by Gilad et al. (Gilad et al., 2007a), native ferritin is a rather weak T2 contrast agent, with the particle magnetic moment orders of magnitude smaller than magnetic nanoparticles like SPIOs (Bulte et al., 1993; Brooks et al., 1998). SPIO labeling typically results in Fe content greater than 5 pg per cell (about 250 times greater than unlabeled cells); in contrast, the observed iron increases induced by ferritin transgenesis in our study were less than double of the original (50-80% increase in our study). Thus, it should not come as a surprise that SPIO labeling has vastly superior detection sensitivity than ferritin reporter genes. In our *in vitro* MRI characterization comparing HFG-mES cell pellets (no iron supplement) with WT-mESC pellets prelabeled with serial dilutions of SPIOs (with 2 hrs incubation with 0.25mg/ml SPIOs as the baseline undiluted condition), it was found that SPIO labeled cells continued to induce stronger MRI contrast until the SPIOs were diluted by a factor of 1024 (Figure III-12). This suggested that transplants labeled with SPIOs may need to undergo on average more than 10 cell divisions (or through other mechanisms) to lose more than 99.9% of nanoparticles before the signal is reduced to the level typical of the FTH reporter. (This admittedly is an oversimplified estimation based on *in vitro* MRI only, and has limited predictive value of *in vivo* behavior). We believe that SPIOs have a clear advantage over MRI reporters for tasks that focus on cellular tracking over a relatively short period of time. Magnetic nanoparticle labeling has already been proven effective in clinical settings to trace stem cell transplants for more than a

month (Zhu et al., 2006); it is neither practical nor necessary for reporter genes to compete against SPIOs in such applications.

None of these limitations, however, should discourage researchers about the future of molecular MRI reporters. Transgenic MRI reporters like FTH are not meant to replace SPIOs, but are likely to complement SPIO labeling by opening up new applications. The new possibilities are linked to the unique properties that come with genetic modifications. For example (1) Expression of molecular reporters could be turned on and off with an inducible system, as previously discussed, not only introducing greater flexibility into experimental designs but also providing a safer, less toxic alternative. (2) Expression of molecular reporters could be made contingent upon cells reaching specific developmental stage/taking certain differentiation pathway; this is especially pertinent to monitoring of transplants derived from pluripotent or other undifferentiated stem cells. (3) Expression of molecular reporters could be readily linked to expression of other genes of interest. (In the current study FTH was linked to EGFP with IRES, with EGFP intended to provide visual confirmation of FTH expression, but it is equally valid to suggest that T2 weighted images on FTH expression can be a predictor of EGFP expression. Future studies could replace EGFP with therapeutic genes to combine MR imaging with gene therapy.) (4) While SPIO-labeled cells start out with intense signals that inevitably diminish overtime, signals from molecular reporter genes are expected to remain stable over time, which could be preferable for the purpose of longitudinal (beyond the limit of SPIOs) monitoring and quantification (The actual picture is more complicated as cell division would dilute ferritin iron as well as SPIOs, but SPIO dilution

is irreversible while ferritin reporters will continue to be replenished, presumably towards a new homeostasis).

To summarize, just as SPIOs dominate short term tracking of stem cell transplants (at the cellular level), transgenic MRI reporters will play an irreplaceable role in monitoring them at the molecular level as well as enabling longitudinal cellular graft monitoring. The current study represents, to our knowledge, the first success with noninvasive monitoring of embryonic stem cells *in vivo* with an MRI reporter. Our findings suggest that FTH, a member of the metalloprotein reporter family, could function effectively as a reporter gene in mESCs without noticeable negative impact on host viability and pluripotency. These results are promising and we hope this proof-of-principle study will encourage efforts to further explore its potential and facilitate translation into clinical practice.

Figure III-1.

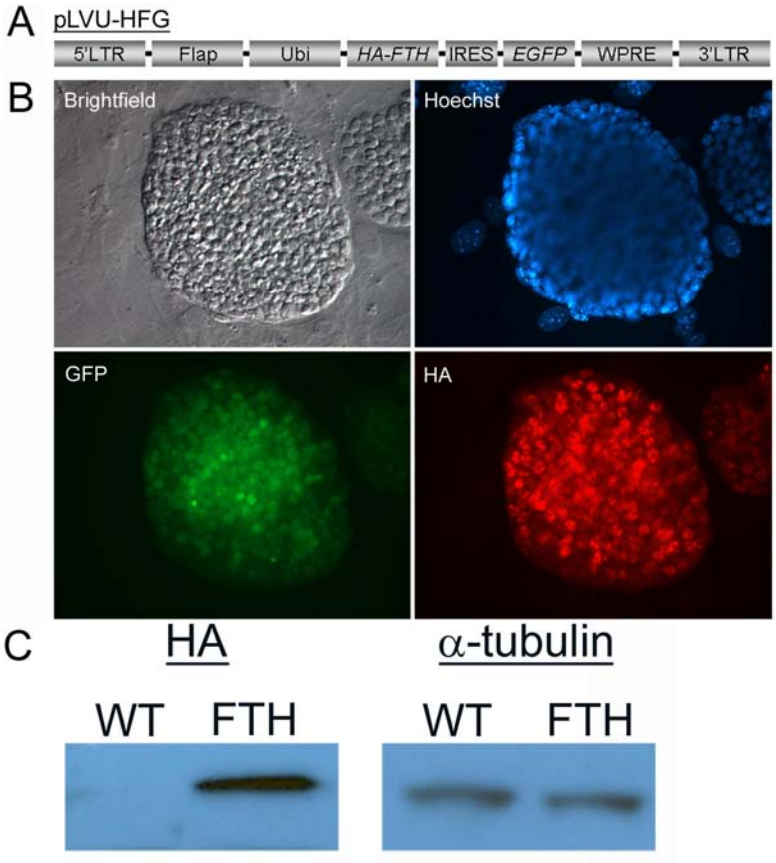

Figure III-1. Generation of HFG-mESCs

(A) Schematic of lentiviral construct: FUGW vector was modified to express HA tagged human FTH under the control of ubiquitin promoter and EGFP linked by IRES.

(B) The homogenous expression of transgene was confirmed by expression of EGFP and immunostaining using antibody that specifically recognized HA tag. All images were from the same HFG-mES colony.

(C) Western blot of HA tagged FTH in WT (left) and FTH transgenic (right) mESC lines, α-tubulin was used as an internal control. Expression of tagged human FTH (predicted molecular weight 22 kDa) was confirmed in HFG-mESCs.

Figure III-2.

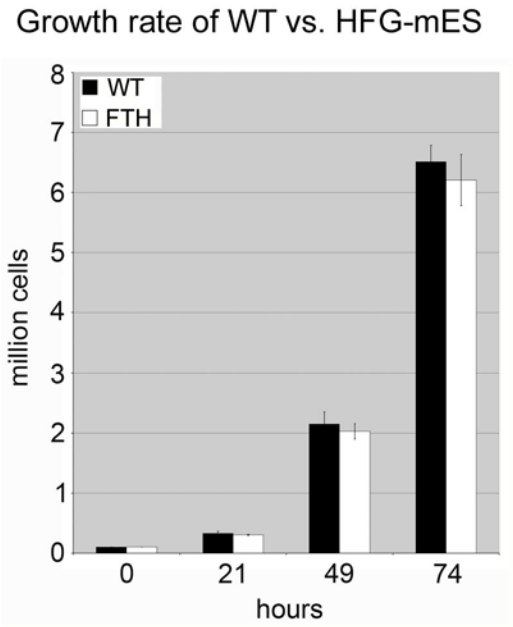

Figure III-2. *In vitro* mESC Proliferation

When seeded at $1x10^4$ per cm^2 and quantified at different time points (21, 49, 74 hrs) during exponential growth phase, HFG-mESCs retained similar growth rate as WT-mESCs, with doubling time estimated at 12.15 hrs (WT) and 12.25 hrs (HFG-mES) respectively (p=0.236 two tailed unpaired t-test, n=3).

Figure III-3.

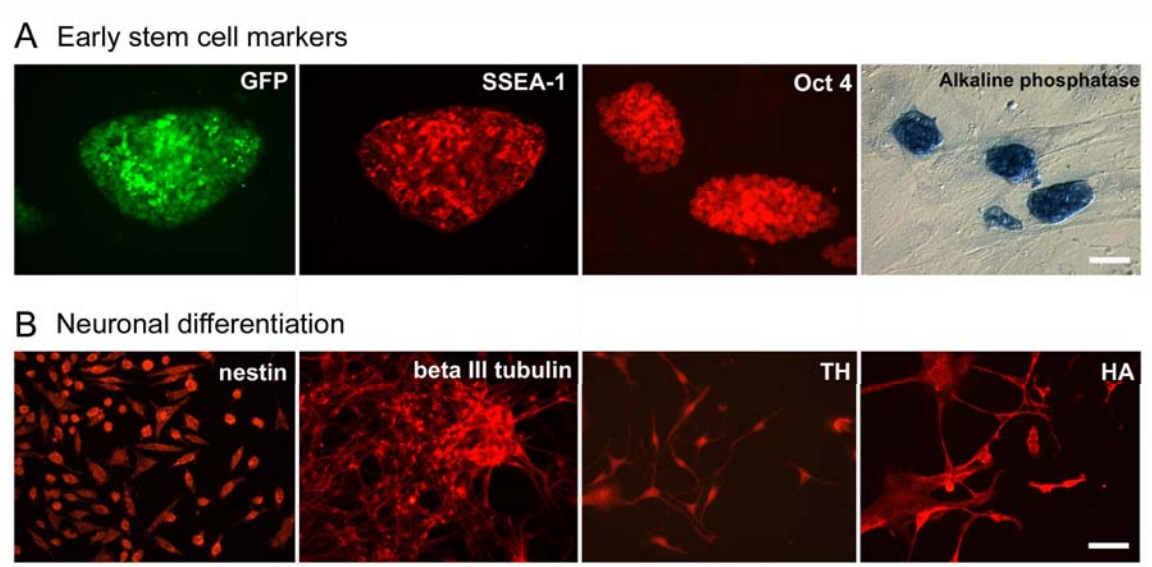

Figure III-3. Early stem cell markers and neuronal differentiation of HFG-mESCs

(A) HFG-mES cell culture was EGFP positive and expressed undifferentiated stem cell markers SSEA-1, Oct 4 and alkaline phosphatase.

(B) Neural differentiation of HFG-mES cells: immunostaining of nestin at neural progenitor stage and beta-tubulin III and tyrosine hydroxylase. HFG-mES derived-neurons maintained homogenous transgene expression shown here with immunostaining for HA. This confirmed HFG-mES cells were capable of neuronal differentiation while maintaining FTH transgene expression.

Figure II-4.

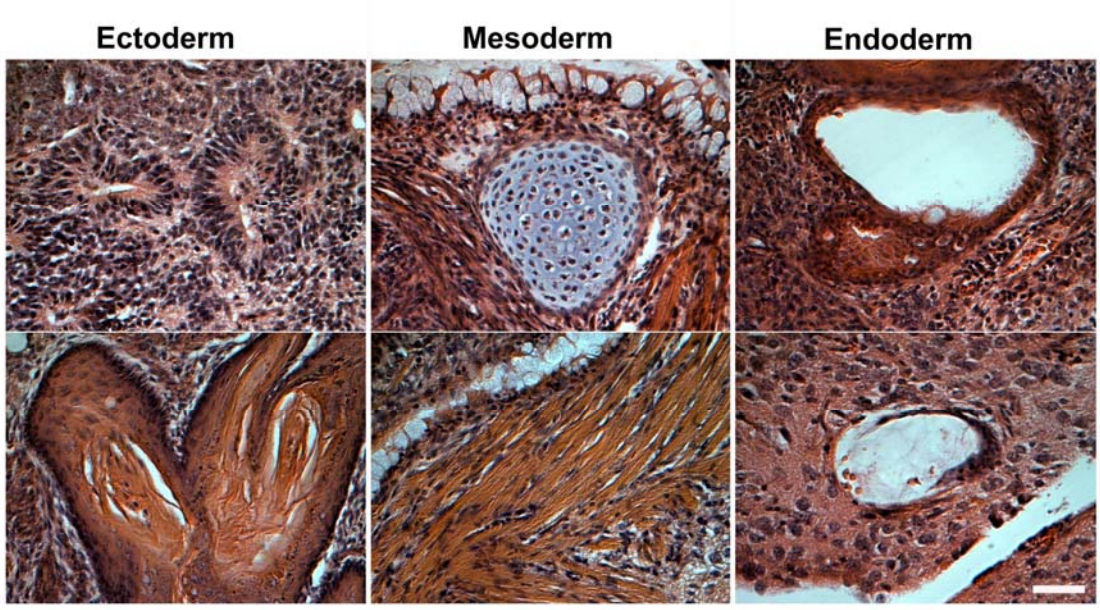

Figure III-4. Teratoma formation from HFG-mES cell transplants

HFG-mESC-derived teratomas contain differentiated tissues representing all three germ layers: ectoderm (top to bottom: neural epithelium and squamous epithelium with keratin deposition), mesoderm (cartilage and striated muscle) and endoderm (ciliated epithelium and gut epithelium). Scale bar, 50 μm.

Figure II-5.

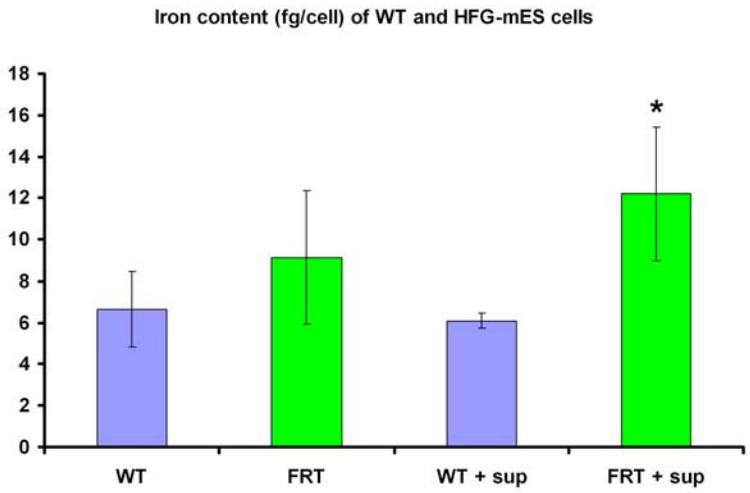

Figure III-5. *In vitro* iron content of WT and HFG-mES cells

Estimation of cellular iron content by O-phenanthroline method showed HFG-mES cells had a positive but not statistically significant increase in iron content (2.46f g/cell p=0.29) over their WT controls. Supplement with Chemically Defined Iron Supplement (Fe 0.54 ug/ml) over 4 days amplified the differences to significant levels (6.10 fg/cell difference, p=0.01).

Figure II-6.

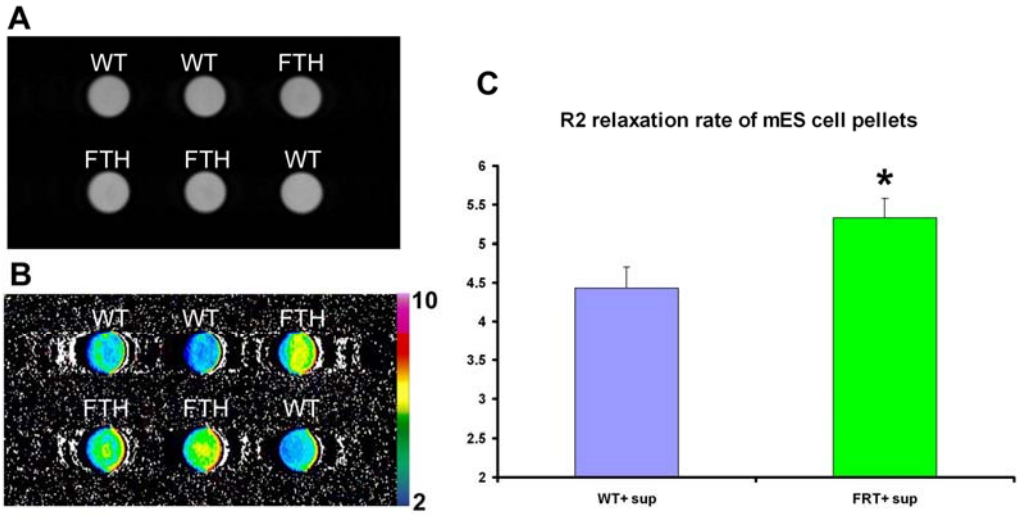

Figure III-6. *In vitro* MRI FTH Transgene Induced MRI Contrast in mES Cell pellets

(A) Representative T2 weighted fast spin echo images of WT and HFG-mES cell pellets at low TE of 20 ms. The position was switched in the right column to rule out possible positional effect from magnetic field inhomogeneity.

(B) Corresponding color coded R2 maps from multi-echo measurements of R2 relaxation rate showed significant increase in R2 relaxation rate in HFG-mES cells (with iron supplement).

(C) FTH overexpression increases R2 relaxation rate (1/T2) in HFG-mES cells *in vitro* p=0.01 two tailed t-test, n=3)

Figure II-7.

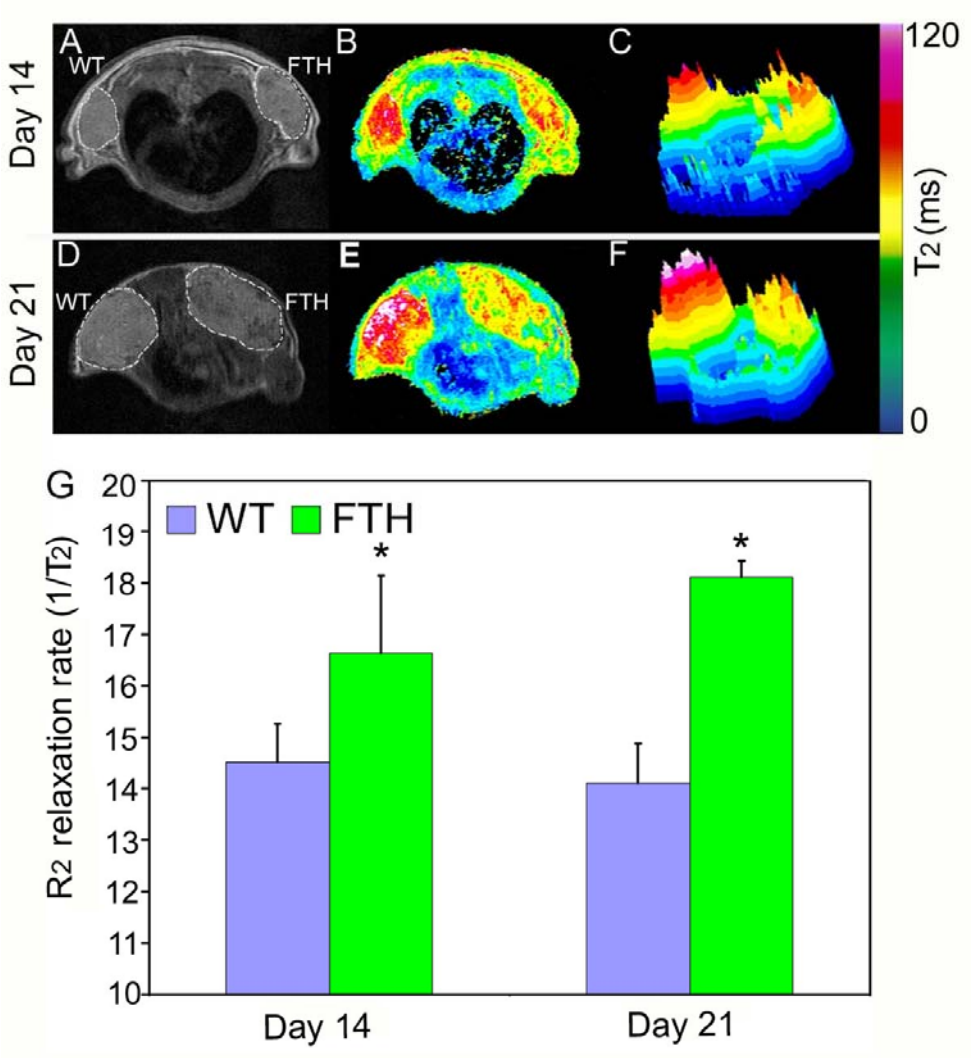
A
WT
FTH
B
C
Day 14
120
T2 (ms)
0
D
WT
FTH
E
F
Day 21
G
WT
FTH
R2 relaxation rate (1/T2)
20
19
18
17
16
15
14
13
12
11
10
*
*
Day 14
Day 21

Figure III-7. *In vivo* MRI Detection of FTH Transgene Induced MRI Contrast in mESC Grafts

(A and D) Representative T2 weighted fast spin echo images showing the same pair of tumors grown from mESC grafts (left: WT, right: FTH transgenic), at day 14 and day 21 post inoculation.

(B and E) Corresponding color coded T2 maps from multi-echo measurements of T2 relaxation time showed significant reduction of T2 relaxation time in the tumor overexpressing FTH transgene at both time points.

(C and F) Surface plots of T2 values suggest greater T2 difference between WT and transgenic tumors with extended period of *in vivo* FTH expression.

(G) FTH overexpression increases R2 relaxation rate (1/T2) in transgenic tumors *in vivo* at both time points (day 14, p=0.038 two tailed paired t-test, n=4; day 21, p=0.019 two tailed paired t-test, n=3).

Figure III-8.

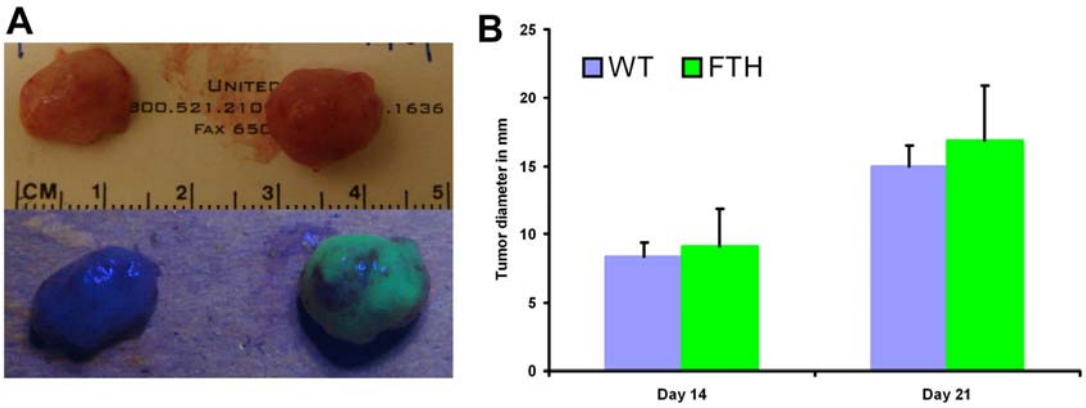

Figure III-8. *In vivo* proliferation of mESC transplants

(A) Images of WT (left) and HFG-mES (right) tumor explants. HFG-mES tumors can be readily identified under fluorescent light by EGFP expression.

(B) Diameter of WT and HFG-mES tumors measured in millimeter (mm) based on MRI images on day 14 and day 21 post transplant. No statistically significant difference in growth rate was observed between WT and transgenic transplants ($p=0.266$ on day 14 and $p=0.215$ on day 21, two tailed paired t-test, $n=3$).

Figure III-9.

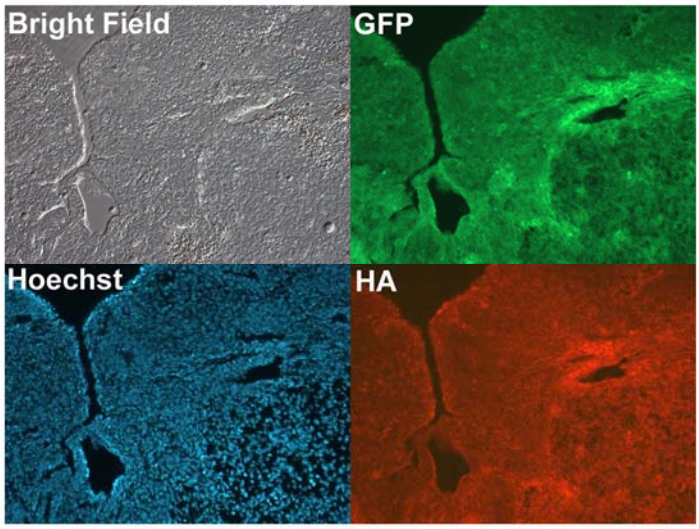

Figure III-9. Histological sections of mESCs transplants

FTH transgene expression in 20 μm HFG-mESC tumor sections was confirmed with fluorescence microscopy of EGFP and immunostaining of HA-tagged FTH. Images of WT type tumor were taken in parallel with the same settings and confirmed not to express the transgene, to rule out background auto-fluorescence. These data provide evidence of the stability and homogeneity of FTH transgene expression *in vivo*.

Figure III-10.

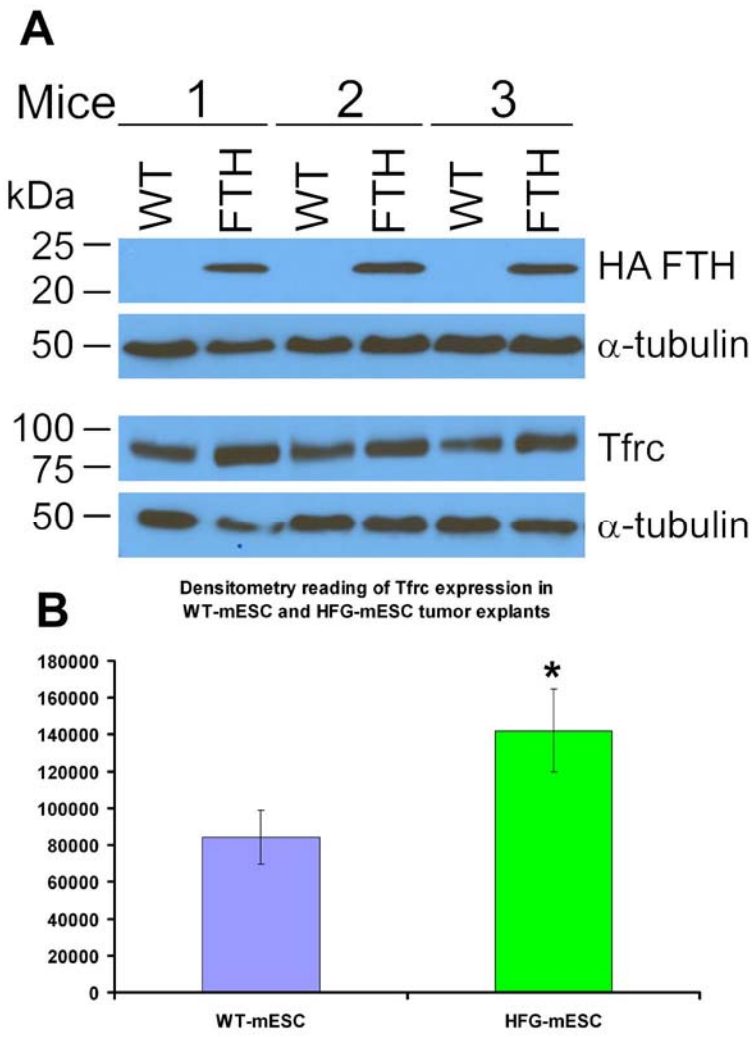

Figure III-10. Western blot analysis of tumor explants

Western blot using antibodies against HA tag and Tfrc further confirmed FTH transgene expression in HFG-mESC transplants and showed *in vivo* up-regulation of Tfrc in FTH transgenic transplants compared to WT controls, with an average increase of 70% estimated by densitometry. (Alpha-tubulin was used as an internal control.) Data are presented as pairs of WT vs. FTH transplants within each individual CD-1 Nude mice; western blot was performed on tumor explants 3 weeks post-transplant.

Figure III-11.

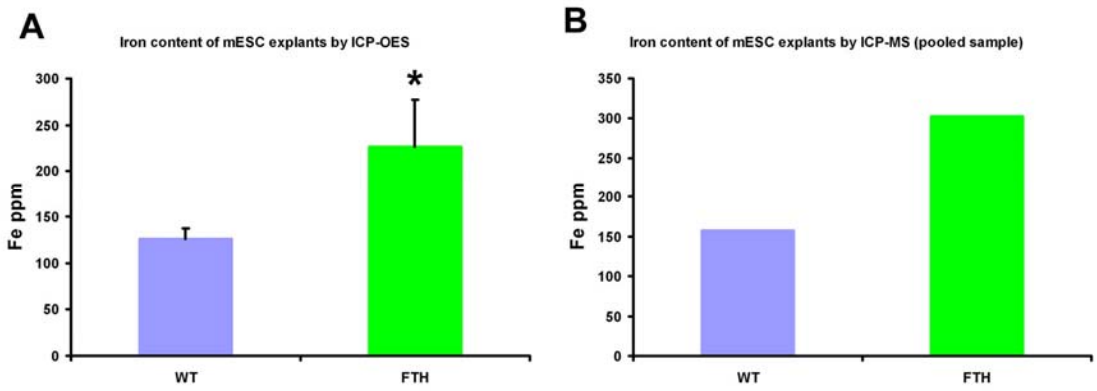

Figure III-11. Post mortem analysis of iron content

(A) ICP-OES analysis of Fe content measured in parts per million (ppm) tissue dry weights of WT and FTH transgenic tumors. Iron content in HFG-mES tumors was 80% higher than that of WT controls ($p=0.029$ two tailed t-test, $n=3$).

(B) ICP-MS analysis of Fe content measured in parts per million (ppm) tissue dry weights of the same WT and FTH transgenic tumor samples pooled. Iron content in HFG-mES tumors was estimated to be 92.4% higher than that of WT controls.

Figure III-12.

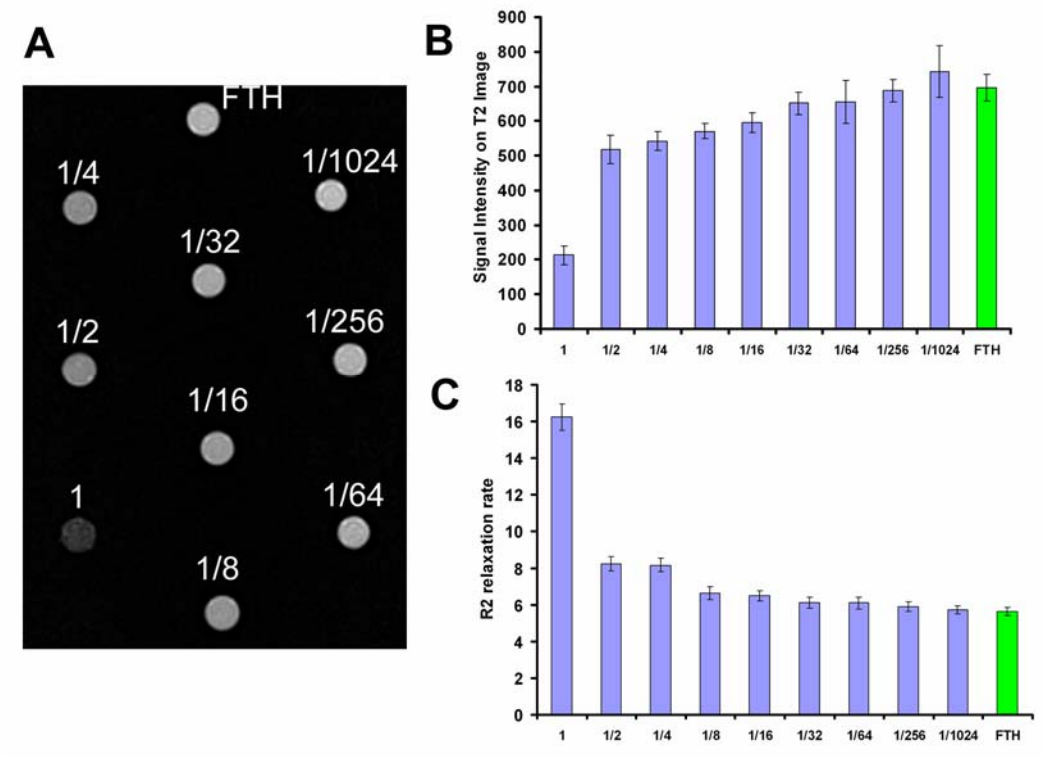

Figure III-12. *In vitro* MRI comparison between SPIO labeling and FTH reporter in mESCs

(A) A T2 weighted MR image (TR=2 s, TE=100 ms) of unlabeled HFG-mES and WT mES cell pellets labeled with serial dilutions of SPIOs (standard undiluted condition equals incubation with SPIOs at concentration of 0.25 mg/ml in culture medium for 2 hrs). Cells with SPIO labeling continued to induce stronger MRI contrast than unlabeled HFG-mES cell until reaching a dilution factor of 1024 (0.24 ug/ml).

(B) Quantification of relative signal intensity of the same T2 image (TR=2 s, TE=100 ms). Greater MRI contrast corresponded to greater hypointensity on T2 images.

(C) R2 relaxation rates of the same cell pellets calculated from multiple T2 FSE images (TR=2 s, TE=10-150 ms with 10 ms increment).

Chapter IV

Conclusions and Future Directions

4.1 Conclusions

Back in 2006, when we began to conceive plans of introducing MRI reporter genes into ESCs, there was clear excitement in the field of molecular imaging following independent confirmations of ferritin function as an MRI reporter *in vivo* (Cohen et al., 2005; Genove et al., 2005). And the level of excitement was matched only by the extent of uncertainties: Ferritin was believed to be a more effective reporter than transferrin receptor, but never confirmed; combination of ferritin and transferrin receptors was proposed to be safer and more effective than individual reporters (Deans et al., 2006), but never proven; introduction into ESCs had obvious appeals, but would it actually work? We consider ourselves lucky that, thanks to the research expertise and the level of collaboration available in this institution, it was possible for us to set out to answer these pressing questions empirically.

Conclusions on reporter gene choices

In chapter II, we made parallel comparisons between WT, FTH, Tfrc and FTH/Tfrc combination to determine the relative efficacy and safety of the popular metalloprotein based reporters. Lentivirus mediated transgenesis led to clonal C6 glioma and 293HEK cell lines with robust transgene expression, which enabled us to make key observations of transgene safety, the impacts of transgenesis on iron homeostasis and how that translated into MRI contrast both *in vitro* and *in vivo*.

Both FTH and Tfrc are relatively safe transgenes; it was possible to maintain constitutive expression of either in clonal lines without much impairment to cell proliferation. At higher expression levels, FTH could lead to an iron deficiency

phenotype with slower growth rate which may offer some protection against iron challenge/overload (consistent with its iron storage protein function); while Tfrc expression slightly increased cells vulnerability to iron toxicity (consistent with its iron uptake function). In stark contrast, co-expression of FTH/Tfrc was associated with clear toxicity both *in vitro* and *in vivo*. Having ruled out all conceivable confounds, we concluded that additional expression of FTH against a Tfrc background was indeed, paradoxically, detrimental to cell viability. The most plausible explanation we have for toxicity was the breakdown of cellular iron regulation when both uptake and storage were beyond normal regulatory feedback control (with IRE removed from transgene sequences).

Both Tfrc and FTH transgenesis led to enhanced iron uptake and increase in cellular iron content, although they exhibited quite different patterns. Tfrc overexpression led to robust and immediate boost to iron uptake capacities, making transgenic cells very responsive to increases in environmental iron. Tfrc transgenesis (no IRE) also largely rendered iron uptake unregulatable: dramatic elevation in Tfrc level and iron content in transgenic transplants persisted one month post-inoculation and theoretically will remain so for the life of the cells. The impacts of FTH on iron homeostasis were more complex: though increased iron uptake from FTH transgenesis was also mediated through increased Tfrc expression, in this case it was a compensatory response to FTH-induced depletion of LIP, and consequently both Tfrc upregulation and iron content increase from FTH overexpression were of smaller magnitude and took longer to materialize than direct Tfrc transgenesis. More importantly, with FTH transgenesis, Tfrc expression remained under regulatory control, making it possible for iron uptake to revert to baseline levels (as

observed in C6-FTH transplant). In the case of FTH/Tfrc combination, Tfrc level and iron content were only slightly greater than in the Tfrc only condition (in the same genetic background). Given the compensatory Tfrc changes from FTH were of smaller magnitude and induced FTH expression was also weaker than with its constitutive expression counterparts, it was not surprising that additional FTH expression against a Tfrc background did not lead to very conspicuous increases.

We have conducted both *in vitro* and *in vivo* MRI of metalloprotein transgene functions. Our *in vivo* characterizations offered the first parallel comparisons among FTH, Tfrc and FTH/Tfrc. The comparisons suggested that both FTH and Tfrc were capable of reporter function and had similar efficacy in creating MR contrast measured by T2 weighted sequences. While the similar efficacy was in a sense coincidental (both are dependent upon transgene expression level and imaging parameters, which would doubtlessly vary between studies), from a practical point of view it suggested both FTH and Tfrc were equally viable reporter options. This conclusion runs counter to the popular idea that FTH transgenesis is sufficiently functional with endogenous iron supply, while Tfrc function as a reporter has to depend upon external iron supplements. The fortuitous coincidence also presented an opportunity to compare similar MR contrast against different tissue iron levels (Tfrc: high, FTH: low), in turn providing support for the ferritin iron loading factor model which postulated the same amount of iron stored in increased ferritin storage would lead to greater MR contrast. In the case of FTH/Tfrc combination, induced FTH expression against Tfrc background only led to non-significant changes in MR contrast.

Our *in vitro* MRI studies led to similar conclusions, though from experience we would caution that these studies have attendant risk of both false positive (especially when it involves amplification from iron supplements) and false negative (especially when iron change is of small magnitude and with delayed onset) prediction for *in vivo* function. *In vivo* MRI (of longer duration of transgene expression and physiologically-relevant iron supply) provided more convincing confirmation of metalloprotein transgene functions and a more accurate picture of relative efficacy.

Our conclusions from Chapter II can be summarized as providing three confirmations while dispelling two misconceptions, which lead to one recommendation. The data support: (1) safety of both human Tfrc and FTH transgenes (2) the iron homeostasis model of metalloprotein based MRI reporter function, in which unregulated transgene expression along with induced compensatory changes in iron homeostasis provide the basis for MR contrast (3) and indirectly, the ferritin iron loading factor hypothesis.

The two misconceptions were: (1) The idea that Tfrc is a weaker reporter gene than FTH and could only function with external contrast agent. FTH and Tfrc each have its advantages and disadvantages, overall they are of comparable efficacy as reporter genes under the current experimental conditions. (2) The appealing but untested idea of FTH/Tfrc co-expression as an MRI reporter was proven unfeasible due to toxicity. The additional benefit to MR contrast was rather limited from co-expression and came at a steep price of significantly reduced viability, which we interpret as the danger of replacing iron regulation with arbitrary iron uptake and storage levels. There may be

further room to improve MR contrast from co-expression, but the toxicity concern has ruled it out for stem cell applications.

The one recommendation we offered was: For introduction of a MRI reporter gene into pluripotent stem cells, we recommended ferritin. Both FTH and Tfrc were viable options, but FTH transgene was believed to be the safer option because it achieved the same level of MR contrast with less iron accumulation and maintained iron uptake in a regulatable state, along with potential to protect against iron overload.

Conclusions on FTH-mESC combination

In chapter III, we introduced the preferred reporter gene, FTH, into mESCs to test the practicality of MRI reporter-ESC combination. Using lentiviral transduction, we succeeded in establishing clonal transgenic mESC lines that retained fast proliferation and normal morphology while constitutively expressing FTH, which provided further support for ferritin safety in the context of cell replacement therapy. Furthermore, FTH expression was not disruptive to mESC pluripotency based on early stem cell marker expression, neuronal differentiation as well as teratoma formation. Functionally, with T2 weighted sequences, the level of MRI contrast achieved with FTH transgenesis was equal to or greater than previous reports on ferritin in other cell models. Thus we conclude a MRI reporter-ESC combination, as exemplified by HFG-mESCs, could be both safe and effective for cell transplant monitoring purposes.

One constant concern we had was that lower transgene expression in ESCs would significantly reduce reporter efficacy. This concern was not borne out with HFG-mESCs *in vivo*. Despite large differences in FTH expression levels (FTH expression in HFG-

mES was estimated below 1/4 of C6-FTH), HFG-mES transplants exhibited similar MR contrast to C6-FTH transplants with comparable levels of iron. In contrast, variations in FTH levels had clear impact on growth rate, *in vitro* MRI, and the time course of MR contrast *in vivo* (low FTH levels took longer to reach similar effects). These seemingly paradoxical phenomena suggested the possibility that regulatory control over intracellular iron balance poses limitations on the maximum compensatory shift in iron homeostasis in response to FTH transgenesis, beyond which point (estimated at below 80% iron increase in most cases we examined) it becomes much less responsive to further increase in transgene expression. Thus for practical purposes increasing FTH level would be more effective in enabling earlier detection of reporter function, but less so in boosting its maximum sensitivity. For the same reason we would also recommend that in the case of low transgene expression, to allow sufficient time for compensatory changes before making final conclusions on the efficacy of ferritin-based reporters.

While HFG-mES was a success story of reporter gene combining safety and function in ESCs, over time we also came to realize the limitations of molecular reporters that rely on changes in endogenous iron homeostasis, especially of their significantly weaker detection sensitivity compared to artificial magnetic nanoparticles. Instead of competing against SPIOs in short term cell tracking, future pursuit of MR reporter genes in stem cells would most likely to pay off in applications exclusive to molecular reporters like stem cell based gene therapy, developmental studies or longitudinal monitoring. With our proof of principle study demonstrating the feasibility of MRI reporter-ESC combination, we expect future studies to focus on improving sensitivity of reporter genes and extend its applications to more clinically relevant models.

4.2 Future Directions:

As a project focusing on enabling novel applications, the future direction of the current study can be revealed by asking a simply question: How will people benefit from this? In its current form for proof-of-principle purposes (i.e. transplant of fast proliferating undifferentiated mESCs and compare the R2 relaxivity of resultant tumor formations), our model is still quite distant from typical research/clinical practices. In a more representative scenario of stem cell based therapy, the cell graft will be at least partially differentiated (for example, neural progenitor cells instead of undifferentiated ESCs) to avoid neoplasia formation, the graft could be migratory and the cell model of choice will not be of murine origin. How useful will ferritin reporters be under such (more relevant) situations?

Let's imagine Professor Inquisitus, a devoted neuroscientist who is interested in testing his many hypotheses of stem cell based therapy for neurodegenerative diseases, traumatic brain injury and stroke. He has just read about the success of ferritin as reporter gene in ESCs and received a generous gift of ferritin transgenic ESC lines, now he is curious about whether his research could benefit from the new tool.

If he plans to track the migration of a stem cell graft with the exact experimental settings employed in our studies on a 4.7T (or below) unit, we would recommend against it. He will most likely find the outcome unsatisfactory because the cell grafts in his experiments are comprised of much fewer cells of undefined localization, which poses much greater challenges for MRI detection than the case with comparing R2 relaxivity of tumors. As for the situations under which we would recommend using ferritin reporters,

embarrassingly right now all we have to offer are educated guesses, so the first priority of future efforts should be to turn the guesswork into a more solid guideline. In addition, more extensive safety studies on the cells would also have to be established.

Establishing a guideline for applicability of ferritin reporter gene

The MR sensitivity for molecular reporting almost certainly needs improvement for the typical applications neuroscientists would be contemplating. There are two proven technical approaches to enhance MR sensitivity of ferritin.

One is to increase the field strength of the MR scanner; it has been shown that the contrast enhancement from ferritin increases linearly with field strength (Vymazal et al., 1992). Our assumption based on previous studies (Gottesfeld and Neeman, 1996; Genove et al., 2005) is on 9.4T and above the contrast from ferritin transgenesis could be sufficient for the purpose of tracing stem cell grafts. This needs to be empirically tested. (To clarify, ferritin iron in the brain can be detected on much lower field strength MRI units. Both aged-related (Bartzokis et al., 1994; Bartzokis et al., 1997) and disease-related (Bartzokis et al., 1999; Bartzokis et al., 2000) iron accumulation can be evaluated under clinical field strength <= 1.5T. The purpose of the high field is to further enhance the contrast to allow easy distinction of much smaller cell masses.)

The other approach is to use T2* weighted gradient echo sequences instead of T2 sequences. As previously discussed, the detection sensitivity for ferritin follows the relationship of T2*>T2>T1; and the reason we chose T2 over T2* in the current study was mostly due to image quality concerns. Fortunately, the brain is a fairly homogenous tissue (with reduced local fluctuation in magnetic susceptibility) that is well suited to

using T2* sequences to monitor neural grafts. A parallel comparison between T2 and T2* of ferritin transgenesis in the brain demonstrating the superior contrast from T2* sequence can be found in the direct viral injection study from Genove (Genove et al., 2005). The same relationship should apply to grafts derived from FTH transgenic ESCs as well.

With extensive testing under optimal imaging methods, ideally a practical guideline would emerge that takes the form of "***X*** million of cells can be detected on ***Y*** T scanner using T2/ T2* sequences after ***Z*** days of transgene expression …" This guideline will help researchers like Professor Inquisitus to readily identify, depending on their access to hardware and the experimental design, whether their research would likely benefit from ferritin reporter gene in its current form.

Demonstration of unique applications of ferritin-ESC combination

While it is a theoretical certainty that a ferritin reporter introduced into ESCs will enable longitudinal monitoring as well as imaging of molecular events, both applications are yet to be demonstrated. Following the establishment of applicability guidelines, efforts should be directed at confirming the unique imaging advantages of transgenic ESCs.

At the cellular level, this means demonstrating the advantage of reporter genes in longitudinal monitoring, in comparison to the current practice of pre-transplant labeling with SPIOs. It is well recognized that SPIOs have clear advantage over native ferritin in short-term tracking applications, however due to inevitable loss of contrast agents

through cell division and metabolism, beyond certain yet to be determined time point, a ferritin transgenic reporter is believed to have a long-term advantage.

That "certain time point" is of great interest and it is difficult to speculate about. Our *in vitro* MRI comparing serial dilutions of SPIO labeling of WT mESCs with HFG-mESCs suggested 1000 times dilution will bring the two to comparable levels, but interpretation of this data proved challenging. From the perspective of iron content it is a reasonable estimate as SPIO labeling typically increases cellular iron to >250 times of baseline levels and 1000 times dilution will bring it down to below transgenic levels (1.5-1.8 times of baseline in our study). However other factors also exert strong influence on their respective T2 enhancement effects; for example, Fe spin alignment which gives SPIO particles greater magnetic moment (Bulte and Kraitchman, 2004; Gilad et al., 2007a), and iron loading factors of ferritin which gives higher relaxivity per iron with lower loading factors (Vymazal et al., 1996; Vymazal et al., 1998). On top of these, the estimate based on *in vitro* MRI with cell suspensions in agrose gel was also susceptible to considerable variations depending on sample preparation and likely deviates significantly from *in vivo* estimates. Consequently the 1000 times difference, while being the best estimate we have, is a rough one at best. Thus we consider it worthwhile to conduct a longitudinal study making parallel comparisons between the neural grafts derived from transgenic ESCs and grafts derived from WT ESCs prelabeled with SPIOs (preferably within the same subjects). This experiment hopefully will provide researchers with an accurate estimate of the dividing line between SPIOs supremacy and ferritin reporter advantages on the time scale applicable to graft monitoring. In Zhu and colleagues' clinical study (Zhu et al., 2006) with SPIO labeled neural progenitor cell transplants, the

graft became un-traceable by week 7 due to cell proliferation (in rodent studies, the traceability of SPIOs labeled stem cells ranged from days (Bos et al., 2004) to months (Stuckey et al., 2006) depending on location and cell type); and we know from experience that FTH transgene-based contrast should be detectable by week 2. So the longitudinal comparison study we are proposing should not take unrealistically long to make a distinction and the outcome will likely be of practical relevance.

At the molecular level, the potential applications are many. Its most basic form, that expression of a transgene can be linked to that of the reporter gene in ESCs, has already been demonstrated in our study linking EGFP with ferritin in ESCs, in the sense that MRI contrast can be predictive of EGFP expression. In applications more pertinent to stem cell research, two are of immediate interests. One is to determine the differentiation status of stem cell grafts; for example one might be interested in knowing whether neural progenitor cell grafts into the striatum have differentiated into dopaminergic cells *in vivo*. We imagine this question can now be answered with MRI by placing the expression of the reporter gene under the control of specific promoter like tyrosine hydroxylase and subsequent detection of reporter will be indicative of desired differentiation. Similar strategy has been previously successfully adopted to monitor differentiation status with GFP (Matsushita et al., 2002). The other pursuit of interest is in stem cell-based gene therapy, in which expression of a therapeutic gene can be linked to the MRI reporter gene (Ichikawa et al., 2002) (through IRES, fusion proteins, or simply incorporated into the same viral vector under two promoters) to enable direct (and potentially quantitative) connections between behavioral/physiologic improvements and therapeutic gene expression. Beyond therapeutic gene expression, it has even been proposed to use MRI

reporters for functional imaging by placing reporter sequence under the control of promoters for immediate early genes that are known to be regulated by neural activity (Jasanoff, 2007).

Solutions from alternative MR reporter genes

The applications discussed so far focused on ferritin-ESCs, with the assumption that researchers will have access to high field strength scanners and their experimental designs are tolerant of delays between transgene expression and reporter detection. What about the situations in which ferritin no longer applies? For example when the research requires very high detection sensitivity and/or immediate detection of transgene expression; or when researchers are concerned about the long term effect of iron accumulation, or simply do not have access to the high field strength MRI units?

To address these concerns, one has to look beyond ferritin (at least its native form) for other possible combinations of reporter genes and stem cells. Here are only a few of the possibilities:

Engineered Tfrc receptor, or other receptor type proteins, could be utilized in specific targeting; and the ligand (Tf or others) could be coupled with high sensitivity magnetic iron particles. This was essentially the strategy behind some of the earlier demonstrations (Weissleder et al., 2000; Ichikawa et al., 2002) of Tfrc reporter function. The clear advantage was that it enabled high sensitivity (thanks to SPIOs/MIONs) detection that was immediate (did not require iron homeostasis change); the disadvantage was mostly associated with delivery of ligand-coupled iron nanoparticles and efficiency of their local uptake (access to CNS will particularly difficult due to blood brain barrier).

Overall, this strategy will be worth pursing in stem cell applications when sensitivity and immediacy are of priority.

MagA, which encodes for bacterial magnetosome (Bazylinski and Frankel, 2004) is another possibility. The reason why native ferritin makes a weak contrast agent is partially due to its antiferromagnetic property with most of its Fe spins canceling out (Gilad et al., 2007a; Cohen et al., 2009); the hope is other forms of iron storage in the cell might be more effective in inducing MR contrast. While we currently know little about how MagA takes up and stores iron in mammalian cells, studies from this lab have demonstrated it could function as a reporter gene in 293HEK cells (Zurkiya et al., 2008) and pilot *in vitro* characterizations suggest it has greater MR sensitivity than ferritin. If MagA turns out to be compatible with ESCs, it has good potential to function as an enhanced version of a ferritin-like metalloprotein reporter.

Lysine rich protein: For researchers most concerned with consequences of long-term iron accumulation, there are also options available to completely bypass iron-based MRI contrast. As has been recently reported, transgenes encoding for synthetic proteins that are rich in lysine residues could have their rapid exchanging amide protons exploited by the process of chemical exchange saturation transfer (CEST) to create MR contrast (Gilad et al., 2007b; McMahon et al., 2008; Sherry and Woods, 2008). This approach has great potential in terms of safety and immediacy, and should be compatible with genetic engineering of stem cells. Right now the main limitations are detection sensitivity, and consequently, applicable only to very high strength MR units.

Multi-model reporter: There is no rule stipulating that monitoring has to be restricted to one imaging modality. Each imaging method has its inherent strengths and

weaknesses, and sometimes rather than exploring different options within the same modality to seek compromises between sensitivity and safety, or short and long term; a simple solution can come from combining the advantages of multiple imaging modalities. A case in point was Hoehn et al's attempt in combining ferritin with luciferase within the same construct to achieve both sensitivity (optical imaging of bioluminescence) and great spatial resolution (MRI) (Hoehn et al., 2008). For stem cell therapy in large animals, a dual reporter system for PET (HSV-TK) and MRI (ferritin) could be ideal in combining many advantages including: great sensitivity, immediate probing of transgene expression, potential suicide gene to protect against tumor formation (from PET) and great resolution, non-invasiveness, functional imaging (from MRI), as well as good tissue penetration (from both). The complementary nature between PET and MRI is well-recognized and PET-MRI systems have growing presence in research and clinical institutions, where dual reporter stem cell lines in the mode of HSV-TK-Ferritin-ESCs could one day find their applications.

Extension to other stem cell models

Last but not least, the success in mESCs should and will be extended to other pluripotent stem cell models for greater clinical and research relevance. The lentiviral transduction approach adopted in the current study has proven effective in other ESC models (Gropp et al., 2003) and we do not foresee major technical challenges to introduce MRI reporter genes into other pluripotent stem cells like human ESCs and monkey ESCs. Of particular interest was the recent development of iPSCs which currently holds enormous promise for patient-specific stem cell therapies and whose

establishment was the consequences of extensive epigenetic engineering (Takahashi et al., 2007; Yu et al., 2007). While the eventual clinical translation of iPSCs and other pluripotent stem cells will almost certainly be free from viral-mediated transgenesis (recent advances have proven the feasibility of generating iPSCs by naked DNA sequences (Kaji et al., 2009) or by recombinant proteins only (Zhou et al., 2009)), establishment of MRI traceable iPSCs could at a minimum serve as a valuable research tool to further our understanding of this new and promising member of pluripotent stem cell family.

Reference:

Aisen P (1998) Transferrin, the transferrin receptor, and the uptake of iron by cells. Met Ions Biol Syst 35:585-631.

Aisen P, Wessling-Resnick M, Leibold EA (1999) Iron metabolism. Curr Opin Chem Biol 3:200-206.

Alfke H, Stoppler H, Nocken F, Heverhagen JT, Kleb B, Czubayko F, Klose KJ (2003) In vitro MR imaging of regulated gene expression. Radiology 228:488-492.

Andrews NC (1999) Disorders of iron metabolism.[see comment][erratum appears in N Engl J Med 2000 Feb 3;342(5):364]. New England Journal of Medicine 341:1986-1995.

Arbab AS, Jordan EK, Wilson LB, Yocum GT, Lewis BK, Frank JA (2004) In vivo trafficking and targeted delivery of magnetically labeled stem cells. Human Gene Therapy 15:351-360.

Arbab AS, Yocum GT, Rad AM, Khakoo AY, Fellowes V, Read EJ, Frank JA (2005) Labeling of cells with ferumoxides-protamine sulfate complexes does not inhibit function or differentiation capacity of hematopoietic or mesenchymal stem cells. NMR in Biomedicine 18:553-559.

Arbab AS, Pandit SD, Anderson SA, Yocum GT, Bur M, Frenkel V, Khuu HM, Read EJ, Frank JA (2006) Magnetic resonance imaging and confocal microscopy studies of magnetically labeled endothelial progenitor cells trafficking to sites of tumor angiogenesis.[erratum appears in Stem Cells. 2006 Apr;24(4):1142]. Stem Cells 24:671-678.

Arosio P, Levi S (2002) Ferritin, iron homeostasis, and oxidative damage. Free Radical Biology & Medicine 33:457-463.

Aziz N, Munro HN (1987) Iron regulates ferritin mRNA translation through a segment of its 5' untranslated region. Proceedings of the National Academy of Sciences of the United States of America 84:8478-8482.

Baker E, Baker SM, Morgan EH (1998) Characterisation of non-transferrin-bound iron (ferric citrate) uptake by rat hepatocytes in culture. Biochim Biophys Acta 1380:21-30.

Bartzokis G, Beckson M, Hance DB, Marx P, Foster JA, Marder SR (1997) MR evaluation of age-related increase of brain iron in young adult and older normal males. Magn Reson Imaging 15:29-35.

Bartzokis G, Mintz J, Sultzer D, Marx P, Herzberg JS, Phelan CK, Marder SR (1994) In vivo MR evaluation of age-related increases in brain iron. AJNR Am J Neuroradiol 15:1129-1138.

Bartzokis G, Sultzer D, Cummings J, Holt LE, Hance DB, Henderson VW, Mintz J (2000) In vivo evaluation of brain iron in Alzheimer disease using magnetic resonance imaging. Arch Gen Psychiatry 57:47-53.

Bartzokis G, Cummings JL, Markham CH, Marmarelis PZ, Treciokas LJ, Tishler TA, Marder SR, Mintz J (1999) MRI evaluation of brain iron in earlier- and later-onset Parkinson's disease and normal subjects. Magn Reson Imaging 17:213-222.

Bazylinski DA, Frankel RB (2004) Magnetosome formation in prokaryotes. Nat Rev Microbiol 2:217-230.

Berlett BS, Stadtman ER (1997) Protein oxidation in aging, disease, and oxidative stress. Journal of Biological Chemistry 272:20313-20316.

Bjorklund A, Lindvall O (2000) Cell replacement therapies for central nervous system disorders. Nat Neurosci 3:537-544.

Bos C, Delmas Y, Desmouliere A, Solanilla A, Hauger O, Grosset C, Dubus I, Ivanovic Z, Rosenbaum J, Charbord P, Combe C, Bulte JW, Moonen CT, Ripoche J, Grenier N (2004) In vivo MR imaging of intravascularly injected magnetically labeled mesenchymal stem cells in rat kidney and liver.[see comment]. Radiology 233:781-789.

Breuer W, Epsztejn S, Cabantchik ZI (1995) Iron acquired from transferrin by K562 cells is delivered into a cytoplasmic pool of chelatable iron(II). Journal of Biological Chemistry 270:24209-24215.

Brissot P, Pigeon C, Loreal O (2002) Regulation of systemic iron transport and storage. Molecular & Cellular Iron Transport:597-612.

Brons IG, Smithers LE, Trotter MW, Rugg-Gunn P, Sun B, Chuva de Sousa Lopes SM, Howlett SK, Clarkson A, Ahrlund-Richter L, Pedersen RA, Vallier L (2007) Derivation of pluripotent epiblast stem cells from mammalian embryos. Nature 448:191-195.

Brooks RA, Vymazal J, Goldfarb RB, Bulte JW, Aisen P (1998) Relaxometry and magnetometry of ferritin. Magnetic Resonance in Medicine 40:227-235.

Bulte JW, Kraitchman DL (2004) Iron oxide MR contrast agents for molecular and cellular imaging. NMR in Biomedicine 17:484-499.

Bulte JW, Duncan ID, Frank JA (2002) In vivo magnetic resonance tracking of magnetically labeled cells after transplantation. J Cereb Blood Flow Metab 22:899-907.

Bulte JW, Vymazal J, Brooks RA, Pierpaoli C, Frank JA (1993) Frequency dependence of MR relaxation times. II. Iron oxides. J Magn Reson Imaging 3:641-648.

Byrne JA, Pedersen DA, Clepper LL, Nelson M, Sanger WG, Gokhale S, Wolf DP, Mitalipov SM (2007) Producing primate embryonic stem cells by somatic cell nuclear transfer.[see comment]. Nature 450:497-502.

Cao F, Drukker M, Lin S, Sheikh AY, Xie X, Li Z, Connolly AJ, Weissman IL, Wu JC (2007) Molecular imaging of embryonic stem cell misbehavior and suicide gene ablation. Cloning Stem Cells 9:107-117.

Casey JL, Koeller DM, Ramin VC, Klausner RD, Harford JB (1989) Iron regulation of transferrin receptor mRNA levels requires iron-responsive elements and a rapid turnover determinant in the 3' untranslated region of the mRNA. EMBO J 8:3693-3699.

Casey JL, Hentze MW, Koeller DM, Caughman SW, Rouault TA, Klausner RD, Harford JB (1988) Iron-responsive elements: regulatory RNA sequences that control mRNA levels and translation. Science 240:924-928.

Caughman SW, Hentze MW, Rouault TA, Harford JB, Klausner RD (1988) The iron-responsive element is the single element responsible for iron-dependent translational regulation of ferritin biosynthesis. Evidence for function as the binding site for a translational repressor. Journal of Biological Chemistry 263:19048-19052.

Cherry SR, Gambhir SS (2001) Use of positron emission tomography in animal research. ILAR J 42:219-232.

Cherry SR, Biniszkiewicz D, van Parijs L, Baltimore D, Jaenisch R (2000) Retroviral expression in embryonic stem cells and hematopoietic stem cells. Mol Cell Biol 20:7419-7426.

Cohen B, Dafni H, Meir G, Harmelin A, Neeman M (2005) Ferritin as an endogenous MRI reporter for noninvasive imaging of gene expression in C6 glioma tumors. Neoplasia (New York) 7:109-117.

Cohen B, Ziv K, Plaks V, Harmelin A, Neeman M (2009) Ferritin nanoparticles as magnetic resonance reporter gene. WIREs Nanomed Nanobiotechnol 1:181-188.

Cohen B, Ziv K, Plaks V, Israely T, Kalchenko V, Harmelin A, Benjamin LE, Neeman M (2007) MRI detection of transcriptional regulation of gene expression in transgenic mice. Nature Medicine 13:498-503.

Conrad S, Renninger M, Hennenlotter J, Wiesner T, Just L, Bonin M, Aicher W, Buhring HJ, Mattheus U, Mack A, Wagner HJ, Minger S, Matzkies M, Reppel M, Hescheler J, Sievert KD, Stenzl A, Skutella T (2008) Generation of pluripotent stem cells from adult human testis. Nature 456:344-349.

Cozzi A, Corsi B, Levi S, Santambrogio P, Albertini A, Arosio P (2000) Overexpression of wild type and mutated human ferritin H-chain in HeLa cells: in vivo role of ferritin ferroxidase activity. Journal of Biological Chemistry 275:25122-25129.

Crichton R, Ward R (1998) Iron homeostasis. Metal Irons in biological systems 633-665.

Dautry-Varsat A, Ciechanover A, Lodish HF (1983) pH and the recycling of transferrin during receptor-mediated endocytosis. Proceedings of the National Academy of Sciences of the United States of America 80:2258-2262.

de Vries IJ, Lesterhuis WJ, Barentsz JO, Verdijk P, van Krieken JH, Boerman OC, Oyen WJ, Bonenkamp JJ, Boezeman JB, Adema GJ, Bulte JW, Scheenen TW, Punt CJ, Heerschap A, Figdor CG (2005) Magnetic resonance tracking of dendritic cells in melanoma patients for monitoring of cellular therapy.[see comment]. Nature Biotechnology 23:1407-1413.

Deans AE, Wadghiri YZ, Bernas LM, Yu X, Rutt BK, Turnbull DH (2006) Cellular MRI contrast via coexpression of transferrin receptor and ferritin. Magnetic Resonance in Medicine 56:51-59.

Efrat S (2002) Cell replacement therapy for type 1 diabetes. Trends Mol Med 8:334-339.

Evans MJ, Kaufman MH (1981) Establishment in culture of pluripotential cells from mouse embryos. Nature 292:154-156.

Freed CR, Greene PE, Breeze RE, Tsai WY, DuMouchel W, Kao R, Dillon S, Winfield H, Culver S, Trojanowski JQ, Eidelberg D, Fahn S (2001) Transplantation of embryonic dopamine neurons for severe Parkinson's disease.[see comment]. New England Journal of Medicine 344:710-719.

Gambhir SS (2002) Molecular imaging of cancer with positron emission tomography. Nat Rev Cancer 2:683-693.

Gambhir SS, Bauer E, Black ME, Liang Q, Kokoris MS, Barrio JR, Iyer M, Namavari M, Phelps ME, Herschman HR (2000) A mutant herpes simplex virus type 1 thymidine kinase reporter gene shows improved sensitivity for imaging reporter

gene expression with positron emission tomography. Proceedings of the National Academy of Sciences of the United States of America 97:2785-2790.

Gambhir SS, Barrio JR, Phelps ME, Iyer M, Namavari M, Satyamurthy N, Wu L, Green LA, Bauer E, MacLaren DC, Nguyen K, Berk AJ, Cherry SR, Herschman HR (1999) Imaging adenoviral-directed reporter gene expression in living animals with positron emission tomography. Proceedings of the National Academy of Sciences of the United States of America 96:2333-2338.

Genove G, DeMarco U, Xu H, Goins WF, Ahrens ET (2005) A new transgene reporter for in vivo magnetic resonance imaging. Nature Medicine 11:450-454.

Gilad AA, Winnard PT, Jr., van Zijl PC, Bulte JW (2007a) Developing MR reporter genes: promises and pitfalls. NMR in Biomedicine 20:275-290.

Gilad AA, McMahon MT, Walczak P, Winnard PT, Jr., Raman V, van Laarhoven HW, Skoglund CM, Bulte JW, van Zijl PC (2007b) Artificial reporter gene providing MRI contrast based on proton exchange. Nature Biotechnology 25:217-219.

Gottesfeld Z, Neeman M (1996) Ferritin effect on the transverse relaxation of water: NMR microscopy at 9.4 T. Magnetic Resonance in Medicine 35:514-520.

Gropp M, Itsykson P, Singer O, Ben-Hur T, Reinhartz E, Galun E, Reubinoff BE (2003) Stable genetic modification of human embryonic stem cells by lentiviral vectors. Mol Ther 7:281-287.

Hanna J, Wernig M, Markoulaki S, Sun CW, Meissner A, Cassady JP, Beard C, Brambrink T, Wu LC, Townes TM, Jaenisch R (2007) Treatment of sickle cell anemia mouse model with iPS cells generated from autologous skin.[see comment]. Science 318:1920-1923.

Hanson ES, Leibold EA (1999) Regulation of the iron regulatory proteins by reactive nitrogen and oxygen species. Gene Expr 7:367-376.

Harrison PM, Arosio P (1996) The ferritins: molecular properties, iron storage function and cellular regulation. Biochim Biophys Acta 1275:161-203.

Henle ES, Linn S (1997) Formation, prevention, and repair of DNA damage by iron/hydrogen peroxide. Journal of Biological Chemistry 272:19095-19098.

Hentze MW, Caughman SW, Casey JL, Koeller DM, Rouault TA, Harford JB, Klausner RD (1988) A model for the structure and functions of iron-responsive elements. Gene 72:201-208.

Hoehn M, Himmelreich U, Kruttwig K, Wiedermann D (2008) Molecular and cellular MR imaging: potentials and challenges for neurological applications. J Magn Reson Imaging 27:941-954.

Hopkins CR, Trowbridge IS (1983) Internalization and processing of transferrin and the transferrin receptor in human carcinoma A431 cells. J Cell Biol 97:508-521.

Ichikawa T, Hogemann D, Saeki Y, Tyminski E, Terada K, Weissleder R, Chiocca EA, Basilion JP (2002) MRI of transgene expression: correlation to therapeutic gene expression. Neoplasia (New York) 4:523-530.

Inman RS, Wessling-Resnick M (1993) Characterization of transferrin-independent iron transport in K562 cells. Unique properties provide evidence for multiple pathways of iron uptake. Journal of Biological Chemistry 268:8521-8528.

Ivanova N, Dobrin R, Lu R, Kotenko I, Levorse J, DeCoste C, Schafer X, Lun Y, Lemischka IR (2006) Dissecting self-renewal in stem cells with RNA interference. Nature 442:533-538.

Jacobs RE, Cherry SR (2001) Complementary emerging techniques: high-resolution PET and MRI. Curr Opin Neurobiol 11:621-629.

Jasanoff A (2007) MRI contrast agents for functional molecular imaging of brain activity. Curr Opin Neurobiol 17:593-600.

Jocobs A, Worwood M (1978) Normal Iron Metabolism. Metals and the Liver.

Kaji K, Norrby K, Paca A, Mileikovsky M, Mohseni P, Woltjen K (2009) Virus-free induction of pluripotency and subsequent excision of reprogramming factors.[see comment]. Nature 458:771-775.

Kaneko K, Yano M, Yamano T, Tsujinaka T, Miki H, Akiyama Y, Taniguchi M, Fujiwara Y, Doki Y, Inoue M, Shiozaki H, Kaneda Y, Monden M (2001) Detection of peritoneal micrometastases of gastric carcinoma with green fluorescent protein and carcinoembryonic antigen promoter. Cancer Res 61:5570-5574.

Kaur D, Rajagopalan S, Chinta S, Kumar J, Di Monte D, Cherny RA, Andersen JK (2007) Chronic ferritin expression within murine dopaminergic midbrain neurons results in a progressive age-related neurodegeneration. Brain Research 1140:188-194.

Kaur D, Yantiri F, Rajagopalan S, Kumar J, Mo JQ, Boonplueang R, Viswanath V, Jacobs R, Yang L, Beal MF, DiMonte D, Volitaskis I, Ellerby L, Cherny RA, Bush AI, Andersen JK (2003) Genetic or pharmacological iron chelation prevents MPTP-induced neurotoxicity in vivo: a novel therapy for Parkinson's disease.[see comment]. Neuron 37:899-909.

Konijn AM, Glickstein H, Vaisman B, Meyron-Holtz EG, Slotki IN, Cabantchik ZI (1999) The cellular labile iron pool and intracellular ferritin in K562 cells. Blood 94:2128-2134.

Koretsky A, Y-J. L, Schorle H, Jaenisch R (1996) Genetic control of MRI contrast by expression of the transferrin receptor. Proceedings of the International Society of Magnetic Resonance Medicine 1.

Kotamraju S, Chitambar CR, Kalivendi SV, Joseph J, Kalyanaraman B (2002) Transferrin receptor-dependent iron uptake is responsible for doxorubicin-mediated apoptosis in endothelial cells: role of oxidant-induced iron signaling in apoptosis. Journal of Biological Chemistry 277:17179-17187.

Kruszewski M (2003) Labile iron pool: the main determinant of cellular response to oxidative stress. Mutat Res 531:81-92.

Lawson DM, Treffry A, Artymiuk PJ, Harrison PM, Yewdall SJ, Luzzago A, Cesareni G, Levi S, Arosio P (1989) Identification of the ferroxidase centre in ferritin. FEBS Lett 254:207-210.

Lee SH, Lumelsky N, Studer L, Auerbach JM, McKay RD (2000) Efficient generation of midbrain and hindbrain neurons from mouse embryonic stem cells. Nature Biotechnology 18:675-679.

Levi S, Luzzago A, Cesareni G, Cozzi A, Franceschinelli F, Albertini A, Arosio P (1988) Mechanism of ferritin iron uptake: activity of the H-chain and deletion mapping of the ferro-oxidase site. A study of iron uptake and ferro-oxidase activity of human liver, recombinant H-chain ferritins, and of two H-chain deletion mutants. Journal of Biological Chemistry 263:18086-18092.

Levi S, Yewdall SJ, Harrison PM, Santambrogio P, Cozzi A, Rovida E, Albertini A, Arosio P (1992) Evidence of H- and L-chains have co-operative roles in the iron-uptake mechanism of human ferritin. Biochem J 288:591-596.

Lois C, Hong EJ, Pease S, Brown EJ, Baltimore D (2002) Germline transmission and tissue-specific expression of transgenes delivered by lentiviral vectors. Science 295:868-872.

Louie AY, Huber MM, Ahrens ET, Rothbacher U, Moats R, Jacobs RE, Fraser SE, Meade TJ (2000) In vivo visualization of gene expression using magnetic resonance imaging. Nature Biotechnology 18:321-325.

Ma Y, Ramezani A, Lewis R, Hawley RG, Thomson JA (2003) High-level sustained transgene expression in human embryonic stem cells using lentiviral vectors. Stem Cells 21:111-117.

Martin GR (1981) Isolation of a pluripotent cell line from early mouse embryos cultured in medium conditioned by teratocarcinoma stem cells. Proceedings of the National Academy of Sciences of the United States of America 78:7634-7638.

Massoud TF, Gambhir SS (2003) Molecular imaging in living subjects: seeing fundamental biological processes in a new light. Genes Dev 17:545-580.

Matsushita N, Okada H, Yasoshima Y, Takahashi K, Kiuchi K, Kobayashi K (2002) Dynamics of tyrosine hydroxylase promoter activity during midbrain dopaminergic neuron development. J Neurochem 82:295-304.

McKay R (2000) Stem cells--hype and hope. Nature 406:361-364.

McMahon MT, Gilad AA, DeLiso MA, Berman SM, Bulte JW, van Zijl PC (2008) New "multicolor" polypeptide diamagnetic chemical exchange saturation transfer

(DIACEST) contrast agents for MRI. Magnetic Resonance in Medicine 60:803-812.

Meneghini R (1997) Iron homeostasis, oxidative stress, and DNA damage. Free Radical Biology & Medicine 23:783-792.

Moore A, Basilion JP, Chiocca EA, Weissleder R (1998) Measuring transferrin receptor gene expression by NMR imaging. Biochim Biophys Acta 1402:239-249.

Naus CC, Elisevich K, Zhu D, Belliveau DJ, Del Maestro RF (1992) In vivo growth of C6 glioma cells transfected with connexin43 cDNA. Cancer Res 52:4208-4213.

Nichols J, Zevnik B, Anastassiadis K, Niwa H, Klewe-Nebenius D, Chambers I, Scholer H, Smith A (1998) Formation of pluripotent stem cells in the mammalian embryo depends on the POU transcription factor Oct4. Cell 95:379-391.

Niwa H, Miyazaki J, Smith AG (2000) Quantitative expression of Oct-3/4 defines differentiation, dedifferentiation or self-renewal of ES cells.[see comment]. Nat Genet 24:372-376.

Okabe S, Forsberg-Nilsson K, Spiro AC, Segal M, McKay RD (1996) Development of neuronal precursor cells and functional postmitotic neurons from embryonic stem cells in vitro. Mechanisms of Development 59:89-102.

Pfeifer A, Ikawa M, Dayn Y, Verma IM (2002) Transgenesis by lentiviral vectors: lack of gene silencing in mammalian embryonic stem cells and preimplantation embryos. Proceedings of the National Academy of Sciences of the United States of America 99:2140-2145.

Pham CG, Bubici C, Zazzeroni F, Papa S, Jones J, Alvarez K, Jayawardena S, De Smaele E, Cong R, Beaumont C, Torti FM, Torti SV, Franzoso G (2004) Ferritin heavy

chain upregulation by NF-kappaB inhibits TNFalpha-induced apoptosis by suppressing reactive oxygen species. Cell 119:529-542.

Picard V, Renaudie F, Porcher C, Hentze MW, Grandchamp B, Beaumont C (1996) Overexpression of the ferritin H subunit in cultured erythroid cells changes the intracellular iron distribution. Blood 87:2057-2064.

Ponka P, Beaumont C, Richardson DR (1998) Function and regulation of transferrin and ferritin. Semin Hematol 35:35-54.

Revazova ES, Turovets NA, Kochetkova OD, Agapova LS, Sebastian JL, Pryzhkova MV, Smolnikova VI, Kuzmichev LN, Janus JD (2008) HLA homozygous stem cell lines derived from human parthenogenetic blastocysts. Cloning Stem Cells 10:11-24.

Rogers WJ, Meyer CH, Kramer CM (2006) Technology insight: in vivo cell tracking by use of MRI. Nat Clin Pract Cardiovasc Med 3:554-562.

Rosenthal MS, Cullom J, Hawkins W, Moore SC, Tsui BM, Yester M (1995) Quantitative SPECT imaging: a review and recommendations by the Focus Committee of the Society of Nuclear Medicine Computer and Instrumentation Council.[see comment]. J Nucl Med 36:1489-1513.

Roy NS, Cleren C, Singh SK, Yang L, Beal MF, Goldman SA (2006) Functional engraftment of human ES cell-derived dopaminergic neurons enriched by coculture with telomerase-immortalized midbrain astrocytes.[see comment][erratum appears in Nat Med. 2007 Mar;13(3):385]. Nature Medicine 12:1259-1268.

Schuldiner M, Itskovitz-Eldor J, Benvenisty N (2003) Selective ablation of human embryonic stem cells expressing a "suicide" gene. Stem Cells 21:257-265.

Shamblott MJ, Axelman J, Wang S, Bugg EM, Littlefield JW, Donovan PJ, Blumenthal PD, Huggins GR, Gearhart JD (1998) Derivation of pluripotent stem cells from cultured human primordial germ cells.[erratum appears in Proc Natl Acad Sci U S A 1999 Feb 2;96(3):1162]. Proceedings of the National Academy of Sciences of the United States of America 95:13726-13731.

Sherry AD, Woods M (2008) Chemical exchange saturation transfer contrast agents for magnetic resonance imaging. Annu Rev Biomed Eng 10:391-411.

Smith AG (2001) Embryo-derived stem cells: of mice and men. Annu Rev Cell Dev Biol 17:435-462.

Solter D, Knowles BB (1978) Monoclonal antibody defining a stage-specific mouse embryonic antigen (SSEA-1). Proceedings of the National Academy of Sciences of the United States of America 75:5565-5569.

Spergel DJ, Kruth U, Shimshek DR, Sprengel R, Seeburg PH (2001) Using reporter genes to label selected neuronal populations in transgenic mice for gene promoter, anatomical, and physiological studies. Prog Neurobiol 63:673-686.

Stadtman ER, Berlett BS (1998) Reactive oxygen-mediated protein oxidation in aging and disease. Drug Metab Rev 30:225-243.

Steinberg D (1997) Low density lipoprotein oxidation and its pathobiological significance. Journal of Biological Chemistry 272:20963-20966.

Stuckey DJ, Carr CA, Martin-Rendon E, Tyler DJ, Willmott C, Cassidy PJ, Hale SJ, Schneider JE, Tatton L, Harding SE, Radda GK, Watt S, Clarke K (2006) Iron

particles for noninvasive monitoring of bone marrow stromal cell engraftment into, and isolation of viable engrafted donor cells from, the heart. Stem Cells 24:1968-1975.

Sturrock A, Alexander J, Lamb J, Craven CM, Kaplan J (1990) Characterization of a transferrin-independent uptake system for iron in HeLa cells. Journal of Biological Chemistry 265:3139-3145.

Takahashi K, Tanabe K, Ohnuki M, Narita M, Ichisaka T, Tomoda K, Yamanaka S (2007) Induction of pluripotent stem cells from adult human fibroblasts by defined factors.[see comment]. Cell 131:861-872.

Theil EC (2000) Targeting mRNA to regulate iron and oxygen metabolism. Biochem Pharmacol 59:87-93.

Thomson JA, Kalishman J, Golos TG, Durning M, Harris CP, Becker RA, Hearn JP (1995) Isolation of a primate embryonic stem cell line. Proceedings of the National Academy of Sciences of the United States of America 92:7844-7848.

Thomson JA, Itskovitz-Eldor J, Shapiro SS, Waknitz MA, Swiergiel JJ, Marshall VS, Jones JM (1998) Embryonic stem cell lines derived from human blastocysts.[see comment][erratum appears in Science 1998 Dec 4;282(5395):1827]. Science 282:1145-1147.

Toomey JR, Kratzer KE, Lasky NM, Broze GJ, Jr. (1997) Effect of tissue factor deficiency on mouse and tumor development. Proceedings of the National Academy of Sciences of the United States of America 94:6922-6926.

Treffry A, Zhao Z, Quail MA, Guest JR, Harrison PM (1997) Dinuclear center of ferritin: studies of iron binding and oxidation show differences in the two iron sites. Biochemistry 36:432-441.

Vymazal J, Zak O, Bulte JW, Aisen P, Brooks RA (1996) T1 and T2 of ferritin solutions: effect of loading factor. Magnetic Resonance in Medicine 36:61-65.

Vymazal J, Brooks RA, Bulte JW, Gordon D, Aisen P (1998) Iron uptake by ferritin: NMR relaxometry studies at low iron loads. J Inorg Biochem 71:153-157.

Vymazal J, Brooks RA, Zak O, McRill C, Shen C, Di Chiro G (1992) T1 and T2 of ferritin at different field strengths: effect on MRI. Magnetic Resonance in Medicine 27:368-374.

Weissleder R, Ntziachristos V (2003) Shedding light onto live molecular targets. Nature Medicine 9:123-128.

Weissleder R, Simonova M, Bogdanova A, Bredow S, Enochs WS, Bogdanov A, Jr. (1997) MR imaging and scintigraphy of gene expression through melanin induction. Radiology 204:425-429.

Weissleder R, Moore A, Mahmood U, Bhorade R, Benveniste H, Chiocca EA, Basilion JP (2000) In vivo magnetic resonance imaging of transgene expression. Nature Medicine 6:351-355.

Wobus AM, Boheler KR (2005) Embryonic stem cells: prospects for developmental biology and cell therapy. Physiol Rev 85:635-678.

Wood JC, Fassler JD, Meade T (2004) Mimicking liver iron overload using liposomal ferritin preparations. Magnetic Resonance in Medicine 51:607-611.

Yang SH, Cheng PH, Banta H, Piotrowska-Nitsche K, Yang JJ, Cheng EC, Snyder B, Larkin K, Liu J, Orkin J, Fang ZH, Smith Y, Bachevalier J, Zola SM, Li SH, Li XJ, Chan AW (2008) Towards a transgenic model of Huntington's disease in a non-human primate.[see comment]. Nature 453:921-924.

Yu J, Vodyanik MA, Smuga-Otto K, Antosiewicz-Bourget J, Frane JL, Tian S, Nie J, Jonsdottir GA, Ruotti V, Stewart R, Slukvin, II, Thomson JA (2007) Induced pluripotent stem cell lines derived from human somatic cells.[see comment]. Science 318:1917-1920.

Zhou H, Wu S, Joo J, Zhu S, Han D, Lin T, Trauger S, Bien G, Yao S, Zhu Y, Siuzdak G, Scholer H, Duan L, Ding S (2009) Generation of Induced Pluripotent Stem Cells Using Recombinant Proteins. Cell Stem Cell.

Zhu J, Zhou L, XingWu F (2006) Tracking neural stem cells in patients with brain trauma. New England Journal of Medicine 355:2376-2378.

Zurkiya O, Chan AWS, Hu X (2008) MagA Is Sufficient for Producing Magnetic Nanoparticles in Mammalian Cells, Making it an MRI Reporter. Magnetic Resonance in Medicine 59:1225–1231.